

**Genome-wide control of H4 K16  
acetylation by the SAS-I complex  
in *Saccharomyces cerevisiae***

Inaugural-Dissertation

zur

Erlangung des Doktorgrades

Dr. rer. nat.

der Fakultät für

Biologie

an der

Universität Duisburg-Essen

vorgelegt von

**Franziska Heise**

aus Halle/ Saale

März 2011

Die der vorliegende Arbeit zugrunde liegenden Experimente wurden in der Abteilung für Genetik der Fakultät Biologie der Universität Duisburg-Essen durchgeführt.

1. Gutachter: Prof. Dr. Ann E. Ehrenhofer-Murray

2. Gutachter: Prof. Dr. Bernhard Horsthemke

3. Gutachter:

Vorsitzender des Prüfungsausschusses: Prof. Dr. Hemmo Meyer

Tag der mündlichen Prüfung: 15.06.2011

---

**Abstract**

The MYST HAT Sas2 is part of the SAS-I complex, which includes the subunits Sas4 and Sas5 and acetylates histone H4 lysine 16 (H4 K16Ac). This Sas2-mediated H4 K16Ac blocks the propagation of heterochromatin at the telomeres of *Saccharomyces cerevisiae* and is further involved in silencing at the *HM* loci and the rDNA locus. In this study, we investigated Sas2-mediated H4 K16Ac on a genome-wide scale, by using chromatin immunoprecipitations combined with high resolution tiling arrays. Because Sas2 interacts with the chromatin assembly factors CAF-I and Asf1, we furthermore investigated the dependence of the Sas2-mediated H4 K16Ac on these factors and found a partial influence of CAF-I and Asf1 on H4 K16Ac. Globally, H4 K16Ac was reduced in the absence of Sas2. Interestingly, H4 K16Ac loss in *sas2Δ* cells outside of the telomeric regions showed a distinctive pattern in that there was a pronounced decrease of H4 K16Ac within the majority of open reading frames (ORFs), but little change in intergenic regions. Significantly, high Sas2-dependent H4 K16Ac correlated with low histone H3 exchange and low H3 K56 acetylation, indicating that this modification was placed on chromatin independently of histone exchange. Consistent with this notion we found evidence that Sas2 mediated H4 K16 acetylation coupled to the S-Phase of the cell cycle. In agreement with the effect of Sas2 within ORFs, *sas2Δ* caused resistance to 6-azauracil, and RNA polymerase II (PolII) occupancy in the 3' region of genes was increased in *sas2Δ* cells, suggesting a positive effect on transcription elongation in the absence of H4 K16Ac. Additionally, we observed a slight accumulation of transcripts at the 3' end of the majority of genes in *sas2Δ* cells. This effect for several reasons was distinct from short transcripts that are caused by cryptic transcription initiation. Nonetheless, this finding completed our picture of the positive impact of *sas2Δ* on PolII-dependent transcription. In summary, our data suggest that Sas2-dependent H4 K16Ac is distributed globally and deposited into chromatin independently of transcription and histone exchange but coupled to DNA replication, and that it has an inhibitory effect on the ability of PolII to travel through the body of the gene.

## Zusammenfassung

Die Histonacetyltransferase (HAT) Sas2 in *Saccharomyces cerevisiae* gehört zur Familie der MYST HATs und bildet mit den Untereinheiten Sas4 und Sas5 den SAS-I Komplex, der Histon H4 an Lysin 16 (H4 K16Ac) acetyliert. Diese Sas2-vermittelte H4 K16Ac verhindert eine Ausbreitung des telomerischen Heterochromatins in euchromatische Bereiche und ist weiterhin an der transkriptionellen Stilllegung der *HM* Loci und des rDNA Locus beteiligt. In der vorliegenden Arbeit wurde die Sas2-vermittelte H4 K16Ac auf genomweiter Ebene unter Anwendung von Chromatinimmunpräzipitation (ChIP) in Kombination mit hoch auflösenden genomischen Tiling Arrays untersucht. Da Sas2 mit den Chromatin-Assemblierungsfaktoren CAF-I und Asf1 interagiert, wurde weiterhin die Abhängigkeit der Sas2-vermittelten H4 K16Ac von diesen Faktoren untersucht. Dabei wurde ein partieller Einfluss von CAF-I und Asf1 auf die Sas2-vermittelte H4 K16Ac festgestellt. In Abwesenheit von Sas2 war die H4 K16Ac auf globaler Ebene reduziert. Interessanterweise verursachte der Verlust der H4 K16Ac in *sas2Δ* Zellen ein charakteristisches Muster außerhalb der telomerischen Region. H4 K16Ac war an der Mehrzahl der offenen Leseraster (ORFs) stark reduziert, während die H4 K16Ac in intergenischen Regionen kaum Veränderungen aufwies. Bezeichnenderweise korrelierte die Sas2-abhängige H4 K16Ac mit einem geringen Histon H3 Austausch und einem geringen Maß an H3 K56 Acetylierung. Dies deutete darauf hin, dass H4 K16Ac unabhängig von transkriptionsgekoppeltem Histonaustausch im Chromatin platziert wurde. Dementsprechend wurden in dieser Arbeit Hinweise gefunden, dass die Sas2 vermittelte H4 K16Ac im Zellzyklus gekoppelt an die S-Phase eingeführt wird. In Übereinstimmung mit dem Effekt von Sas2 innerhalb von ORFs wurde weiterhin festgestellt, dass eine Deletion von *SAS2* zur Resistenz gegenüber 6-Azauracil führte sowie die Konzentration der RNA Polymerase II (PolII) an den 3' Regionen der Gene erhöhte. Diese Resultate ließen auf einen positiven Effekt der fehlenden H4 K16Ac auf die Elongationphase der Transkription schließen. Zusätzlich dazu wurde eine geringfügige Akkumulation von Transkripten an den 3'-Enden in der Mehrzahl der Gene in *sas2Δ* Zellen beobachtet. Zusammenfassend lassen die Resultate dieser Arbeit darauf schließen, dass die Sas2-abhängige H4 K16Ac global im Genom von *S. cerevisiae* positioniert wird, unabhängig von Transkription und Histonaustausch in das Chromatin eingebaut wird und daher vor allem in schwach transkribierten ORFs verbleibt. Es wurde gezeigt, dass die Acetylierung von H4 K16 gekoppelt an die DNA-Replikation erfolgt und dass die Sas2-vermittelte H4 K16Ac die Fähigkeit der PolIII, ein Gen zu transkribieren, inhibiert.

---

**Table of contents**

<b>ABSTRACT .....</b>	<b>3</b>
<b>ZUSAMMENFASSUNG .....</b>	<b>4</b>
<b>LIST OF TABLES AND FIGURES .....</b>	<b>8</b>
<b>ABBREVIATIONS.....</b>	<b>10</b>
<b>1. INTRODUCTION .....</b>	<b>11</b>
1.1 THE ORGANIZATION OF DNA IN EUKARYOTES .....	11
1.2 STRUCTURAL ORGANIZATION OF EUKARYOTIC CHROMATIN .....	11
1.3 HISTONE MODIFICATIONS AND HISTONE-MODIFYING ENZYMES .....	13
1.3.1 Histone acetyltransferases.....	14
1.3.2 Histone deacetylases .....	15
1.3.3 The histone acetyltransferase complex SAS-I in <i>Saccharomyces cerevisiae</i> .....	16
1.3.4 Further roles of H4 K16 acetylation in the control of gene expression.....	18
1.4 TRANSCRIPTIONAL SILENCING AND HETEROCHROMATIN IN <i>SACCHAROMYCES CEREVISIAE</i> .....	19
1.5 CHROMATIN AND TRANSCRIPTION .....	20
1.6 PERVASIVE TRANSCRIPTION IN THE YEAST GENOME .....	21
1.7 CHROMATIN DYNAMICS .....	24
1.7.1 Replication-coupled chromatin assembly by CAF-I and Asf1 .....	25
1.7.2 Replication-independent assembly of histones by Asf1 .....	27
1.8 RETROTRANSPOSONS IN <i>SACCHAROMYCES CEREVISIAE</i> .....	28
1.9 OUTLINE OF THIS THESIS.....	29
<b>2. MATERIAL AND METHODS .....</b>	<b>31</b>
2.1 <i>ESCHERICHIA COLI</i> STRAINS.....	31
2.2 MEDIA GROWTH CONDITIONS .....	31
2.3 <i>SACCHAROMYCES CEREVISIAE</i> STRAINS.....	31
2.4 GENETIC MANIPULATION OF <i>SACCHAROMYCES CEREVISIAE</i> STRAINS.....	33
2.4.1 Crossing, sporulation and dissection of asci.....	33
2.4.2 DNA techniques in <i>Saccharomyces cerevisiae</i> .....	34
2.5 MOLECULAR CLONING .....	34
2.6 GENETIC ASSAYS IN <i>SACCHAROMYCES CEREVISIAE</i> .....	35
2.7 ANTIBODIES.....	35
2.8 CHROMATIN IMMUNOPRECIPITATION.....	36

2.9 QUANTITATIVE REAL-TIME PCR.....	37
2.10 TILING ARRAY (CHIP-CHIP).....	39
2.10.1 ChIP-chip sample preparation.....	39
2.10.2 Processing and hybridization of ChIP DNA.....	39
2.10.3 Tiling Array data analysis.....	40
2.10.3.1 Normalization.....	40
2.10.3.2 Identification of H4 K16Ac – enriched and – depleted regions.....	40
2.10.3.3 Average profiles of H4 K16Ac along transcriptional units.....	40
2.10.3.4 H3 exchange and H3 K56 acetylation data.....	41
2.11 RNA EXPRESSION ANALYSIS.....	41
2.11.1 RNA sample preparation.....	41
2.11.2 Reverse transcription (RT) and measurement of 3': 5' ratios.....	42
2.11.3 Hybridization to expression arrays.....	42
2.11.4 Expression array data analysis.....	42
2.12 PREPARATION OF <i>SACCHAROMYCES CEREVISIAE</i> PROTEIN EXTRACTS.....	42
2.13 SDS PAGE AND IMMUNOBLOTTING (WESTERN BLOT).....	43
2.14 SYNCHRONIZATION OF <i>SACCHAROMYCES CEREVISIAE</i> CELLS.....	43
<b>3. RESULTS.....</b>	<b>44</b>
3.1 GENOME-WIDE INFLUENCE OF SAS2-MEDIATED H4 K16 ACETYLATION.....	44
3.1.1 <i>sas2Δ</i> caused a global reduction of H4 K16 acetylation.....	44
3.1.2 Acetylation of H4 K16 at telomeric regions was dependent on Sas2, but only partially dependent on the chromatin assembly factors CAF-I and Asf1.....	47
3.1.2.1 H4 K16Ac was depleted at subtelomeric regions in <i>sas2Δ</i> .....	47
3.1.2.2 H4 K16Ac at telomeric regions was partially influenced by the chromatin assembly factors CAF-I and Asf1.....	51
3.1.3 Retrotransposons showed H4 K16 acetylation that depended on Sas2.....	52
3.1.4 H4 K16 acetylation was decreased at the 3' ends of long ORFs in <i>sas2Δ</i> cells.....	57
3.1.5 <i>sas2Δ</i> cells showed resistance to 6-azauracil.....	61
3.1.5.1 Comparable <i>IMD2</i> expression level in wt and <i>sas2Δ</i> cells.....	63
3.1.5.2 Increased processivity of transcription in <i>sas2Δ</i> cells.....	63
3.1.6 Accumulation of transcripts at the 3' end of genes in <i>sas2Δ</i> cells.....	66
3.1.7 Partial interdependence of Sas2 and Set2.....	69
3.1.8 Sas2-dependent H4 K16 acetylation was predominantly found in regions of low histone exchange and low H3 K56 acetylation.....	71

---

3.1.9 H4 K16Ac in CAC1 and/ or ASF1 deletion strains was less changed in regions with low histone exchange.....	73
3.2 CELL-CYCLE DEPENDENT DEPOSITION OF H4 K16 ACETYLATION BY SAS2.....	75
3.2.1 Generation of a repressible SAS2 allele was achieved by construction of a heat-inducible N-degron.....	75
3.2.2 Dynamics of H4 K16 acetylation by Sas2 were cell-cycle dependent.....	80
<b>4. DISCUSSION .....</b>	<b>82</b>
4.1 SAS2 INFLUENCED H4 K16AC ON A GLOBAL SCALE .....	82
4.2 THE POSSIBLE FUNCTION OF SAS2 AT TY ELEMENTS.....	84
4.3 THE DELETION OF SAS2 INFLUENCED TRANSCRIPTION ELONGATION .....	85
4.4 SAS2 $\Delta$ INFLUENCED THE LEVEL OF TRANSCRIPTION ON A GLOBAL SCALE.....	86
4.5 COOPERATION OF SAS2 AND SET2 IN THE REPRESSION OF TRANSCRIPTION ELONGATION .....	89
4.6 SAS2-DEPENDENT H4 K16 ACETYLATION WAS ASSOCIATED WITH REGIONS OF LOW H3 EXCHANGE.....	90
4.7 THE INFLUENCE OF CAF-I AND ASF1 ON H4 K16AC.....	90
4.8 REPLICATION-COUPLED DEPOSITION OF H4 K16AC BY SAS2 .....	92
4.9 A GENOME-WIDE FUNCTION OF SAS2-MEDIATED H4K16AC .....	93
<b>5. REFERENCES .....</b>	<b>95</b>
<b>DANKSAGUNG .....</b>	<b>109</b>
<b>LEBENS LAUF .....</b>	<b>110</b>
<b>ERKLÄRUNG .....</b>	<b>112</b>

## List of Tables

Table 1. Abbreviations .....	10
Table 2. Yeast strains used in this study.....	31
Table 3. Plasmids used in this study.....	34
Table 4. Oligonucleotides used in this study.....	37

## List of Figures

Figure 1. Acetylation of H4 K16 by the SAS-I complex prevents spreading of SIR-mediated heterochromatin into centromere-proximal regions. ....	17
Figure 2. Model for transcription and pervasive transcription. ....	23
Figure 3. Model for replication-coupled chromatin assembly and disassembly. ....	26
Figure 4. H4 K16 acetylation (H4 K16Ac) was more abundant in regions with less histone H4. ....	45
Figure 5. Relative H4 K16Ac levels in <i>sas2Δ</i> were globally reduced. ....	47
Figure 6. H4 K16Ac at subtelomeric regions showed dependence on Sas2, and a partial influence of the chromatin assembly factors CAF-I and Asf1. ....	48
Figure 7. H4 K16Ac at subtelomeric regions depended on Sas2, and displayed a partial influence of the chromatin assembly factors CAF-I and Asf1. ....	49
Figure 8. Relative H4 K16Ac was decreased around <i>HMR</i> in <i>sas2Δ</i> cells. ....	50
Figure 9. H4 K16Ac was partially dependent on the chromatin assembly factors CAF-I and Asf1. ....	51
Figure 10. H4 K16Ac at Ty elements depended on Sas2.....	54
Figure 11. H4 K16Ac was unaffected deletion of the chromatin assembly factors <i>CAC1</i> and <i>ASF1</i> . ....	56
Figure 12. The influence of Sas2 at Ty1 differed from that of the 5'-3' exoribonuclease Xrn1. ....	56
Figure 13. H4 K16Ac was depleted along ORFs in <i>sas2Δ</i> cells. ....	57
Figure 14. Depletion of H4 K16Ac at the <i>CSF1</i> gene, in <i>sas2Δ</i> . ....	59
Figure 15. <i>sas2Δ</i> caused a decrease of H4 K16 acetylation in the 3' region of ORFs.....	60
Figure 16. Deletion of <i>SAS2</i> caused resistance to 6-azauracil (6-AU).....	62
Figure 17. <i>IMD2</i> induction upon 6-AU treatment did not increase in <i>sas2Δ</i> .....	63
Figure 18. PolIII was present at elevated levels at 3' region of ORFs in <i>sas2Δ</i> .....	64
Figure 19. PolIII dissociation was slowed down at the 3' end of <i>GAL1pr::FMP27</i> in <i>sas2Δ</i> . ....	65

---

Figure 20. Levels of PolIII CTD phosphorylation at S5 and S2 of were not altered by <i>sas2Δ</i> . .....	65
Figure 21. <i>sas2Δ</i> caused an accumulation of transcripts at 3' ends within coding regions.	67
Figure 22. Accumulation of transcripts at 3' ends in <i>sas2Δ</i> . .....	69
Figure 23. Influence of Sas2 on Set2-mediated H3 K36 methylation.....	70
Figure 24. H4 K16Ac was present in regions with low H3 K56 Ac and low histone H3 exchange. ....	72
Figure 25. Less average change in relative H4 K16Ac in <i>cac1Δ</i> , <i>asf1Δ</i> and <i>cac1Δ asf1Δ</i> in regions with low histone exchange.....	74
Figure 26. Myc-tagged Sas2 under the control of the methionine repressible promoter <i>MET3</i> . ....	76
Figure 27. Repression of <i>GALLpr-SAS2</i> was still able to complement the <i>HMRa-e**</i> silencing defect. ....	77
Figure 28. <i>GALLpr-SAS2</i> segregants derived from a genetic cross, did not derepress <i>TEL-VII L::URA3</i> under repressive conditions. ....	78
Figure 29. <i>GALLpr-SAS2</i> on a plasmid showed less complementation of <i>sas2Δ</i> <i>TEL-VI L::URA3</i> than a genomic integration, but still insufficient repression of Sas2 under repressive conditions. ....	78
Figure 30. Under restrictive conditions the heat-inducible degron mutant Sas2-td decreased H4 K16Ac and caused derepression of <i>HMLα</i> silencing. ....	79
Figure 31. Sas2-mediated H4 K16 acetylation was dependent on progression through S- phase. ....	81
Figure 32. Model for the influence of Sas2 on transcription.....	87

## Abbreviations

**Table 1. Abbreviations**

5-FOA	5-fluoro-orotic acid
6-AU	6-azauracil
Ac	acetylation (e.g. at H4 K16 = H4 K16Ac)
Asf1	anti-silencing function (chromatin assembly factor)
bp	base pair
CAF-I	Chromatin Assembly Complex I
ChIP	chromatin immunoprecipitation
CTD	carboxy-terminal domain of RNA Polymerase II
Gal	galactose
HAT	histone acetyltransferase
<i>HML</i>	homothallic mating left
<i>HMR</i>	homothallic mating right
kb	kilo bases
<i>MAT</i>	mating type locus
Me3	trimethylation (e.g. at H3 K36 = H3 K36Me3)
MYST	family of histone acetyltransferases, to which Sas2 belongs
o/n	over night
ORF	open reading frame
Ph	phosphorylation (e.g. H3 S10Ph)
PolII	RNA Polymerase II
qPCR	quantitative real-time polymerase chain reaction
RT-qPCR	quantitative PCR from reverse transcribed RNA
rt	room temperature
SAS-I	HAT complex containing Sas2, Sas4, Sas5
Sas2	something about silencing
S2-P	phosphorylation of serine 2 at CTD
S5-P	phosphorylation serine 5 at CTD
Sir	silent information regulator
w/o	without
wt	wild-type
YM	yeast minimal medium
YP	yeast peptone medium
YPD	yeast peptone dextrose medium

Yeast (*Saccharomyces cerevisiae*) genes were named according to nomenclature conventions of *Saccharomyces cerevisiae* genome database (SGD).

Amino acids were given in the single-letter code, e.g. K = lysine, R = arginine.

# **1. Introduction**

## **1.1 The organization of DNA in eukaryotes**

The carrier of the genetic information, the deoxyribonucleic acid (DNA) is located in the nucleus of eukaryotic cells. The regions of DNA that encode proteins are referred to as genes, and the entity of an organism's DNA as the genome. Sequencing of whole genomes of many eukaryotic organisms so far has revealed the different sizes and complexity of genomes, which, next to coding regions, also consist of noncoding DNA. Complex organisms possess large genomes with an increasing proportion of noncoding and repetitious DNA, for instance the 3.1 Gb large human genome contains about 25 000 genes and comprises about 95% of noncoding DNA. In contrast, the unicellular model organism *Saccharomyces cerevisiae* contains about 6300 genes on 16 chromosomes. It was the first completely sequenced eukaryotic organism (Goffeau et al. 1996). In this compact genome, a protein-coding gene can be found every 2 kb, and the majority of the sequence consists of open reading frames (ORFs) (Dujon 1996). To achieve fitting of the large DNA molecule into the nucleus, the DNA exists in a nucleoprotein complex, packaged with histones and non-histone proteins, the chromatin.

## **1.2 Structural organization of eukaryotic chromatin**

The first level of DNA compaction is obtained by wrapping 146 bp DNA around an octamer of histones to form the nucleosome. Each histone octamer is formed of two copies of each core histone –H2A, H2B, H3 and H4 (Luger et al. 1997). The histones are highly conserved among species and are small basic proteins that consist of a histone fold, histone fold extensions and the flexible histone tails that protrude from the nucleosome (Luger and Richmond 1998). Histones are subject to posttranslational modifications and thus have a high impact on chromatin structure. The nucleosome is the basic repeating unit, which is completed by the H1 linker histone and is spaced at 165 bp in *S. cerevisiae*. The yeast histone H1, Hho1 is structurally distinct from mammalian H1 (Patterton et al. 1998), and was shown to be inhibitory to homologous recombination (Downs et al. 2003). From the 10 nm “beads-on-a-string” structure, in which the “beads” represent the nucleosome and the “string” the linker DNA, the DNA is proposed to be further compacted into the 30 nm chromatin fiber (Finch and Klug 1976; Widom and Klug 1985), which is until today controversially discussed in the scientific community (Maeshima et al.). However, the

DNA can be furthermore compacted with the help of scaffold proteins and forms the visible metaphase chromosomes during mitosis.

In general, chromatin is historically and cytologically differentiated into two forms, the compact heterochromatin and the less condensed euchromatin. Euchromatin contains the most active genes and serves as a template for transcription. Heterochromatin contains few genes, is repressive to transcription and is found at repetitive DNA regions, transposable elements, centromeric and telomeric regions where it forms a highly compacted higher order structure. These regions, which are referred to as constitutive heterochromatin, remain condensed throughout the cell cycle and are crucial for maintaining genome integrity. In contrast, regions of facultative heterochromatin occur at coding regions and change their chromatin state in response to developmental processes (Grewal and Jia 2007). Heterochromatin displays the ability to spread and to influence gene expression in a time and region-dependent manner by inactivating chromosomal domains, a process referred to as silencing (Rusche et al. 2003). Heterochromatin can even form along long distances at chromosomes, for instance in dosage compensation that equals the dosage of sex chromosome-linked gene expression. In mammals, one of the two female X chromosomes is inactivated by the noncoding Xist RNA that triggers silencing (Okamoto and Heard 2009). Heterochromatin is region-specific but not promoter-specific. Furthermore, chromatin states can be altered by positioning a euchromatic region adjacent to heterochromatin, which was described as position-effect variegation (PEV) in *Drosophila melanogaster* by Muller (Muller 1930). The introduced euchromatic region is subsequently silenced and transcriptionally repressed due to the spreading of the adjacent heterochromatin. This phenomenon is not uniquely found in *Drosophila melanogaster*, but also in a variety of organisms, e.g. also in *S. cerevisiae*, where reporter genes that are inserted adjacent to telomeres are silenced, a process that is referred to as telomere position effect (Gottschling et al. 1990).

Silencing in metazoans can be mediated by histone modifications and the subsequent binding of repressive proteins, e.g. methylation of H3 K9 (H3 K9Me) and the heterochromatic protein HP1, as well as by RNA transcript-related mechanisms or RNAi, CpG methylation or the presence of histone variants (Grewal and Jia 2007). The yeast *Saccharomyces cerevisiae* lacks HP1 and also an RNAi machinery. In *S. cerevisiae*, heterochromatin formation at three distinct loci is mediated by the highly conserved histone deacetylase Sir2 (Moazed 2001).

As mentioned above, changes in chromatin state can also be mediated by the incorporation of histone variants. H3.3 is a mark for actively transcribed genes and is deposited upon

gene activation into coding regions that were previously displaced of both H3 and H3.3 (Wirbelauer et al. 2005). This histone deposition mode of H3.3 and other histone variants outside of S-Phase is distinct to that of canonical histones, which are deposited during replication. H2A.Z, a variant of the canonical H2A, is another histone variant associated with active chromatin and is found in several eukaryotes. In contrast to H2A, H2A.Z is incorporated next to silent chromatin in *S. cerevisiae* and inhibits the spreading of heterochromatin into euchromatic regions (Meneghini et al. 2003). H2A.Z is also found flanking nucleosome free regions (NFR) around promoters, and therefore plays a vital role for transcription activation (Workman 2006).

Since histones do not only function in condensing DNA, but furthermore govern access to the DNA in all nuclear processes like DNA replication, repair, and gene expression, several mechanisms have evolved to allow DNA accessibility. These mechanisms include site exposure of DNA by histone fluctuation, remodeling of histones and eviction. Taken together, the combination of nucleosome positions and their covalent modifications are key regulators of processes in the genome (Jiang and Pugh 2009).

### **1.3 Histone modifications and histone-modifying enzymes**

Histones contain a variety of amino acid residues that can be modified by several histone-modifying enzymes. Lysines can be acetylated and methylated, arginines can be methylated and serine and threonine show phosphorylation. Further modifications imply ubiquitylation, sumoylation, ADP ribosylation, deimination and proline isomerization (Kouzarides 2007). More complexity of the modifications is introduced by three possible forms of methylation that can appear as mono-, di- or trimethylation at lysine residues, e.g. the methylation of H3 K36 (H3 K36Me). Covalent modifications of nucleosomes occur primarily at the N-terminal tails, for example H4 K16 acetylation (H4 K16Ac), but also the globular histone domains are subject to modifications, e.g. H3 K56Ac (Xu et al. 2005). Each core histone possesses multiple sites that can be subject to modification. H4 displays four possible lysine residues at the N-terminal tail that can be acetylated, K5, K8, K12 and K16. Mostly, these sites are not modified all at once. An analysis in *S. cerevisiae* shows that 12% of the residues are not acetylated, 36% are monoacetylated, 28% diacetylated, 13% trimethylated and 12% tetraacetylated (Smith et al. 2003). The H4 K16Ac in *S. cerevisiae* is found in 80% of all H4 molecules, and most of the monoacetylated H4 is acetylated at K16 (Clarke et al. 1993; Smith et al. 2003). H4 K16Ac has a special implication in chromatin organization, because it inhibits higher-order chromatin

formation, whereas the residues H4 1-13 are dispensable for the formation of higher-order chromatin (Shogren-Knaak et al. 2006). This disruption of contacts between nucleosomes is one mechanism of the modifications, whereas the second mechanism is the recruitment of effector proteins. Lysine acetylation, for example constitutes a binding platform for proteins containing a bromodomain, e.g. Gcn5, Bdf1 or Brd4. Some of these proteins have enzymatic activities by which they subsequently influence the chromatin. For example, the bromodomain of Gcn5 as a part of the SAGA complex is essential for gene activation of a subset of genes (Barbaric et al. 2003). Specific domains have also been identified both for the recognition of lysine methylation, which are chromo-like domains and PHD domains, and for phosphorylation recognized by a domain within 14-3-3 proteins (Kouzarides 2007). As an example, Eaf3, a subunit of the Rpd3S HDAC complex, recognizes H3 K36Me3 by virtue of its PHD domain, and Rpd3S subsequently deacetylates coding regions after the passage of PolIII (Krogan et al. 2003; Carrozza et al. 2005; Keogh et al. 2005).

The variety of modifications and their abundance make it likely that the modifications also influence each other. Indeed, crosstalk between many modifications that influences the generation of another modification or the binding of effector proteins have been reported. For example, phosphorylation of H3 at serine 10 by the Snf1 kinase promotes the acetylation of H3 K14 by Gcn5 (Cheung et al. 2000; Lo et al. 2000).

Many enzymes have by now been characterized that carry out histone modifications. Among them are acetyltransferases, lysine- and arginine methylases, serine- and threonine kinases. Most modifications are dynamic and reversible by a different kind of enzymes, like e.g. deacetylases and lysine demethylases (Kouzarides 2007). Besides the enzymatic removal, there are more mechanisms to remove or change modifications of histones, for instance the eviction of histones, the substitution with histone variants or, more seldom, events like histone cleavage (Suganuma and Workman 2008).

### **1.3.1 Histone acetyltransferases**

Histones can be modified by a variety of enzymes that introduce specific posttranslational modifications and have an impact on the conformation of the chromatin structure or subsequent binding of regulatory factors. The probably best-characterized modification is histone acetylation that is known since the 1970s and is carried out by histone acetyltransferases (HATs). In the enzymatic process of acetylation, an acetyl group from acetyl-coenzyme A is transferred to the  $\epsilon$ -amino residue of a lysine side chain of a histone,

which leads to the neutralization of the positive charged lysine (Sternier and Berger 2000). Based on sequence homologies, there are three distinct groups of HATs: 1) the acetyltransferases related to Gcn5, the GNAT family, 2) the family of MYST HATs, including MOZ, Sas3, Sas2, Tip60, Esa1, human and Drosophila MOF and 3) the remaining group with p300/CBP, Hat1, TAF<sub>II</sub>250 and others (Fukuda et al. 2006).

The GNAT family of HATs mainly functions in the regulation of cell growth and development by their influence on transcription and DNA repair (Carrozza et al. 2003). Many of these enzymes belong to one or more multisubunit HAT complexes. Gcn5 for example is a transcriptional adaptor protein being part of the SAGA complex that is recruited to activators upon transcription and acetylates H3 at promoter-proximal nucleosomes at K9, 14, 18, 23 (Carrozza et al. 2003). The physiological function of the ADA complex, which also includes Gcn5, is less clear, although it is also related to histone acetylation (Sternier and Berger 2000).

MYST HAT family members display a variety of functions, such as transcriptional activation (Esa1), participation in transcriptional gene silencing (Sas2, Sas3), dosage compensation (dMOF) and many more (Sternier and Berger 2000; Carrozza et al. 2003). The MYST HAT family member Sas2 will be introduced in more detail below. Esa1 targets histone H4 at K5, 8, 12 and 16 as well as K14 of H2A.Z and is the only HAT in *S. cerevisiae* that is essential. It is part of two distinct complexes, the larger complex NuA4 that is recruited to promoters, and a smaller one, piccolo NuA4, which functions in a global manner (Millar and Grunstein 2006). However, as suggested by the genome-wide localization analysis of Gcn5 and Esa1, these HATs are associated globally with protein-coding genes in correlation with transcription besides their specific targeting to promoters (Robert et al. 2004).

The acetylation of histones is a reversible process mediated by a class of enzymes referred to as histone deacetylases. Therefore, the addition and removal of acetylation marks is a highly dynamic process.

### 1.3.2 Histone deacetylases

Lysine acetylation is removed by specific enzymes, the histone deacetylases (HDACs) that thereby influence gene activity and other DNA-related processes. HDACs are classified into four groups. The yeast Rpd3 belongs to the Class I HDACs and deacetylates lysines residues of all four core histones. The enzymes of Class I, as well as Class II HDACs can be inhibited by Trichostatin A (TSA). The HDACs of Class II are similar to yeast Hda1

that deacetylates H3 and H2B (Fukuda et al. 2006). A third class of HDACs depends on NAD<sup>+</sup> for the deacetylation reaction and are referred to as the Sirtuins, including their prominent member Sir2. Class IV includes a single enzyme, HDAC11, which does not show sequence similarities with enzymes of the other groups (Fukuda et al. 2006). Rpd3 and Hda1 in yeast are general deacetylases that act on promoters, genome-wide, whereas Hos1, Hos2 and Hos3 deacetylate the rDNA locus and thereby affect ribosomal protein encoding genes (Ekwall 2005).

The HDAC Sir2, which targets H4 K16Ac, interacts with Sir3 and Sir4 to form the SIR complex and thereby forms heterochromatin in *S. cerevisiae* (Imai et al. 2000). A deletion of *SIR2* causes hyperacetylation of H4 K16 at telomere-proximal regions and the *HM* and rDNA loci, which are regions that are known to bind Sir2 (Robyr et al. 2002).

### 1.3.3 The histone acetyltransferase complex SAS-I in *Saccharomyces cerevisiae*

The histone acetyltransferase (HAT) Sas2 belongs to the MYST family of HATs. This family is a group of evolutionarily related HATs that share sequence similarities: it was named after its founding members: **MOZ**, **Ybf2/ Sas3**, **Sas2** and **Tip60**. MYST HATs that were identified later include Esa1, *Drosophila* MOF and human MOF (Sternier and Berger 2000). The *SAS2* gene was identified in a screen for defects in silencing in a *sir1Δ* background (Reifsnyder et al. 1996) and additionally in a screen for suppressors of silencing and therefore named “something about silencing” (Ehrenhofer-Murray et al. 1997). In the latter study, *SAS2* was linked to transcriptional silencing, because *sas2Δ* represses silencing defects at the *HMR* locus (Ehrenhofer-Murray et al. 1997). Intriguingly, Sas2 has opposite effects on silencing at *HML* and telomeres compared to the effects at *HMR*. Specifically, a deletion of *SAS2* causes a further derepression of *HML* in a *sir1Δ* strain and leads to a loss of silencing at telomeres, whereas *sas2Δ* represses the silencing defects of a defective *HMR* allele (*HMRa-e\*\**) (Reifsnyder et al. 1996; Ehrenhofer-Murray et al. 1997).

Sas2 in the cell exists in a nuclear complex, the SAS-I complex, together with two additional subunits, Sas4 and Sas5, being essential for the HAT activity of SAS-I and displaying similar effects on silencing (Xu et al. 1999; Meijsing and Ehrenhofer-Murray 2001; Sutton et al. 2003). In the complex of SAS-I, Sas4 forms the central subunit that connects Sas2 and Sas5 (Schaper et al. 2005). The main acetylation target of the HAT Sas2 is H4 K16 and, to a much lesser extent, acetylation at H3 K14 (Sutton et al. 2003). The H4 K16 acetylation (H4 K16Ac) by Sas2 in *S. cerevisiae* plays an important role in the

maintenance of euchromatic identity by opposing the spreading of SIR-mediated heterochromatin at telomeres, which is referred to as boundary function. In the absence of Sas2, SIR is allowed to spread farther away from the telomeres into centromer-proximal, euchromatic regions, leading to the formation of heterochromatin and repression of genes located in these regions (Fig. 1) (Kimura et al. 2002; Suka et al. 2002). The establishment of a boundary against heterochromatin furthermore involves other factors, for instance the histone variant H2A.Z that requires H4 K16Ac for its incorporation next to telomeres (Shia et al. 2006). Another factor important for boundary formation is the HDAC Rpd3L of which a deletion in a *sas2Δ* background has been shown to be lethal (Ehrentraut et al. 2010). A deletion of *SAS2* is not lethal, but severely affects transcriptional silencing (see above) and reduces the overall levels of H4 K16Ac (Kimura et al. 2002; Shia et al. 2006). Furthermore, due to its effect at subtelomeric genes, the expression of telomere-proximal genes is affected in the absence of Sas2 (Kimura et al. 2002; Shia et al. 2006).

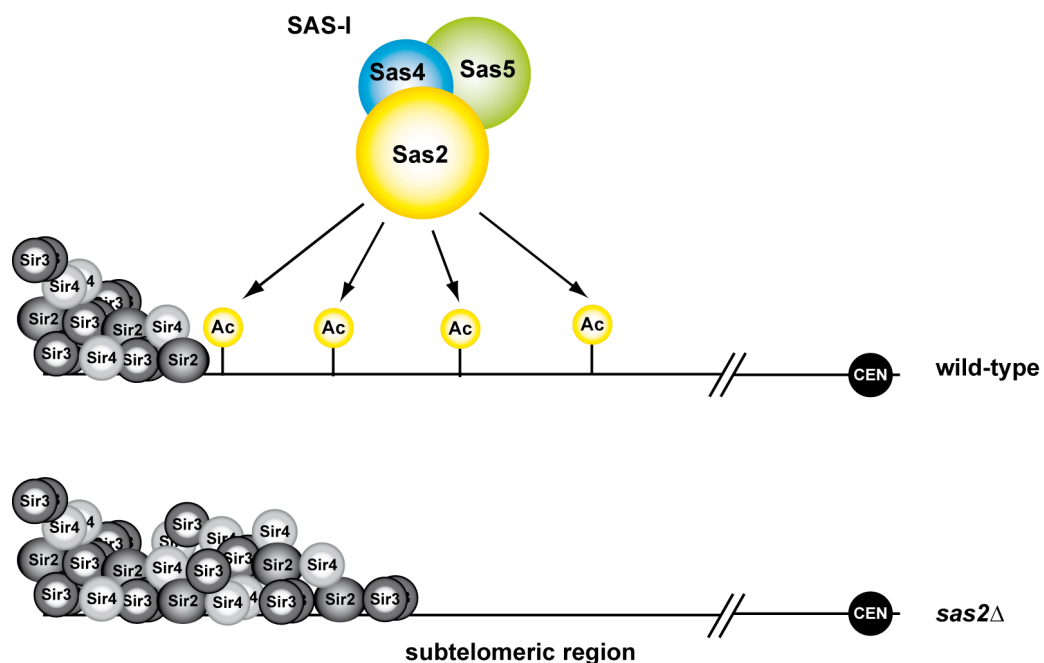


**Figure 1. Acetylation of H4 K16 by the SAS-I complex prevents spreading of SIR-mediated heterochromatin into centromer-proximal regions.**

In the wild-type (upper panel) SAS-I, with its catalytic subunit Sas2, acetylates H4 K16 at the subtelomeric region. In the absence of Sas2 (*sas2Δ*, lower panel) heterochromatin that is mediated by the SIR complex (Sir2, Sir3, Sir4) propagates into euchromatic centromer-proximal regions. (Kimura et al. 2002; Shia et al. 2006)

Besides its function in the maintenance of euchromatic identity, Sas2 may be furthermore important for the reestablishment of euchromatic patterns after DNA replication. This hypothesis is suggested by the interaction of Sas2 identified with the chromatin assembly factors CAF-I and Asf1 (Meijsing and Ehrenhofer-Murray 2001; Osada et al. 2001). One possible scenario is that the SAS-I complex is recruited to freshly replicated DNA via its

interaction with CAF-I and Asf1, which themselves are able to interact with PCNA at the replication fork, and subsequently introduces H4 K16 acetylation (Meijsing and Ehrenhofer-Murray 2001).

Recently, Sas2 was related to ageing through its deletion delaying senescence driven by the shortening of telomeres (Kozak et al. 2010). Furthermore, H4 K16Ac undergoes changes during the lifespan of a yeast cell. H4 K16Ac levels are increased in replicatively old cells in combination with a loss of Sir2 abundance at the telomeres. Since a deletion of SAS2 in old cells stabilizes SIR and thereby extends lifespan, this finding was suggestive of a role of H4 K16Ac in the regulation of cellular lifespan.

### 1.3.4 Further roles of H4 K16 acetylation in the control of gene expression

The roles of H4 K16Ac mediated by Sas2 in *S. cerevisiae* were introduced above. This section briefly introduces the functions of H4 K16Ac in species other than *S. cerevisiae*.

In *Drosophila*, MOF acetylates H4 K16 that is enriched on the male X chromosome and is a key component of the MSL dosage compensation complex (Rea et al. 2007). This enrichment of MOF leads to an increase of X-linked gene expression in male flies by two-fold (Kind et al. 2008). Besides its role as a transcriptional regulator in dosage compensation, MOF may also act as a general transcriptional regulator since it is also associated with autosomes (Kind et al. 2008). H4 K16Ac in *Drosophila* is furthermore influenced by different kinds of H3 K36Me3. The knock-down of H3 K36 di- and trimethylation by dMes-4 leads to a severe reduction of H4 K16Ac. By contrast, the reduction of H3 K36Me3 mediated by dHypb causes elevated levels of H4 K16Ac (Bell et al. 2007).

Like *Drosophila* MOF, human MOF also displays enzymatic activity for H4 K16Ac. Knock-down of hMOF causes a pronounced reduction or a complete loss of H4 K16Ac, and therefore hMOF is responsible for most of H4 K16Ac in human cells (Rea et al. 2007). Cells depleted of hMOF arrest in G2/ M, suggesting a possible role for MOF in the G2/ M cell-cycle checkpoint in mammals (Taipale et al. 2005). Interestingly, a loss of H4 K16Ac seems to be one characteristic of cancer cells (Fraga et al. 2005). Therefore, the research for treatments as HDAC inhibitors is of special interest with respect to clinical aspects.

H4 K16Ac is furthermore involved in transcription elongation at the *FOSL1* gene in human cells. A crosstalk between H3 S10P and H4 K16Ac is triggered by H3 S10P, which leads to the recruitment of hMOF and H4 K16Ac. Together, the two modifications provide a

binding platform for BRD4, which recruits the positive transcription elongation factor P-TEFb (Zippo et al. 2009).

#### **1.4 Transcriptional silencing and heterochromatin in *Saccharomyces cerevisiae***

Heterochromatin in *S. cerevisiae* is found at three distinct regions, the telomeres, the silent mating-type loci *HMR* and *HML* and the rDNA locus. Whereas silent chromatin in higher eukaryotes is mediated by H3 K9Me that is recognized by HP1 and can furthermore involve the RNAi machinery, silencing in *S. cerevisiae* is mediated by the Sir proteins Sir2, Sir3 and Sir4 (Perrod and Gasser 2003; Rusche et al. 2003). Heterochromatin is assembled in a step-wise manner, upon which the Sir2/ 4 subcomplex first binds to regulatory sites, the silencers. Subsequently, Sir2 deacetylates H4 K16 of neighboring nucleosomes and thereby provides binding sites for Sir3 and Sir4 that further recruit additional Sir2 protein, such that the Sir2/ 3/ 4 holocomplex spreads along deacetylated chromatin (Rusche and Lynch 2009).

The actively transcribed *MAT* allele determines the mating type in haploid *S. cerevisiae* cells that can be *MAT a* or *MAT  $\alpha$* . Additionally, the cell contains two more loci, *HML* and *HMR*, containing cryptic copies of  $\alpha$  and *a* information, respectively (Rusche et al. 2003). Epigenetic silencing at these regions is necessary to maintain the mating ability of yeast cells. A derepression of the *HM* loci causes expression of both *a* and  $\alpha$  genes, rendering cells unable to mate, since the cell then has the cell-type characteristics of a nonmating diploid cell (Perrod and Gasser 2003). The *HM* loci are flanked by the silencers *E* and *I*, to which the Sir proteins bind to mediate silencing (Rusche et al. 2003).

Telomeres represent the ends of chromosomes and serve to stabilize and protect the DNA ends. They consist of irregular TG-rich repeats of approximately 300 bp length that are situated terminal to the subtelomeric regions. The latter, contain Y' elements, short TG repeats and a core X element (Perrod and Gasser). The subtelomeric repeats contain nucleosomes, whereas the regions of TG-rich repeats lack nucleosomes (Wright et al. 1992). The TG repeats include a Rap1 binding site, which is bound by Rap1 that subsequently recruits Sir4 followed by Sir2 and Sir3, thus enabling the spreading of SIR and heterochromatin (Perrod and Gasser 2003). The silencing at the telomeres by SIR is terminated in a competition zone that creates an equilibrium between silenced and active chromatin (Rusche and Lynch 2009). The SIR complex is thereby antagonized by Sas2-mediated H4 K16Ac (Kimura et al. 2002; Suka et al. 2002). This mechanism can be

explained by the creation of a binding site for Sir3 by the unacetylated H4 K16 at telomeric heterochromatin, therefore the acetylation of H4 K16 prevents binding of Sir3 (Carmen et al. 2002).

The rDNA locus of *S. cerevisiae* consists of tandem array repeats. Although half of these genes are expressed, this locus is also subject to transcriptional silencing in order to protect the region from recombination. Silencing of the rDNA locus requires *SIR2*, but none of the other *SIR* genes (Rusche et al. 2003). Less silencing at these repeats is related to shortened life span caused by increased recombination and excision of the rDNA repeats (Perrod and Gasser 2003).

## **1.5 Chromatin and transcription**

During eukaryotic transcription, the protein-coding genes are transcribed into RNA by RNA polymerase (PolII). The transcription cycle proceeds in a stepwise manner. It starts with the binding of sequence-specific activators proteins upstream of the promoter, which leads to the recruitment of acetyltransferase-coactivator or mediator complexes that facilitate binding of general transcription factors (Li et al. 2007a). The preinitiation complex (PIC) is formed, and PolII enters the complex at the promoter. Upon unwinding of the DNA, an open PIC is formed, and the promoter is subsequently cleared of PolII, which produces RNA by transcribing the first bases of DNA. PolII pausing is then mediated by negative elongation factor (NELF), amongst others, and the carboxy-terminal domain (CTD) is phosphorylated at serine 5 (S5) by the Ctk kinase. In higher eukaryotes, it is P-TEFb that subsequently phosphorylates serine 2 (S2) of the PolII CTD domain, upon which PolII escapes from pausing and enters the productive elongation cycle. Finally, transcription is terminated by the dissociation of PolII from the DNA and release of the RNA (Fuda et al. 2009).

Since the DNA is packaged into chromatin, the nucleosomes present a barrier that both has to be overcome by PolII and influences all stages of transcription. At silent genes that are in an inducible, poised state, there is a nucleosome-free region around the promoter flanked with H2A.Z containing nucleosomes (Workman 2006). Upon activation of the gene, factors that are involved in nucleosome displacement and chromatin remodeling are recruited in order to facilitate the binding of the transcription machinery and subsequent transcription through the chromatin. The histone chaperone FACT facilitates the eviction of H2A/ H2B dimers, whereas Asf1 disassembles H3/ H4 tetramers (Adkins et al. 2007; Kulaeva et al. 2007). Thereby, nucleosomes are disassembled not only at the promoters,

but also within the coding region (Lee et al. 2004). Specific modifications of histones facilitate their displacement, for example the SAGA complex facilitates the displacement of H2A.Z by acetylating histones around the promoter, and additional histones are removed by the remodeler SWI/SNF. Many histone modifications have been related to active transcription. One marker for actively transcribed genes is H3 K4Me3 by Set1 (Santos-Rosa et al. 2002), which is associated with the S5-phosphorylated PolII (Ng et al. 2003). H3 K4Me3 is located primarily at the 5' end of ORFs. This region contains furthermore other typical modifications, e.g. H3 K9Ac, H3 K14Ac, H4 K5Ac, and H4 K12Ac that flank the 5' NFR and are correlated with gene expression (Kurdistani et al. 2004; Liu et al. 2005; Pokholok et al. 2005).

After the progression of PolII through a coding region, it is important to ensure the restoration of the chromatin structure in order to maintain genome integrity. This requirement involves several processes. An important mark for this purpose is H3 K36Me3 that is mediated by Set2. This histone methyltransferase recognizes the elongating PolII, which is phosphorylated at S2 of its CTD domain (Krogan et al. 2003; Li et al. 2003). H3 K36Me3 levels are high at the 3' end of ORFs and are correlated with transcription frequency (Pokholok et al. 2005). H3 K36Me3 is then recognized by the chromodomain-containing subunit of the HDAC Rpd3S, which is Eaf3. Thereby, H3 K36Me3 recruits Rpd3S that catalyzes the histone deacetylation in the coding region in association with transcription elongation (Carrozza et al. 2005; Joshi and Struhl 2005; Keogh et al. 2005). Spt6 and Spt16 are other elongation factors associated with the elongating PolII, and play an important role for the redeposition of histones during elongation (Kaplan et al. 2003; Schwabish and Struhl 2004). Furthermore, the histone chaperone and chromatin assembly factor Asf1 functions in the dis- and reassembly of histones during elongation and prevents intragenic transcription (Schwabish and Struhl 2006). These events lead to the restoration of a chromatin structure repressive for PIC formation and transcription, making these pathways crucial to prevent aberrant transcription initiation at cryptic promoters from within a coding region.

## **1.6 Pervasive transcription in the yeast genome**

Several recent studies indicate that transcription in eukaryotes is more complex than previously thought. PolII is not only located at coding regions, but also at low levels at intergenic regions in *S. cerevisiae* (Steinmetz et al. 2006). In line with these findings, transcription not only emanates from protein-coding genes or specific non-coding RNAs,

but can arise from intragenic and intergenic regions, as well as at known ORFs or in the opposite orientation (see Fig. 2). Recent high-resolution transcript maps in *S. cerevisiae* show the pervasive occurrence of cryptic unstable transcripts (CUTs) and stable unannotated transcripts (SUTs) (Neil et al. 2009; Xu et al. 2009). The CUTs are about 200 – 800 nt long, transcribed by PolIII and furthermore capped and polyadenylated. Their appearance depends on the exosome, for instance its catalytic subunit Rrp6 a 3'-5' exonuclease (Xu et al. 2009). The SUTs present a new class of transcripts without any previous annotation: they present 12 % of all yeast transcripts (Xu et al. 2009). These types of transcription do not occur randomly, but in defined transcription units, and the transcription start sites correlate with 5' nucleosome-depleted NFR of a neighboring transcription unit. They arise from single bidirectional promoters (Neil et al. 2009; Xu et al. 2009), which engage different preinitiation complexes and compete for the same transcription factors (Neil et al. 2009). Furthermore at 5' regions, the histone variant H2A.Z suppresses antisense transcription in cooperation with components of the RNAi machinery in *S. pombe* (Zofall et al. 2009). Antisense transcription at 3' regions is prevented by the chromatin remodeler Isw2 preventing shifting of nucleosomes from the 3' intergenic regions (Whitehouse et al. 2007). The transcription elongation factors Spt6 and Spt16 and the H3 K36 methyltransferase Set2 prevent transcription initiation from cryptic initiation sites within a coding region by distinct mechanisms. Spt6 and Spt16 replace removed nucleosomes and thereby restore the chromatin structure after the passage of PolIII (Kaplan et al. 2003; Berretta and Morillon 2009; Jamai et al. 2009). Set2 is associated with the elongating PolIII and methylates H3 K36. The Rpd3S complex subsequently recognizes H3 K36Me3 and deacetylates histones within the coding region that is being transcribed. The acetylation signals that are associated with the elongating PolIII are thus removed, and the repressive chromatin along an ORF is restored, which prevents aberrant transcription initiation (Carrozza et al. 2005; Keogh et al. 2005).

Non-coding transcripts can furthermore derive from retrotransposons. Ty1 generates an antisense RNA that plays a role in the regulation of this Ty element. This antisense transcript depends on the cytoplasmic 5'-3' exonuclease Xrn1 (Berretta et al. 2008). Moreover, heterochromatic regions, e.g. telomeres, have been shown to give rise to non-coding transcripts, which was shown for humans, mouse, zebrafish and yeast (Luke et al. 2008; Berretta and Morillon 2009).

The function's character of all these transcripts is still subject of intense discussions. In plants and *Drosophila*, sense-antisense pairs and antisense transcripts can become substrates for the ribonuclease II-like enzyme dicer, which subsequently produces siRNAs

and miRNAs that are involved in RNA-based silencing pathways (Beiter et al. 2009). However, such pathways do not exist in *S. cerevisiae*, although recent studies show that functional RNAi systems can be introduced from other organisms into yeast (Suk et al. 2011; Drinnenberg et al. 2009).

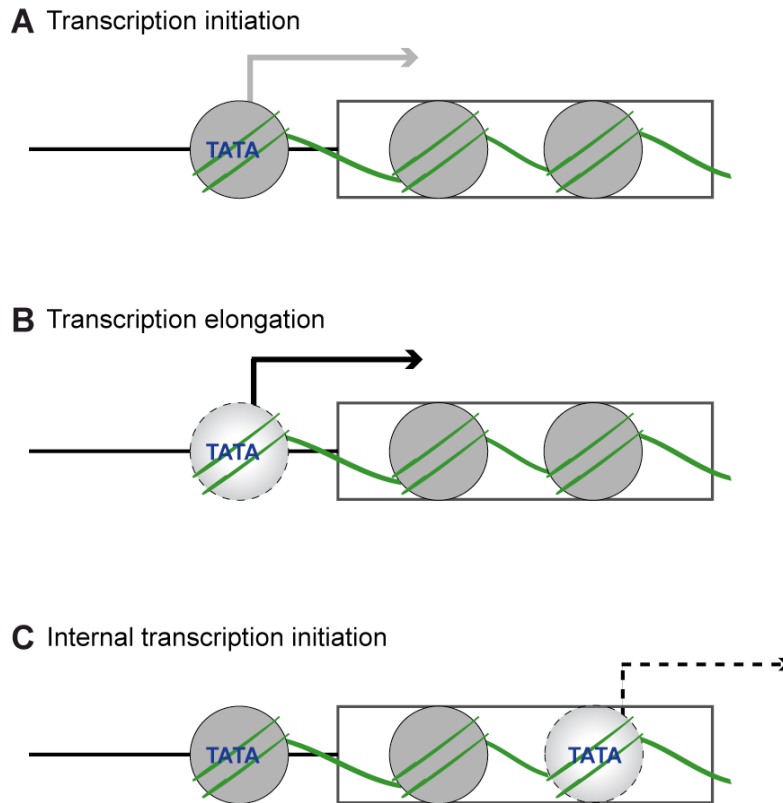


**Figure 2. Model for transcription and pervasive transcription.**

(A) Before activation of transcription genes are in a poised state. Transcription is initiated at the promoter, here symbolized by the TATA box. (B) After the eviction of nucleosomes (nucleosome with a dashed line) the elongation phase begins during which PolII proceeds through the coding region (PolII is not shown). (C) If the chromatin structure is not restored properly after the progression of PolII transcription initiation from within the coding region, starting at cryptic promoters (cryptic TATA box) can take place.

It has been suggested that pervasive transcription may be a side effect of normal transcription, and that nucleosome depletion leads to more “accidental” transcription. Alternatively, pervasive transcription of CUTs, for example, may be a test trial for normal transcription, because the transcripts are usually rapidly degraded since depending on the exosome (Berretta and Morillon 2009). However, there are also stable transcripts, the SUTs, that are conserved between yeast strains, and some transcripts only occur under specific growth conditions. These facts suggest a biological function and significance of the transcripts, maybe an adaptation to nutritional changes in the environment (Xu et al. 2009). CUTs can also fulfill regulatory tasks, like e.g. the CUT derived from Ty1 (Berretta et al. 2008) or the non-coding RNA, *SRG1* that controls repression of the *SER3* gene (Martens et al. 2004). The reason why some transcripts occur to be stable and others

unstable remains to be determined. Intriguingly, some transcripts are translated into proteins that are not normally produced (Cheung et al. 2008).

## **1.7 Chromatin dynamics**

Chromatin is not present in a fixed state, but undergoes changes during diverse cellular processes, such as DNA replication, DNA repair and transcription. During these phases, its structure and the position of nucleosomes are subject to dynamic changes to support these processes and to allow access to the DNA. The nucleosomes throughout the genome are well positioned (Liu et al. 2005; Yuan et al. 2005; Lee et al. 2007). The yeast ORFs are characterized by a decreased nucleosome density 5' to the transcription start site, the nucleosome-free region (NFR) that is flanked by two well-positioned nucleosomes (Workman 2006; Rando and Chang 2009).

The structure of chromatin can be altered by the introduction or removal of histone modifications, or by the incorporation of histone variants. Furthermore, the nucleosomes can be moved by ATP-dependent chromatin remodeling complexes, which slide the histones along the DNA fiber and therefore lead to histone destabilization and restructuring of chromatin (Clapier and Cairns 2009). Besides the replacement of histones (and their modifications) during replication, histones are furthermore exchanged and removed outside of DNA replication. Histones are evicted at promoters during gene activation and are reassembled upon gene repression. In *S. cerevisiae*, the nucleosome exchange at promoters occurs rapidly, whereas the exchange over ORFs is much slower (Rando and Chang 2009).

Histone H3 in yeast is exchanged in the body of highly transcribed genes, upon the travelling of PolIII through the gene. The rate of exchange differs between SAGA-regulated and TFIID-regulated genes, the latter being exchanged more slowly (Huisinga and Pugh 2004; Dion et al. 2007). However, not all histone-turnover is due to the passage of PolIII. Most notably, the exchange of nucleosomes at promoters is poorly correlated with occupancy of PolIII and strength of transcription (Dion et al. 2007). In summary, exchange of histones independently of replication provides a mechanism for gene regulation in that access is provided to the DNA for DNA-binding factors (Williams and Tyler 2007). High rates of histone exchange have an impact on the occurrence of histone modifications. For instance, H4 K16Ac is anticorrelated with gene expression (Kurdistani et al. 2004; Liu et al. 2005) and is high in regions with low histone turnover (Liu et al. 2005; Dion et al. 2007), suggesting that nucleosomes carrying this modification are replaced by unmodified

histones during transcription. Interestingly, the acetylation of H3 K56 is linked to several exchange-related processes. H3 K56Ac is correlated with replication-independent H3 exchange (Rufiange et al. 2007), occurs related to S-phase (Masumoto et al. 2005) and is furthermore involved in DNA repair and genome stability (Driscoll et al. 2007; Chen et al. 2008). The assembly and disassembly of histones is guided by factors referred to as histone chaperones or chromatin assembly factors.

### 1.7.1 Replication-coupled chromatin assembly by CAF-I and Asf1

Proliferating yeast cells generate genetically identical daughter cells. In order to pass on the genetic information to their progeny, a careful duplication of the DNA as well as the chromatin during the process of DNA replication is necessary. Chromatin represents the template for the replication machinery, but at the same time restricts access for the DNA. For that reason, the chromatin structure is opened by chromatin remodeling machineries prior to the initiation of replication at the origins of replication (Ehrenhofer-Murray 2004). Thus, in the process of replication, the chromatin structure is affected: firstly by the disassembly of parental nucleosomes ahead of the replication fork that are subsequently transferred onto the nascent DNA. Secondly, the chromatin structure is impacted by the deposition of newly synthesized histones, a process referred to as *de novo* nucleosome assembly (Groth et al. 2007). The histones incorporated during replication are newly synthesized during S-Phase (Osley 1991; Scharf et al. 2009) and carry acetylation marks prior to their deposition (Sobel et al. 1995; Loyola et al. 2006). For the reestablishment of parental modification patterns, the histones are rapidly deacetylated after their assembly into chromatin (Annunziato and Seale 1983; Benson et al. 2006).

*De novo* deposition of histones coupled to DNA replication is tightly associated with the action of CAF-I (chromatin assembly factor-I), a chromatin assembly factor or histone chaperone that was identified by virtue of its ability to deposit the histones H3 and H4 onto replicated DNA *in vitro* (Fig. 3) (Verreault et al. 1996). The replication-coupled action of CAF-I is mediated by its interaction with PCNA (proliferating nuclear cell antigen) (Shibahara and Stillman 1999). In *S. cerevisiae*, the CAF-I complex consists of the three subunits Cac1, Cac2 and Cac3. The *CAC* genes are not essential for the viability of yeast and show similar phenotypes of increased sensitivity to UV irradiation and defects in telomeric and *HM* silencing (Kaufman 1996; Enomoto et al. 1997; Enomoto and Berman 1998). The silencing defect caused by the mutation of CAF-I is explained by reduced H3

levels upon *CAC1* deletion, leading to a reduced recruitment of SIR to heterochromatic loci (Tamburini et al. 2006).

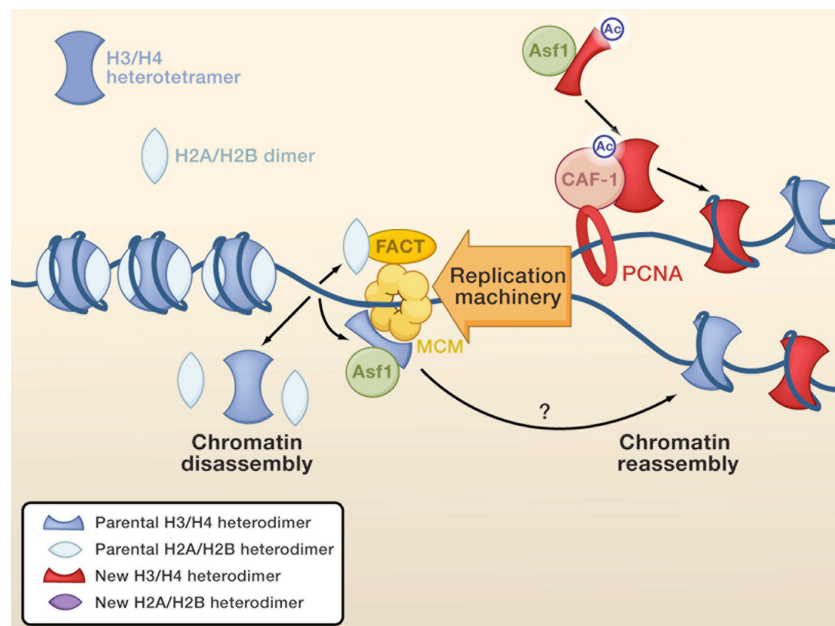


**Figure 3. Model for replication-coupled chromatin assembly and disassembly.**

FACT is involved in the disassembly of H2A/ H2B dimers. Asf1 removes parental H3/ H4 heterodimers. CAF-I and Asf1 cooperate to assemble histones onto the replicated DNA. (modified from Ransom et al. 2010)

Since the deletion of the CAF-I subunits is not lethal, it was assumed that another chromatin assembly factor participates in replication-coupled nucleosome assembly. This factor is Asf1, a homolog of *D. melanogaster* RCAF, cooperates with CAF-1 to assemble histones onto newly replicated DNA (Fig. 3) (Tyler et al. 1999). Asf1 (anti-silencing function 1) was originally discovered as a factor that caused derepression of silencing when overexpressed (Le et al. 1997). A deletion of *ASF1* alone is not lethal, but the proliferation of cells is slowed down (Le et al. 1997; Singer et al. 1998; Tyler et al. 1999). Cells with simultaneous deletions of *ASF1* and *CAC1* are defective in growth and grow more slowly than either single mutant. Furthermore, silencing in this strain is decreased at telomeres and the *HMR* locus (Tyler et al. 1999). Although CAF-I and Asf1 cooperate in the assembly of histones during S-phase, they show different silencing phenotypes and thus do not share overlapping functions in all areas (see also below). The influence of Asf1 on nucleosome density has led to contradictory results, in contrast to that reported for the deletion of *CAC1*, although the reported changes upon deletion of *ASF1* were less severe (Adkins and Tyler 2004; Prado et al. 2004). However, also in the absence of Cac1 and Asf1 there are still nucleosomes present within chromatin, indicating mechanisms for histone assembly and disassembly independent of these chromatin assembly factors.

In the course of replication, the parental patterns of modification have to be reestablished to ensure the reliable propagation of genetic information to the next generation. A hint to a respective mechanism was found by the discovery of an interaction of Sas2 with the largest subunit Cac1 of CAF-I and also with Asf1 (Meijsing and Ehrenhofer-Murray 2001). This result suggests that Sas2 acetylates H4 K16 coupled to replication, a question that has been addressed during the course of this study. Furthermore, two possibilities evolved for how the H4 K16Ac pattern can be reestablished: prior to assembly, or after the assembly of the histones onto the DNA. So far, freshly synthesized histones H4 were found to carry cytoplasmic acetylation marks at K5 and K12 (Sobel et al. 1995), and it therefore remains an open question how H4 K16Ac marks are reestablished and when.

### **1.7.2 Replication-independent assembly of histones by Asf1**

Asf1, the chromatin assembly factor introduced above, is highly conserved and assembles histones not only during DNA replication, but also during transcription and DNA repair. Asf1 is associated with the soluble histone pool and binds to a heterodimer of H3 and H4. It is therefore assumed that Asf1 buffers the possible toxic effects of free histones (Groth et al. 2005). The binding is mediated by the interaction of Asf1 with H3 as well as with the C-terminus of the H4 tail (English et al. 2006).

Asf1 mediates replication-independent histone deposition throughout the cell cycle (Robinson and Schultz 2003; Green et al. 2005) and is additionally involved in the disassembly of nucleosomes. Upon deletion of Asf1, chromatin becomes less susceptible to the digestion with nucleases, which indicates that Asf1 acts *in vivo* in the disassembly of nucleosomes and in genome-wide manner (Adkins and Tyler 2004). Furthermore, studies at the *PHO5* and *PHO8* promoters show that Asf1 is involved in the eviction of histones at these promoters upon gene activation (Adkins et al. 2004; Korber et al. 2006). However, Asf1 is also required for the incorporation of H3 at promoters during transcription. The processes upon transcriptional regulation at *PHO5* depend on the disassembly of histones by Asf1 to recruit the general transcription machinery (Adkins et al. 2007). In line with this involvement in transcription, Asf1 furthermore travels along actively transcribed genes with PolIII. Thereby, it assembles and disassembles histones H3 and H4 during elongation and is a critical factor to inhibit transcription initiation from cryptic intragenic promoters (Schwabish and Struhl 2006). Taken together, Asf1 is a major regulator of replication-independent histone exchange.

Apart from Asf1, many more histone chaperones are involved in replication-independent chromatin assembly, for example FACT that disassembles H2A/ H2B dimers during transcription (Fig. 3) (Belotserkovskaya et al. 2003). Furthermore, HIR has been shown to deposit histones that are reused into DNA, in contrast to Asf1 that mediates the deposition of new histones (Kim et al. 2007). Of note, the replication-associated CAF-I chromatin assembly factor may also be involved in transcription, since it is recruited to actively transcribed regions (Kim et al. 2009).

### **1.8 Retrotransposons in *Saccharomyces cerevisiae***

Transposable elements are retrovirus-like genetic elements, present in all eukaryotic genomes and can influence the genome organization of their hosts, e.g. by causing mutations and rearrangements of genomic regions (Kim et al. 1998). Transposons are generally categorized into retrotransposons and DNA transposons. Whereas DNA transposons are transposed by a “cut-and-paste” mechanism, retrotransposons (like retroviruses) replicate through reverse transcription of an RNA intermediate, and the resulting cDNA product integrates into new sites of the host genome (Kim et al. 1998; Malone and Hannon 2009). The class of retrotransposons furthermore classifies into elements flanked by long terminal repeats (LTR) and elements without LTRs. The LTR elements encode Gag and Pol proteins homologous to retroviral proteins and mediating the replicative transfer to sites in the host genome.

The proportion and nature of transposable elements varies in the different eukaryotic genomes. Within the mammalian genome, 50% of the genome consists of transposons, whereas *Drosophila* only contains 5% of many different element families. *S. cerevisiae* contains elements of the LTR retrotransposon family referred to as Ty elements that constitute 3.1% of the genome (Kim et al. 1998; Malone and Hannon 2009). These Ty elements, namely Ty1, Ty2, Ty4 and Ty5 belong to the Ty1-*copia* group, whereas Ty3 belongs to the Ty3-*gypsy* group of retrotransposons. Throughout the yeast genome, there are insertions of full-length retrotransposons with two flanking LTRs as well as fragments and solo LTRs. Ty1, Ty2, Ty3, and Ty4 elements preferentially integrate upstream of genes that are transcribed by RNA polymerase III (PolIII), e.g. tRNA genes. Interestingly, Ty1 integration is dependent on *CAC3*, a subunit of the chromatin assembly factor CAF-I, and on *HIR3*, a regulator of transcription of histone genes (Huang et al. 1999). The insertions of Ty5 elements are located within heterochromatic regions at telomeres and the silent mating-type loci (Kim et al. 1998). This targeting to silent regions is mediated by the

C-terminal targeting domain of the integrase of Ty5 that interacts with Sir4 (Zhu et al. 2003). In summary, the regions where Ty elements are integrated, namely the adjacent to tRNA genes, *HM* loci and telomeres are gene poor and thus devoid of coding information. This led to the suggestion that the targeting of retrotransposons to these regions is a mechanism to prevent mutations caused by transposition of Ty elements in the host genome. Furthermore, this mechanism allows retrotransposons to persist in their host genome (Boeke and Devine 1998).

Recent findings show that the control of Ty transposition can be carried out by non-coding RNAs. For example, the cryptic unstable antisense transcript RTL regulates the *TY1* retrotransposon (Berretta et al. 2008). Furthermore, antisense RNAs derived from Ty1 inhibit reverse transcription by limiting the levels of integrase and reverse transcriptase that are necessary for retrotransposition (Matsuda and Garfinkel 2009).

## **1.9 Outline of this thesis**

Sas2, a member of the MYST HAT family is part of the SAS-I complex that acetylates H4 K16 and was previously shown to be involved in *HM*, rDNA and telomeric silencing in *Saccharomyces cerevisiae*. In addition to these distinct local influences, it has been argued that Sas2 might also display a global function in mediating H4 K16 acetylation on a genome-wide level. One specific goal of this thesis was to examine the genome-wide influence of Sas2-mediated H4 K16Ac. To follow this approach, we performed chromatin immunoprecipitation combined with high resolution tiling arrays (ChIP-chip) and compared the genome-wide H4 K16Ac levels from wild-type and *sas2Δ* cells. Because Sas2 was shown to interact with the chromatin assembly factors CAF-I and Asf1 (Meijsing and Ehrenhofer-Murray 2001), we furthermore sought to test the model that Sas2 performed H4 K16 acetylation on histones brought to the DNA by these chromatin assembly factors. Concerning this matter, we hypothesized that H4 K16Ac might also be influenced by the loss of one or both of these chromatin assembly factors, the latter due to the fact that CAF-I and Asf1 were previously shown to exhibit overlapping functions.

In summary, the aim of this study was to provide a detailed map of the genome-wide influence of Sas2 and the chromatin assembly factors CAF-I and Asf1 on H4 K16 acetylation. Interestingly, we found that Sas2 displayed a global influence on H4 K16 acetylation, whereas the influence of CAF-I and Asf1 was only partially observed. Unexpectedly, the major influence of Sas2, besides the subtelomeric regions was discovered at ORFs. Upon deletion of *SAS2*, H4 K16Ac was decreased towards the 3' end

of ORFs. In contrast to intergenic regions, the ORFs are the region where the RNA Polymerase II (PolII) is in the elongation phase of transcription. For this reason, we further investigated the influence of Sas2 on transcription elongation. We made the surprising observation that *sas2Δ* displayed resistance to 6-AU, which implied that transcription was facilitated in the absence of SAS2. An explanation for this result might be an increased occupancy of PolII at 3' ends that was discovered by ChIP analysis. Additionally, in a genome-wide expression analysis, we observed that transcript levels were slightly elevated at the 3' end of ORFs in *sas2Δ* cells.

Furthermore, the deposition of H4 K16Ac was independent of histone exchange, since high levels of Sas2-mediated H4 K16Ac correlated with low levels of H3 K56Ac and thus low H3 exchange. Therefore, the question remained, when Sas2 performed acetylation of H4 K16. The previously observed interaction of Sas2 with the chromatin assembly factors CAF-I and Asf1 (Meijsing and Ehrenhofer-Murray 2001) suggested that Sas2 might act in a cell-cycle dependent fashion. Indeed, we found evidence that Sas2-mediated H4 K16 acetylation was incorporated in an S-Phase-coupled manner.

In summary, this study provides novel insights into the global function of the MYST HAT Sas2. Sas2 not only displays a role in silencing, but also influences ORFs and exerts an inhibitory effect on transcription elongation by PolII. Our results furthermore suggest that Sas2 acetylated H4 K16 dependent on DNA replication.

In the following, the contribution of other scientists to this study will be listed alphabetically: Dr. Ho-Ryun Chung from the Max-Planck-Institut für molekulare Genetik, Department of Computational Molecular Biology, Berlin performed the data analysis of the ChIP-chip and expression data; Sandra Clauder-Münster from the group of Dr. Lars Steinmetz from the European Molecular Biology Laboratory, Heidelberg performed the processing and hybridization of RNA to the expression arrays; Dr. Ludger Klein-Hitpass from the Institut für Zellbiologie, Universitätsklinikum Essen performed the hybridization of the ChIP DNA onto the tiling arrays; Dr. Zhenyu Xu from the group of Dr. Lars Steinmetz from the European Molecular Biology Laboratory, Heidelberg performed data analysis of the RNA expression array.

## 2. Material and Methods

### 2.1 *Escherichia coli* strains

DH5 $\alpha$	F <sup>-</sup> $\phi$ 80d <i>lacZ</i> $\Delta$ M15 $\Delta$ ( <i>lacZYA-argF</i> )U169 <i>recA1 endA1 hsdR17</i> ( <i>r<sub>k</sub><sup>-</sup>, m<sub>k</sub><sup>+</sup></i> ) <i>phoA supE44 thi-1 gyrA96 relA1</i> $\lambda$ <sup>-</sup> (Invitrogen)
DH5 $\alpha$	F <sup>-</sup> <i>endA1 hsdR17</i> ( <i>r<sub>k</sub><sup>-</sup>, m<sub>k</sub><sup>+</sup></i> ) <i>supE44 thi-1</i> $\lambda$ <sup>-</sup> <i>recA1 gyrA96 relA1</i> $\Delta$ ( <i>lacZYA-argF</i> )U169 $\phi$ 80d <i>lacZ</i> $\Delta$ M15
GM272	<i>dam3 dam6</i> F <sup>-</sup> <i>r<sub>k</sub><sup>-</sup>, m<sub>k</sub><sup>+</sup> metB1 galK2 galT22 lacY tsx78 supE44 thi<sup>-</sup> tonA3 mt1-1</i>
BL21 (DE3)	F <sup>-</sup> <i>ompT hsdS</i> ( <i>r<sub>B</sub><sup>-</sup>m<sub>B</sub><sup>-</sup></i> ) <i>dcm<sup>+</sup> Tet<sup>r</sup> gal</i> $\lambda$ (DE3) <i>endA Hte</i> [ <i>argU ileY leuW Cam<sup>r</sup></i> ]

### 2.2 Media growth conditions

*E. coli* strains used for plasmid amplification were cultured according to standard procedures (Sambrook et al. 1989) at 37°C in Luria-Bertani (LB) medium supplemented with either 100  $\mu$ g/ml ampicillin or 50  $\mu$ g/ml kanamycin. For the growth of *Saccharomyces cerevisiae* media, were prepared as described previously (Sherman 1991). Unless indicated otherwise, yeast was grown on full medium (YPD: 10 g/l yeast extract, 20 g/l peptone, 2 g/l glucose). Full medium without a carbon source (YP: 10 g/l yeast extract, 20 g/l peptone) was supplemented with 2% galactose (YP-Gal). Yeast minimal (YM) medium (6,7 g/l yeast nitrogen base w/o amino acids) was supplemented with 2% glucose or 2% galactose and as required with 20  $\mu$ g/ml for adenine, uracil, tryptophan, methionine and histidine or 30  $\mu$ g/ml leucine and lysine. YM + 5-FOA (5-fluoroorotic acid; US Biological) medium contained 5-FOA at 1 mg/ml and 20  $\mu$ g/ml uracil. Growth assays with 6-azauracil (6-AU) were performed by supplementing YM with the indicated concentration of 6-AU (stock: 20 mg/ml in 1 M NaOH). Mating assays containing methionine for the repression of *MET3-SAS2* were performed with 400  $\mu$ M methionine final concentration. Strains were grown at 30 °C, unless indicated otherwise.

### 2.3 *Saccharomyces cerevisiae* strains

Yeast strains used in this study are given in Table 2. Yeast was grown and manipulated according to standard procedures (Sherman 1991). Marker selection was performed on selective minimal plates (YM), and plates containing 5-FOA were used to select against *URA3*.

**Table 2. Yeast strains used in this study**

Strain	Genotype	Source <sup>a</sup>
AEY1	<i>MAT<math>\alpha</math> ade2-101 his3-11,15 trp1-1 leu2-3,112 ura3-1 can1-100</i> (= W303-1B)	
AEY2	<i>MAT<math>\alpha</math> ade2-101 his3-11,15 trp1-1 leu2-3,112 ura3-1 can1-100</i> (= W303-1A)	
AEY264	<i>MAT<math>\alpha</math> his4</i>	

AEY265	<i>MAT<math>\alpha</math> his4</i>
AEY266	AEY2, <i>MATa sas2<math>\Delta</math>::TRP1</i>
AEY269	AEY1, <i>MAT<math>\alpha</math> sas2<math>\Delta</math>::TRP1</i>
AEY345	AEY2, <i>MATa sir1<math>\Delta</math>::LEU2</i>
AEY346	AEY2, <i>MATa sir1<math>\Delta</math>::LEU2 sas2<math>\Delta</math>::TRP1</i>
AEY403	AEY1, <i>HMRa-e**</i>
AEY474	AEY1, <i>HMRa-e** sas2<math>\Delta</math>::TRP1</i>
AEY1017	AEY1, <i>TEL-VII L::URA3</i>
AEY1190	AEY1017, <i>sas2<math>\Delta</math>::TRP1</i>
AEY 1647	AEY1, <i>MAT<math>\alpha</math> HMR-SS (GAL4-RAP-ABF) <math>\Delta</math>I sas2::TRP1 sir2<math>\Delta</math>::kanMX</i>
AEY1956	AEY1, <i>MAT<math>\alpha</math> HMRa-e** hht1-hhf1<math>\Delta</math>::LEU2 hht2-hhf2<math>\Delta</math>::HIS3</i> pRS414[HHT1 hhf1-21 (K16R)]
AEY1958	AEY1, <i>MAT<math>\alpha</math> HMRa-e** hht1-hhf1<math>\Delta</math>::LEU2 hht2-hhf2<math>\Delta</math>::HIS3 pOS 107</i> (TRP1 HHT1 HHF1)
AEY2426	AEY1, <i>asf1<math>\Delta</math>::kanMX</i>
AEY2450	AEY2426, <i>cac1<math>\Delta</math>::LEU2</i>
AEY2475	AEY1956, <i>MAT<math>\alpha</math> HMRa-e** hht1-hhf1<math>\Delta</math>::LEU2 hht2-hhf2<math>\Delta</math>::HIS3</i> <i>sas2<math>\Delta</math>::kanMX</i> pRS414[HHT1 hhf1-21 (K16R)]
AEY3462	AEY1, <i>cac1<math>\Delta</math>::LEU2</i>
AEY4148	AEY2, <i>natNT2-GALLpr-3HA-SAS2</i>
AEY4245	AEY403, <i>natNT2-GALLpr-3HA-SAS2</i>
AEY4247	AEY1017, <i>natNT2-GaLLpr-3HA-SAS2</i>
AEY4250	AEY403, <i>natNT2-GALSpr-3HA-SAS2</i>
AEY4251	AEY1017, <i>natNT2-GALSpr-3HA-SAS2</i>
AEY4253	<i>MAT<math>\alpha</math> ade2-101 his3-11,15 leu2-3,112 natNT2-GALLrp-3HA-SAS2</i> <i>TEL-VII L::URA3</i>
AEY4254	<i>MATa ade2-101 his3-11,15 leu2-3,112 sas2<math>\Delta</math>::TRP1 TEL-VII L::URA3</i>
AEY4322	<i>MATa ade2-101 his3-11,15 trp1-1 leu2-3,112 ura3-1 can1-100</i> T. Mizushima <i>ubr1<math>\Delta</math>::GAL-MYC-UBR1::HIS3</i>
AEY4324	AEY4254, pRS315-SAS2
AEY4330	AEY4254, pRS315
AEY4331	AEY4324, pRS315- <i>natNT2-GALLpr-3HA-SAS2</i>
AEY4392	AEY4322, <i>sir1<math>\Delta</math>::kanMX</i>
AEY4488	AEY4322, <i>sas2::Ub-Arg-DHFR<sup>ts</sup>-HA-SAS2-URA3</i> (= SAS2-td) (BclI linearisation of pAE1426)
AEY4490	AEY4392, <i>sas2::Ub-Arg-DHFR<sup>ts</sup>-HA-SAS2-URA3</i> (= SAS2-td) (BclI linearisation of pAE1426)
AEY4495	AEY1, pRS316
AEY4496	AEY269, pRS316
AEY4658	AEY1, <i>MAT<math>\alpha</math> ADE2 lys2<math>\Delta</math> sir3<math>\Delta</math>::HIS3 sas2<math>\Delta</math>::TRP1</i>
AEY4499	<i>MATa ura3<math>\Delta</math>0 his3<math>\Delta</math>I leu2<math>\Delta</math>0 met15<math>\Delta</math>0 TY1 his3AI[<math>\Delta</math>]-3114</i>

A. Morillon

AEY4500	AEY4499, <i>xrn1Δ::kanMX</i>	A. Morillon
AEY4529	AEY4499, <i>sas2Δ::TRP1</i>	
AEY4501	<i>MATa ade2-101 his3-11,15 trp1-1 leu2-3,112 ura3-1 can1-100 ML2::URA3</i>	A. Morillon
AEY4502	AEY4501, <i>xrn1Δ::ADE2</i>	A. Morillon
AEY4527	AEY4501, <i>sas2Δ::TRP1</i>	
AEY3058	<i>MATα HMRA-e** ade2 his3Δ1 leu2Δ0 ura3Δ0 isw1Δ::kanMX</i>	
AEY3718	<i>MATα sas2Δ::TRP1 set2Δ::kanMX ade2 leu3 his3 ura3</i>	
AEY4534	<i>MATa his3Δ1 leu2Δ0 met15Δ0 ura3Δ0 set2::kanMX pRS316</i>	
AEY4584	<i>MATα ade2-101 his3-11,15 leu2-3,112 ura3-1 dst1Δ::kanMX</i>	
AEY4588	<i>MATα ade2-101 sas2Δ::HIS3 his3 leu2Δ0,112 ura3-1 dst1Δ::kanMX</i>	
AEY4493	<i>MATa ura3-52::HHF1-pGAL1/10-Flag-HHT1-URA3 lys2-801 his3Δ200 leu2Δ1 hht1-hhf1::LEU2 hht2-hhf2::HIS3 trp1Δ63 bar1Δ::NATMX4 KANMX6-pGAL1::FMP27 /pNOY 439 [CEN6 ARS4-TRP1 HHF2 MYC-HHT2]</i>	A. Nourani
AEY4565	AEY4493, <i>sas2Δ::TRP1</i>	
AEY4630	<i>MATα his3Δ200 leu2Δ1 lys2-128Δ trp1Δ63 ura3-52 kanMX-GAL1pr-FLO8-HIS3 spt6-1004-FLAG</i>	F. Winston
AEY4631	<i>MATa arg4-12 his3Δ200 lys2-128Δ ura3-52 kanMX GAL1pr-FLO8-HIS3 spt16-197</i>	F. Winston
AEY4676	AEY 4630 <i>sas2Δ::URAMX</i>	
AEY4677	AEY 4631 <i>sas2Δ::URAMX</i>	

<sup>a</sup>Unless indicated otherwise, strains were constructed during the course of this study or were from the laboratory strain collection. Groups of strains between horizontal lines are isogenic.

## **2.4 Genetic manipulation of *Saccharomyces cerevisiae* strains**

Yeast strains used in this study are listed in Table 2. Unless indicated otherwise, yeast strains were either generated in this study by direct deletion, genomic integration, integration of plasmids, by crossing of yeast strains, or they originated from the laboratory strain collection.

### **2.4.1 Crossing, sporulation and dissection of asci**

Two haploid yeast strains of different mating types were crossed by mixing the strains on a YPD plate and subsequent incubation for eight hours at 30 °C. Diploids were isolated by subsequently streaking on a selective YM plate. Sporulation was induced by plating the diploids on sporulation medium (19 g/l KAc; 0.675 mM ZnAc; 20 g/l agar) and incubated for at least three days at 30 °C. For dissection of asci, cell walls were degraded with zymolyase (5 mg/ml zymolyase, 1 M Sorbitol, 0.1 M NaCitrate, 60 mM EDTA pH 8.0) for 6 min at room temperature and the reaction was stopped by adding 100 μl H<sub>2</sub>O. The dissection of the digested ascospores was carried out using a micromanipulator (Narishige) connected to a Zeiss Axioscope FS microscope. The plates with the dissected ascospores were incubated for two to three days at 30°C. To follow the segregation of markers, plates were replica plated on selective medium.

### 2.4.2 DNA techniques in *Saccharomyces cerevisiae*

Gene deletions with *kanMX* were performed as described (Wach et al. 1994). The PCR-mediated knockout technique was used for *HIS3* or *URAMX* knockouts, whereby the complete open reading frame was replaced by the *HIS3* or *URAMX* sequence. The deletion of *SAS2* by *TRP1* was performed as described (Ehrenhofer-Murray et al. 1997). Double mutant strains were generated by isogenic crosses, subsequent tetrad dissection and the analysis of marker segregation. N-terminal tagging of *SAS2* was performed using a *natNT2-GALLpr-3HA* or *natNT2-GALSpr-3HA* cassette (Janke et al. 2004) that was amplified by PCR. Oligonucleotides used for the amplification are given in Table 4. The amplified cassette was integrated into the yeast genome by homologous recombination, replacing the natural *SAS2* promoter. Correct integration in all cases was verified by PCR analysis.

## 2.5 Molecular cloning

Plasmid generation was performed according to standard cloning techniques (Sambrook et al. 1989). Plasmid isolation and gel elution kits were purchased from Qiagen and Macherey-Nagel. Restriction endonucleases and respective buffers were purchased from NEB, T4 DNA Ligase from Roche and pGEMT vector systems Kit from Promega. *MET3pr-6xMyc-SAS2* was constructed by liberating *6xMyc-SAS2* with *AfeI*/ *SpeI* from pAE782. This fragment was then ligated into pAE136 linearized with *EcoRV*/ *SpeI*. For the N-terminal tagging of *SAS2* on a plasmid, the *natNT2-GALLpr-3HA* cassette (Janke et al. 2004) was amplified by PCR and integrated by homologous recombination in a *sas2Δ* strain bearing a *SAS2* plasmid. For the fusion of a heat-inducible degron to *SAS2* (*SAS2-td*), a truncated *sas2* was generated and subsequently integrated into pAE928, a plasmid containing the heat-inducible degron. The truncated *sas2* was used to avoid the presence of a second functional form of *SAS2* after integration to yeast. Therefore, *SAS2* ORF was amplified from pAE410, simultaneously creating a truncated *sas2* (807 bp) with *HindIII* and *ClaI* restriction sites at the 5' and 3' region, respectively. The truncated *sas2* was ligated into pGEMT and subsequently transformed into GM272. GM272, a *dam<sup>-</sup>* *E. coli* strain was used here and furthermore for plasmid isolation of pAE928, in order to avoid the blocking of the *ClaI* recognition site by overlapping Dam methylation at this specific site. pAE928 and the truncated *sas2* pGEMT clone were digested with *ClaI* and *HindIII*. After gel elution, the *sas2* fragment and pAE928 were ligated and subsequently transformed into GM272 and subjected to sequencing for positive clones. pAE928-truncated-*sas2* was linearized at the unique restriction site of *BclI* within *sas2* and integrated into yeast by homologous recombination. Plasmids are listed in Table 3, oligonucleotides used for molecular cloning in Table 4.

**Table 3. Plasmids used in this study**

Plasmid	Description	Source <sup>a</sup>
pAE136	pRS313- <i>MET3pr</i>	C. Trueblood
pAE261	pRS315	
pAE262	pRS316	
pAE410	pRS315- <i>SAS2</i>	
pAE782	pRS416- <i>6xMyc-SAS2</i>	

pAE928	pRS306- <i>CUP1pr-Ub-Arg-DHFR<sup>ts</sup>-HA-CDC28-5'</i>	C. Liang
pAE1207	pRS313- <i>SAS2</i>	
pAE1261	pRS313- <i>MET3pr-6xMyc-SAS2</i>	
pAE1298	<i>natNT2-GaLLpr-3HA</i> (pYM-N28)	M. Knop
pAE1339	<i>natNT2-GaLSpr-3HA</i> (pYM-N32)	M. Knop
pAE1426	pRS306- <i>CUP1pr-Ub-Arg-DHFR<sup>ts</sup>-HA-sas2</i> (Contains a truncated <i>sas2</i> [807 bp]. Plasmid was linearized with BclI within <i>sas2</i> for integration into yeast. For details, see section 2.5 above.)	

<sup>a</sup> Unless indicated otherwise, plasmids were constructed during the course of this study or were from the laboratory strain collection.

## **2.6 Genetic assays in *Saccharomyces cerevisiae***

Telomeric silencing assays were performed using a telomeric *URA3* reporter (Gottschling et al. 1990). *HM* silencing was measured by determining the mating ability of a strain with a mating tester strain in a patch-mating assay. For this purpose, 2 OD of a tester strain AEY264 (*MATa his4*) or AEY265 (*MATα his4*) were plated on a YM plate. The master plate with the candidate strains was then replicated onto the tester strain plate and incubated for 2 days at 30 °C. For the test of the *SAS2-td* strain, the candidate strain patches (master plates) were previously grown on glucose at 30 °C (permissive conditions) or medium containing galactose at 37 °C (restrictive conditions). Growth assays with 6-azauracil (6-AU) were performed by supplementing minimal medium (YM) with the indicated concentration of 6-AU (stock: 20 mg/ ml in 1 M NaOH). Strains used in the 6-AU assay were previously transformed with an *URA3* containing plasmid (pRS316).

## **2.7 Antibodies**

Antibody	Company	Catalog and Lot #	Application	Application notes
<b>α-H4 K16Ac</b>	Upstate	#07-329; lot #32214	ChIP; ChIP-chip, Western Blot	4 μl IP; Protein G Agarose; 3% Blocking Agent; 0,05% Tween; o/n 4 °C
<b>α-H4 K16Ac</b>	Active Motif	am39167; #107	ChIP	4 μl IP; Protein G Agarose
<b>α-H4 K16Ac</b>	Millipore	NG1532401 05-1232	Western Blot	1:1000; 3% Blocking Agent; 0,05% Tween; 2h rt or o/n 4 °C
<b>α-H4</b>	Abcam	ab31827; lot #386566	ChIP; ChIP-chip	4 μl IP; Protein G Agarose
<b>α-H4</b>	Abcam	ab31827 lot #418330	ChIP; ChIP-chip; Western Blot	1:1000; 5% milk; 0,1% Tween; 1h rt

<b><math>\alpha</math>-H4</b>	Abcam	ab17036; lot #546284	ChIP-chip	3 $\mu$ l IP; Protein G Agarose
<b><math>\alpha</math>-H3 K36Me3</b>	Abcam	ab9050; lot #707981	ChIP	4 $\mu$ l IP; Protein G Agarose
<b><math>\alpha</math>-HA</b>	Covance	4921802 MMS-101P Purified Antibody	Western Blot	1:1000; 5% milk; 0,1% Tween; 1h rt; o/n 4 °C
<b><math>\alpha</math>-myc</b>	Sigma	M4439	Western Blot	1:5000; 3% milk; 0,1% Tween; o/n 4 °C
<b><math>\alpha</math>-PolIII (H-224)</b>	Santa Cruz	sc-9001	ChIP	4 $\mu$ l IP; Protein G Agarose
<b><math>\alpha</math>-S5-P (PolII H14)</b>	Covance	MMS-134R	ChIP	4 $\mu$ l IP; Protein G Agarose
<b><math>\alpha</math>-S2-P (PolII H5)</b>	Covance	MMS-129R	ChIP	4 $\mu$ l IP; Protein G Agarose
<b><math>\alpha</math>-TU27 (<math>\beta</math>-tubulin)</b>	Covance	MMS-410P	Western Blot	1:2000; 5% milk; 0,1% Tween; o/n 4 °C
<b><math>\alpha</math>-rabbit-HRP</b>	Sigma	A0545	Western Blot	1:5000; in solution according to primary antibody; 1h rt
<b><math>\alpha</math>-mouse-HRP</b>	Sigma	A9044	Western Blot	1:1000; in solution according to primary antibody; 1h rt

The specificity of all  $\alpha$ -H4 K16Ac antibodies was tested in ChIP and Western blot application in wild-type and *sas2 $\Delta$*  cells. For ChIP analysis, a typical region at chromosome VI-R was examined for the depletion of the H4 K16Ac signal upon *SAS2* deletion. The specificity of the  $\alpha$ -H3 K36Me3 antibody was tested in Western blot in wild-type and *set2 $\Delta$*  cells.

## **2.8 Chromatin immunoprecipitation**

ChIPs were carried out essentially as described (Weber et al. 2008), with the following modifications. For the subsequent use of antibodies specific for histone ( $\alpha$ -H4) or histone modifications ( $\alpha$ -H4 K16,  $\alpha$ -H3 K36Me3), cross-linking of 100 OD yeast cells was performed for 30 min at room temperature. For  $\alpha$ -PolIII,  $\alpha$ -S5-P,  $\alpha$ -S2-P antibodies, 100 OD cells were cross-linked for 20 min at room temperature, unless indicated otherwise. Samples were sonicated at 4 °C, seven cycles 30 s on and 60 s off. 4  $\mu$ l antibody was used per ChIP. RNase (10 mg/ ml) digestion was carried out 1hour 37 °C prior to incubation with proteinase K. DNA clean-up was performed with Qiaquick Gel Extraction Kit and ERC cDNA Binding Buffer (Qiagen). DNA precipitates for ChIP-chip analysis were eluted with distilled water from the Qiaquick binding columns. Quantitative real-time PCR for the analysis of ChIP samples was performed as described (Weber et al. 2008) except that SYBR Green Real MasterMix (5 PRIME) was used (see section 2.9). Oligonucleotides used for amplification are given in Table 4. Significance levels were calculated using

student's t-test. ChIP analysis of H4 K16Ac and H3 K36Me3 at *CSF1* and *PMA1* was performed by Dr. Jan Weber, University of Duisburg Essen, Department of Genetics, group of Prof. Ann Ehrenhofer-Murray.

For the analysis of PolIII association with *GALIpr::FMP27*, cells were grown to mid-exponential phase in galactose-containing medium. They were subsequently shifted to glucose medium, and samples (50 OD cells) were harvested immediately. Cells were cross-linked with 1% formaldehyde for 20 minutes. ChIP was performed as described above. Relative occupancy of PolIII was calculated by dividing the percent of enrichment of the target DNA sequence against PolIII enrichment at a steadily transcribed gene, *POL1* (for qPCR procedure, see also below). For determining the occupancy of PolIII at *PMA1*, cells were grown in full medium with glucose. Cells were harvested (100 OD cells) and cross-linked. ChIP was performed as described above.

## 2.9 Quantitative real-time PCR

Quantitative real-time PCR (qPCR) was performed in Rotor Gene 3000 (Corbett Research). The qPCR reactions were prepared with real master mix (5 PRIME) containing SYBR green according to the manufacturer's instructions. Cycling was carried out for 15 sec at 94 °C, 30 sec at 56 °C and 40 sec at 68 °C for 45 times with a 2 min 94 °C initial denaturation step, unless stated otherwise. Melt curve detection was performed after hold at 40 °C for 2 min and ramping from 50 °C to 95 °C every 5 sec. The  $C_i$  value for each reaction was determined, and a standard curve of input samples (or genomic DNA calibration curve for RT-qPCR) was used to calculate the amounts of DNA precipitated during the ChIP experiment relative to input DNA (genomic DNA). The amount of DNA precipitated with the  $\alpha$ -H4 K16Ac and  $\alpha$ -H3 K36Me3 antibody was calculated relative to the amount of histone H4 precipitated for the respective regions. For PolIII occupancy, precipitated DNA at one locus was normalized to precipitation at the *POL1* gene. Three technical replicates from three independent ChIPs were analyzed, unless indicated otherwise, and standard deviations were calculated. Oligonucleotide sequences used for amplification are provided in Table 4.

**Table 4. Oligonucleotides used in this study**

Oligonucleotide	Sequence (5' – 3' direction)
GALL_HA Ki Sas2 fwd (S1)	<u>GGAGGCTCCTATTTTCTAGTTGCTTTTTGTTTTCACTCGCAAAAAAATG</u> CGTACGCTGCAGGTCGAC
GALL_HA Ki Sas2 rev (S4)	<u>CCTTTTAGCTTCTGGGTAGTCGCTGTGAGTGATTGACTTAAAGATCTTGC</u> CATCGATGAATTCTCTGTCTG
HindIII_Sas2_fwd ClaI_Sas2_rev	GTGagcttCGATGGCAAGATCTTTAAGTCAATCACTCACAGCG GTGatgatCAGTCACCTTCAATAAGGTGCCAACAGAGTATCTG
Chr10 Ty1-1 (A) fwd Chr10 Ty1-1 (B) rev	CATCAGCTTTCGTTTTAACATGTTTGC CATACTAATATTACGATTATTCCTCATTCGG <sup>1</sup>
Chr10 Ty1-2 (E) fwd Chr10 Ty1-2 (F) rev	CGGTGTAAAGATGATGACATAAGTTATGAGAAGC <sup>1</sup> CTTCACTTCTGTTATCTTCTGTTAAAGTAAGGC
Chr XII Ty2-1(A) fwd Chr XII Ty2-1(B) rev	GCGTCAGAGCACATTAATTAGTGACATATACC CCTATTACATTATCAATCCTTGCCTTTCAGC <sup>1</sup>
Chr XII Ty2-1(E) fwd	GGAAGCTGAAACGCAAGGATTGATAATG <sup>1</sup>

Chr XII Ty2-1(F) rev	CTATCGGAGAAGTGAAGAGAATGT GG
Chr XII Ty2-1(C) fwd	CGCCTTACATCCGTCACGAAACTC <sup>1</sup>
Chr XII Ty2-1(D) rev	CCGATTGATAGTCATGATCAGATTCTG <sup>1</sup>
TelVIR 0,5 up (2)	CGAGTGGATGCACAGTTCAGAG
TelVIR 0,5 down	CGCGTTATGACAATTTTATGTAGATATCC
Tel VI R 1 (2) up	GTTATGTTAGAGATAACTGTGAG
Tel VI R 1 down	GCTTGTTAACTCTCCGACAG
Tel VI R 1.75 fwd	GCGCAATACCCTGTAGTAGTCG
Tel VI R 1.75 rev	CGGCATGTAGACTTTACATATCTCG
Tel VI R 2.5 rev	GCAATGAATCTTCGGTGCTTGG
Tel VI R 2.5 rev	CCATACCAATATCAACTTCACGG
Tel VI R 3.75 fwd	GCGCATATGGCTCTGAAATATCG
Tel VI R 3.75 rev	GGAGTAAATTCAAGTCCATGCGG
Tel VI R 5.0 fwd	CCCCGCCTTTGAAGATTGTCCC
Tel VI R 5.0 rev	CGAGACCCACTTGTATTCTTAGTGC
Tel VI R 7.5 fwd	CCTCTATAGGACCTGTCTCATGG
Tel VI R 7.5 rev	GGAAGTCTACACTAATAGCTATGCG
Tel VI R 15.0 up	GCGCAATATATAGCAGAAGAGC
Tel VI R 15.0 dwn	CAATTCGTCGATAAAGTGC
CSF1 (0) fwd	CTTCTATTGACGGTAATAAGTTAGCAAGC
CSF1 (0) rev	GATTTTCGCTCGTTTCCATAGTAGCC
CSF1 (4,4) fwd	GACTTTCCAAAGGGCATGTGCG
CSF1 (4,4) rev	GCCGTATATATACGACCTTGCAACATC
CSF1 (8,8) fwd	CGATCCCAGGTAGCAAATATTTC
CSF1 (8,8) rev	GCTTTTGGACGGGGATAACTG C
CSF1 (tis) fwd	GTGAGAGGTTACGATGCGTTC
CSF1 (tis) rev	CAATAGAAGACTTGAGTCAGGTGGC
MPS3 (5') fwd	GCATAGGCGGGAAGAGGCAG
MPS3 (5') rev	CGTCATCATTATGTTGGTCTAACGG
MPS3 center fwd	CGTCGCTTTTAATAATCCCTGAATTGC
MPS3 center rev	CCCAAATCTCCTGTTTGTAGATTGC
MPS3 (3') fwd	CATCAACGGAGTGACACCGC
MPS3 (3') rev	GATCTAGCTCATC TTGGCCAAATG
MPS3 (tis_2) fwd	GGGGCATTGTAGACCTCTAAC <sup>2</sup>
MPS3 (-30/ -2) rev	CCAGCACTTCCAGGATAAAAGTTACTACC <sup>2</sup>
POL1 (5') fwd	GCTGCAAGCCGCTCGAAATG
POL1 (5') rev	CCAGTGTCTTCATCACTTGAAC TG
PMA1 5' fwd	CTGATACATCATCTCTTCATCATCC
PMA1 5' rev	CGGAAGTTAAACCGTAAGATGGG
PMA1 center fwd	GGGTTTGGATGCTATTGATAAGGCTTTC
PMA1 center rev	CCTTGTTTTTCGTAGTTTTTCATGGACATC

PMA1 3' fwd	CCTTATTCGGTTGGTGGTCTG
PMA1 3' rev	GGTTTCCTTTTCGTGTTGAGTAGAG
FMP27 3' ORF fwd	GGAGATGACGATGATGGAGCTTCC (only for ChIP and genomic DNA)
FMP27 3' ORF rev	GGCAAGTAATAGATCTGTGACCCTC (only for ChIP and genomic DNA)
FMP27 5 kb fwd	GCAACTAAGTCCCAACGGGTTCC
FMP27 5 kb rev	GATCGGCATCAGCGTTGTGG
FMP27 3 kb fwd	CGCACTCCCAAATGGCCTTAG
FMP27 3 kb rev	GGTTATGGCGGATGGTAATTTTCC
IMD2 -18/+2 fwd	CCACAAGTAGCAAAAAGCAATGGC
IMD2 +220/ +240 rev	CACCGTGTCCATTGGAGAGG

<sup>1</sup> More than one genomic binding site. <sup>2</sup> In qPCR programm: 58 °C annealing, 60s elongation time. Underlined sequences indicate region homologous to the genomic target region. Sites for restriction endonucleases are shown in lower case letters.

## **2.10 Tiling array (ChIP-chip)**

### **2.10.1 ChIP-chip sample preparation**

For ChIP-chip 200 OD cells were harvested and ChIP was performed as described above (section 2.8). For each strain, subjected to ChIP-chip analysis, three independent chromatin preparations were used, representing three biological replicates. Of one chromatin preparation at least 3 x 10 OD for  $\alpha$ -H4 K16Ac IP; 3 x 10 OD for  $\alpha$ -H4 IP; 1 x 10 OD for w/o antibody; 1 x 5 OD for sheared sample (for gel analysis, not on tiling arrays); 10 x 5 OD for input preparation. For subsequent processing a minimum of 300 – 400 ng was required of IPs and up to 7000 ng of Input DNA, which was used for determining the conditions for digestion with DNaseI (see below 2.10.2). Whether the amount of precipitated DNA was sufficient, was determined by measuring the DNA content of the combined samples at the NanoDrop spectrophotometer (peqlab). One chromatin preparation of one strain therefore resulted in three tiling arrays (H4 K16Ac, H4, Input).

### **2.10.2 Processing and hybridization of ChIP DNA**

Tiling arrays representing the complete *S. cerevisiae* genome with ~ 3.2x10<sup>6</sup> perfect match/mismatch probes tiled at an average resolution of 5 bp (Affymetrix GeneChIP® *S. cerevisiae* Tiling 1.0R arrays) were used. ChIP DNA (300 ng) was fragmented by limited DNaseI digestion to an average size of approximately 200 bp and labeled with Terminal Deoxynucleotidyl Transferase using the reagents of the Human Mapping 250K Sty Assay Kit (Affymetrix). Hybridization, washing and scanning of tiling arrays was performed according to the Affymetrix Chromatin Immunoprecipitation Assay protocol. Hybridization was carried out by Ludger Klein-Hitpass, Institut für Zellbiologie, Universitätsklinikum Essen.

### 2.10.3 Tiling Array data analysis

#### 2.10.3.1 Normalization

The intensities measured for perfect match probes were extracted from the binary cel files along with their coordinates in the *S. cerevisiae* genome as annotated by Affymetrix. The intensities were transformed by taking the natural logarithm of the intensities. The resulting values are referred to as log-intensities. The log-intensities for each microarray were normalized by the PMT method (Chung and Vingron 2009). The results were manually inspected, and it was found that normalization has the desired effect, i.e. the distributions were markedly more similar after than before normalization. Moreover, the different conditions, i.e. input, H4, H4 K16Ac, are more similar to each other than in the different genotypes, i.e. wt and *sas2Δ*, indicating that the experiments are highly reproducible. Bioinformatic analysis was performed by Ho-Ryun Chung, Max-Planck-Institut für molekulare Genetik, Department of Computational Molecular Biology.

#### 2.10.3.2 Identification of H4 K16Ac – enriched and – depleted regions

The mean values of the normalized log-intensities across the three replicates for H4 K16Ac were further normalized for the nucleosome density by subtracting the corresponding average values for H4 both from wt and *sas2Δ* samples. Subsequently, a moving average of length 200 base pairs was calculated. Regions were identified that correspond to local maxima in the data, which was defined to be regions whose average enrichment of H4 K16Ac over H4 was higher than any other overlapping region. To extract the statistically significant peaks in the signal, the so-derived distribution was fitted to a normal distribution, with the mean and the standard deviation as parameters. We took the probability that a peak value is greater or equal to the actual peak from the fitted normal distribution as p-value, which were corrected for multiple testing by the application of a false discovery rate of 10% (Benjamini and Hochberg 1995).

For the depleted regions in *sas2Δ*, the mean log-intensities for H4 K16Ac in *sas2Δ* were normalized by subtracting the corresponding average values for H4 K16Ac in wt samples, which should reveal changes on the H4 K16Ac level upon deleting *SAS2*. A moving average of length 200 base pairs was calculated, and this time local minima were determined. The depleted regions were identified by fitting a normal distribution and taking the probability that the trough value is smaller or equal to the actual trough as p-value at a false discovery rate of 10%. Bioinformatic analysis performed by Ho-Ryun Chung.

#### 2.10.3.3 Average profiles of H4 K16Ac along transcriptional units

The transcript boundaries of verified ORFs (4749 genes) were taken from the supplementary table 3 of Xu et al. (Xu et al. 2009). For each TU, we determined the signal in 2% bins of the TU length starting from –18% and ending at +118%. To account for the bias from the different length of the TUs, we divided each bin by the length of the TU. The TUs were ranked according to their expression and were separated into five groups, i.e. starting from the 20% least expressed genes to the 20% most expressed genes. For each of these groups, we calculated the average profile of H4 K16Ac against H4. Bioinformatic analysis performed by Ho-Ryun Chung.

### 2.10.3.4 H3 exchange and H3 K56 acetylation data

We downloaded the H3 exchange and H3 K56Ac data (Rufiange et al. 2007) from NCBI GEO (H3 exchange: GSM205557 and GSM205586; H3 K56Ac: GSM205799 and GSM205821). We extracted the probe sequences from the \*.gpr files. Normalization was performed separately for the two channels per array using PMT (Chung and Vingron 2009). For the H3 exchange, we subtracted from the H3-flag (H3-flag is expressed in G1) the H3-myc (H3-myc is expressed from its endogenous promoter) normalized log intensities. For the H3 K56Ac, we subtracted from the H3 K56Ac the H3 normalized log intensities. The replicates were combined by taking the average value for each probe.

The H3 exchange and H3 K56Ac data has a lower resolution than the H4 K16Ac data. Therefore, we calculated for every position measured in the H3 exchange and H3 K56Ac data an average value from the H4 K16Ac data. We used a Gaussian kernel with zero mean and a standard deviation of 48.33 (145 / 3). We multiplied the H4 K16Ac values by the kernel value corresponding to the H4 K16Ac position relative to the H3 exchange or H3 K56Ac positions in a window from -145 base pairs to +145 base pairs. Bioinformatic analysis performed by Ho-Ryun Chung.

## **2.11 RNA expression analysis**

### **2.11.1 RNA sample preparation**

For RNA expression arrays (David et al. 2006), strains were grown in YPD to mid-exponential phase, and RNA was extracted using the hot phenol method. Further procedures were carried out as described (Xu et al. 2009) except that 20  $\mu$ g DNaseI treated total RNA was used for first strand cDNA synthesis. The RNA was incubated with 0.0034  $\mu$ g Oligo(dT) and 1.8  $\mu$ g random hexamers for 10 min at 70°C for denaturation, followed by 10 min at 25°C and on hold at 4°C for annealing. The synthesis was performed in a thermal cycler and included 2,000 units of SuperScript II Reverse Transcriptase, 50 mM TrisHCl, 75 mM KCl, 3 mM MgCl<sub>2</sub>, 0.01 M DTT, 0.25 mM dCTP, dATP and dGTP, 0.2 mM dTTP, 0.05 mM dUTP, 20  $\mu$ g/mL actinomycin D in a total volume of 105  $\mu$ L. The following program was used: 25 °C for 10 min.; 37 °C for 30 min; 42 °C for 30 min and 70 °C for 10 min to inactivate the enzyme. Finally, 5.5  $\mu$ g cDNA was used for fragmentation and labeling. RNA processing and labeling performed by Sandra Clauder-Münster, European Molecular Laboratory (EMBL), gene expression group of Dr. Lars Steinmetz.

For the *IMD2* expression analysis, total RNA was prepared from 5 OD liquid culture. Samples were harvested and snap frozen in liquid nitrogen. RNA of all samples was prepared simultaneously, and Total RNA isolation Nucleo Spin RNA II (Macherey-Nagel) was used for preparation. After thawing, samples were resuspended in ice-cold water and centrifuged. Cell disruption was performed by vortexing sample containing 3.5  $\mu$ l  $\beta$ -Mercaptoethanol, 350  $\mu$ l Buffer RA1 (M&N) and acid washed glass beads up to half of the volume for 10 min in Turbo Mix, 4 °C. Lysate was transferred to Nucleo Spin Filters (Macherey-Nagel) and centrifuged to clear the lysate. 350  $\mu$ l 70% ethanol were added to flow-through and RNA preparation was continued according to standard protocol of manufacturers instruction step 5.

### 2.11.2 Reverse transcription (RT) and measurement of 3': 5' ratios

For *IMD2* expression analysis 1.7  $\mu\text{g}$  total RNA was used for cDNA synthesis with Invitrogen SuperScriptIII. cDNA synthesis was performed with 50 ng random hexamers according to manufacturers instructions. Inactivation of enzymes was carried out at 95 °C for 10 min.

For analysis of 3': 5' ratio, 2  $\mu\text{g}$  DNaseI treated total RNA was used for first strand cDNA synthesis using Invitrogen SuperScriptIII with 50 ng random hexamers according to supplier's instructions. Inactivation of enzymes was carried out at 95 °C for 10 min. For RT-qPCR analysis, genomic DNA-based calibration curves were used for each amplification. Samples were diluted using carrier RNA 100 ng/  $\mu\text{l}$  f.c. (tRNA, from E.coli MRE 600, 100 mg, Roche). The quantitative analysis was carried out as described above in the quantitative real-time PCR section.

### 2.11.3 Hybridization to expression arrays

An Affymetrix custom yeast tiling array (PN 520055), (David et al. 2006) was used in this study. The labeled cDNA samples were denatured in a solution containing 100 mM Mes, 1 M [Na<sup>+</sup>], 20 mM EDTA, 0.01% Tween-20, 50 pM control oligonucleotide B2 (Affymetrix), 0.1 mg/ml herring sperm DNA, and 0.5 mg/ml BSA in a total volume of 300  $\mu\text{l}$ , from which 250  $\mu\text{l}$  were hybridized per array. Hybridizations were carried out at 45 °C for 16 h with 60 rpm rotation. Hybridization performed by Sandra Clauder-Münster.

### 2.11.4 Expression array data analysis

Arrays were normalized with W303 genomic DNA as reference (Huber et al. 2006). The transcript boundaries were taken from the supplementary table 3 of Xu et al. (Xu et al. 2009). For each transcript, expression level was estimated by the midpoint of the shorth (shortest interval that covers half the values) of the normalized probe intensities (log<sub>2</sub> scale) lying within the transcript. The expression level cut-off for calling a transcript expressed was obtained using the same procedure as previously described (David et al. 2006). To classify genes according to their expression changes in *sas2* $\Delta$  compared to wt, the signal obtained by RNA hybridization to tiling microarrays in *sas2* $\Delta$  and wt was used, where we subtracted from the values for *sas2* $\Delta$  the corresponding ones for the wt. After length normalization, the profiles were clustered using *k*-means clustering with four classes, initialized by 100 randomly chosen centers. Data analysis performed by Zhenyu Xu, EMBL, gene expression group of Lars Steinmetz, and Ho-Ryun Chung.

## 2.12 Preparation of *Saccharomyces cerevisiae* protein extracts

For whole cell extracts, cells were grown in 1.5 ml liquid culture over night. OD<sub>600nm</sub> was measured and 5 - 10 OD were harvested and centrifuged 7000 rpm, 5 min. Cells were washed once with TBS. For cell disruption, 30  $\mu\text{l}$  acid washed glass beads and 100  $\mu\text{l}$  1x Lämmli buffer were added, and cells were vortexed in turbo mix 3x for 20 s with tubes stored on ice in between. Samples were heated at 95 °C, 5 min with lid of tubes perforated and either loaded on a SDS-gel (per lane 1.5 – 2 OD) or stored at -80 °C.

For the determination of HA-tagged Sas2 protein, whole cell extracts were prepared from 100 OD cells with extraction buffer containing 50 mM Tris pH 7.5, 150 mM NaCl, 2.5 mM MgCl<sub>2</sub>, 1% Triton X-100, 10%

Glycerol, 1% SDS, 1 mM DTT, 1 mM PMSF and Roche complete proteinase inhibitor (+ EDTA). For this purpose, cells were washed in PBS + Roche complete proteinase inhibitor (+ EDTA) and disrupted with acid washed glass beads in turbo mix 7x for 30 s, 4 °C. 100  $\mu$ l extraction buffer was added, mixed and centrifuged 5 min, 5000 rpm, 4 °C. Supernatant was transferred to fresh tube with additional 100  $\mu$ l extraction buffer, centrifugation was repeated and supernatant transferred to fresh reaction tube. Aliquots were stored at -80 °C.

### **2.13 SDS PAGE and Immunoblotting (Western blot)**

SDS-PAGE in Tris-glycine buffer according to standard methods (Laemmli 1970) was used for protein separation. For histone analysis a 15% SDS-gel, for Sas2 detection 12% SDS-gel was used. Transfer to nitrocellulose membranes (Amersham Hybond ECL, GE Healthcare) was accomplished by blotting with the BIO-RAD Tank Transfer System with 5.5 mA x h/cm<sup>2</sup>. Transfer buffer with 39 mM Glycine, 48 mM Tris base, 0.037% SDS, 20% Methanol was used (Sambrook et al. 1989). The blot membrane was subsequently blocked for at least 45 min at room temperature in TBST, 3% milk (50 mM Tris-HCl pH7.5, 150 mM NaCl, 0,05% Tween-20, 3% milk powder) or TBST, BA (ECL *Advance* blocking agent, GE Healthcare), depending on antibody used (see section 2.7). After incubation with the primary antibody for 1 h at room temperature or over-night at 4 °C (for details see section 2.7) in TBST, 3% milk (or appropriate solution), the membrane was washed up to 5 times, in total no longer than 1 h in TBST. Secondary antibody (for details see section 2.7) was incubated in TBST, 3% milk (or appropriate solution) 1h at room temperature and membrane was subsequently washed 3 times for 10 min with TBST and in the end, twice shortly with TBS. For signal detection, Amersham ECL Western Blotting Analysis System (GE Healthcare) and Amersham Hyperfilm ECL chemiluminescence films (GE Healthcare) were used.

### **2.14 Synchronization of *Saccharomyces cerevisiae* cells**

The strain bearing the repressible SAS2 allele (*SAS2-td*) (AEY4488) was freshly grown on YP-Gal and used to inoculate a liquid culture of YP-Gal, grown at 37 °C (repressive conditions) during the day. An over night culture was subsequently inoculated to a final OD of at least 0,025 OD. Cells were grown to OD 0,4 – 0,5 until the next day (doubling time between 3 – 4 h, depending on start OD). Cells were harvested in a sterile beaker, washed with YP-Gal pH 4.0 and subsequently suspended in YP-Gal pH 4.0 + nocodazole (f.c. 10  $\mu$ g/ml) for a G2/ M cell cycle arrest. To control the cell cycle arrest, a small sample was sonicated 3 times for 250 ms, setting high and checked under the microscope. The pre-arrested cells were harvested in a sterile beaker, washed with YP-Gal pH 4.0 subsequently suspended in YP-Gal pH 4.0 +  $\alpha$ -factor (f.c. 1.62  $\mu$ g/ml) for a G1 cell cycle arrest. Cells were grown at 37 °C for 1.5 – 3 h and cell cycle arrest was checked under the microscope as described above. Sample “0” was taken and processed for Western blot (5 OD) or ChIP analysis (50 – 200 OD) and residual culture was split in half. One half was maintained in  $\alpha$ -factor and shifted to glucose (YPD) and 30 °C (permissive conditions), the other half was also shifted to glucose, 30 °C and pronase (f.c. 0.02 mg/ml) was added to release the cells from G1-arrest. Samples for subsequent Western blot or ChIP analysis were taken after 1 or 2h. For a schematic presentation of the experiment, see also Fig. 31.

## 3. Results

### 3.1 Genome-wide influence of Sas2-mediated H4 K16 acetylation

#### 3.1.1 *sas2Δ* caused a global reduction of H4 K16 acetylation

Chromatin organization is directly impacted by posttranslational modifications such as histone acetylation. Due to charge neutralization and subsequent opening of the chromatin structure by the acetylation of histones, histone acetyltransferases (HATs) are mediating several DNA-dependent processes. Many HATs are functioning in cooperation with transcription factors and other DNA binding proteins e.g. for regulating gene expression in a local manner (Fukuda et al. 2006). In contrast, the MYST HAT Sas2 in *Saccharomyces cerevisiae* was found to display an anti-silencing function, since a deletion of *SAS2* causes specific silencing defects at the three heterochromatic loci of yeast, the *HM* loci, the rDNA locus and the telomeres (Reifsnyder et al. 1996; Ehrenhofer-Murray et al. 1997). Sas2, the HAT subunit of the SAS-I complex was furthermore shown to exhibit activity for H4 K16 in vitro (Sutton et al. 2003) and by this site-specific modification to inhibit the proliferation of SIR-mediated heterochromatin at telomeres (Kimura et al. 2002; Suka et al. 2002). Still, the question remains how SAS-I is recruited to its specific sites of acetylation. A new consideration was brought to this issue by the finding that both the chromatin assembly factors CAF-I, via its largest subunit Cac1, and Asf1 interact with Sas2 (Meijsing and Ehrenhofer-Murray 2001). Thus, the hypothesis was established that Sas2 might act coupled to replication due to the fact that CAF-I and Asf1 also interact with the replication fork via proliferating cell nuclear antigen (PCNA) (Meijsing and Ehrenhofer-Murray 2001). Since SAS-I so far was shown to act in the vicinity of heterochromatic sites, we sought to investigate the loss of SAS-I and its effect on genome-wide H4 K16 acetylation. Due to the hypothesis that CAF-I and Asf1 might recruit SAS-I to chromatin and also due to the findings of earlier work that CAF-I and Asf1 display overlapping functions (Sharp et al. 2001; Kim and Haber 2009), the absence of each and/or their simultaneous absence might subsequently cause a loss of H4 K16 acetylation. Thus, we furthermore sought to identify regions of Sas2-mediated H4 K16Ac that were dependent on Cac1 and/ or Asf1. To test this, chromatin immunoprecipitations (ChIP) using an antibody against acetylated H4 K16 (H4 K16Ac) and H4 were prepared in triplicate, in wild-type, *sas2Δ*, *cac1Δ*, *asf1Δ* and *cac1Δ asf1Δ* cells and hybridized to high-resolution tiling arrays (ChIP-chip). In order to normalize H4 K16Ac level to nucleosome density, ChIP-chip was performed in parallel

with an antibody against unmodified H4. The antibodies used in this study, were carefully validated for specificity: to test the  $\alpha$ -H4 K16Ac antibody, Western blot analysis was performed in wild-type, *sas2* $\Delta$ , and cells in which H4 K16 was mutated to arginine (H4 K16R) in order to mimic positive charge and thus the unacetylated state of the lysine residue. The signal of H4 K16 acetylation was reduced in *sas2* $\Delta$  compared to wild-type and absent in H4 K16R cells, indicating specificity for this site of acetylation (data not shown). Furthermore, the  $\alpha$ -H4 K16Ac antibody was tested in ChIP in wild-type and *sas2* $\Delta$  cells and precipitates were analyzed by quantitative real-time PCR (qPCR). H4 K16 acetylation, the known target of Sas2, was decreased at the subtelomeric region upon deletion of *SAS2* compared to wild-type (data not shown) confirming the specificity of the antibody. The tiling arrays used in our approach comprised 25-mer oligonucleotides with a 5 bp resolution (Affymetrix), thus tiling the complete *S. cerevisiae* genome. The hybridization of the ChIP precipitates onto the tiling arrays was performed by Ludger Klein-Hitpass from the BioChip lab at the Universitätsklinikum Essen. The bioinformatic data analysis was carried out by Ho-Ryun Chung from the Department of Computational Molecular Biology at the Max-Planck-Institut für molekulare Genetik, Berlin. Furthermore, a validation of the H4 tiling arrays was performed. The H4 signals matched the expected spaces of 165 bp between the yeast nucleosomes (data not shown).

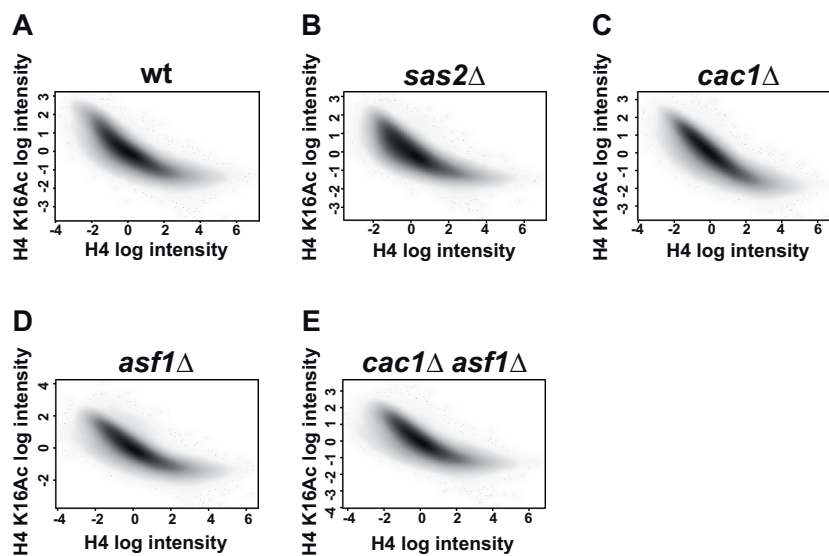


**Figure 4. H4 K16 acetylation (H4 K16Ac) was more abundant in regions with less histone H4.**

(A-E) Overall analysis correlating the total tiling array data of relative H4 K16Ac signals (H4 K16Ac/ H4) to H4 levels for wild-type (wt) (A), *sas2* $\Delta$  (B), *cac1* $\Delta$  (C), *asf1* $\Delta$  (D), *cac1* $\Delta$  *asf1* $\Delta$  (E). Relative global H4 K16Ac levels dropped in *sas2* $\Delta$  (B), but not in the other delete strains. ChIP-chip was performed by hybridizing DNA from H4 K16Ac and H4 chromatin immunoprecipitations (ChIP) to high-resolution tiling arrays. Experiments were performed in triplicate. Data was subjected to normalization procedures. Hybridization was carried out by L. Klein-Hitpass, bioinformatic analysis by H.-R. Chung.

In a first overall analysis, the global distribution of H4 K16Ac relative to H4 in wild-type, *sas2Δ*, *cac1Δ*, *asf1Δ* and *cac1Δ asf1Δ* cells was analyzed (Fig. 4A-E). The data of the overall detected log intensities of H4 K16Ac was plotted against log intensities of H4. Each data point corresponds to a signal from one oligonucleotide of the tiling array. In wild-type, high levels of H4 K16Ac correlated with lower H4 levels and vice versa (Fig. 4A). Compared to wt, *sas2Δ* resulted in a decreased H4 K16Ac signal in regions with low levels of H4 (Fig. 4B), as indicated by the “cloud” of dots that is shifted towards the lower left-hand corner of the graph. However, as expected, H4 K16Ac was not completely absent in *sas2Δ*, because previous analyses have shown that H4 K16 is also targeted by another HAT, Esa1 (Clarke et al. 1993; Suka et al. 2002). In the chromatin assembly factor mutant strains (*cac1Δ*, *asf1Δ* and *cac1Δ asf1Δ*), the H4 K16Ac signal did not show the same general decrease as in *sas2Δ* (Fig. 4C-E). Only the simultaneous deletion of *CAC1* and *ASF1* showed slightly decreased H4 K16 acetylation as compared to *cac1Δ* or *asf1Δ* alone (compare Fig. 4E with 4C and D), but this decrease of H4 K16Ac was still less pronounced than in *sas2Δ* cells, showing that the deletion of *SAS2* caused the highest impact on H4 K16 acetylation.

This finding was confirmed by the correlation of the H4 K16Ac data from *sas2Δ* and wild-type cells. This time the global data of H4 K16Ac of the mutant strains was correlated to the wild-type H4 K16 acetylation data. Thereby, the wild-type acetylation data was subtracted of the H4 K16Ac data of each mutant strain, resulting in a negative correlation trend of the data sets. In agreement with the above data, the analysis showed that regions with high levels of acetylation in the wild-type strain showed diminished H4 K16Ac signals in *sas2Δ*, as visible by the “cloud” of data points bent to the lower right corner of the graph (Fig. 5A). This “bending” was not observed in *cac1Δ* and *asf1Δ* (Fig. 5B, C), thus indicating that the major part of H4 K16Ac remained unchanged in these cells as compared to wild-type. Correlation of *cac1Δ asf1Δ* and wild-type data revealed a minimal “bending” and therefore a slight reduction of H4 K16Ac in this strain (Fig. 5D). Taken together, the biggest change in H4 K16 acetylation was observed upon deletion of *SAS2*, which demonstrated that Sas2 displayed a global influence on H4 K16Ac as opposed to an exclusive role at regions of silent chromatin. However, as shown below, in all mutant strains the loss of H4 K16Ac was not uniformly distributed over the yeast genome.

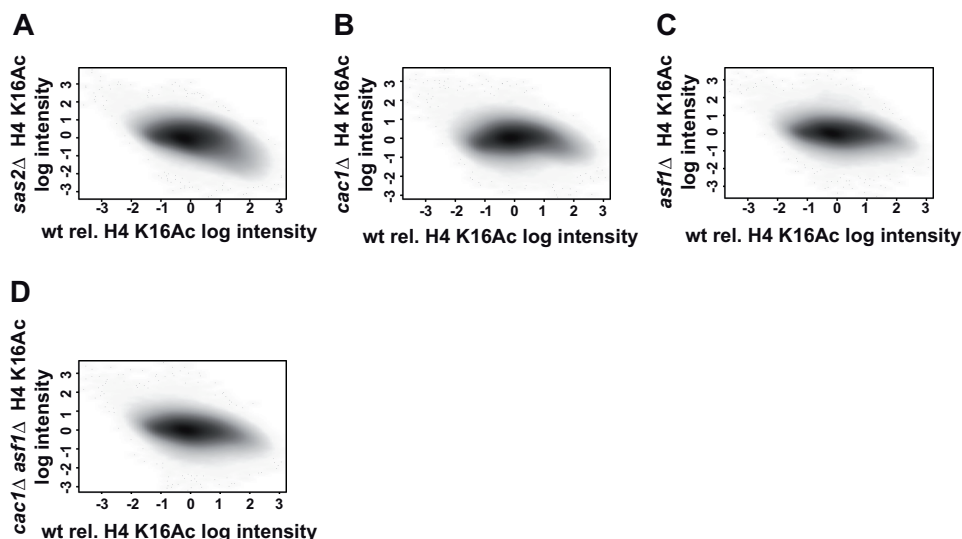


**Figure 5. Relative H4 K16Ac levels in *sas2Δ* were globally reduced.**

(A-D) H4 K16Ac data from wild-type (wt) were plotted against H4 K16Ac from the indicated mutant strains to analyze strain specific global changes. All datasets were normalized to their levels of H4. Furthermore, wild-type relative H4 K16Ac was subtracted from relative H4 K16Ac data of each mutant strain (*sas2Δ* (A), *cac1Δ* (B), *asf1Δ* (C), *cac1Δ asf1Δ* (D)). *sas2Δ* caused a global decrease of H4 K16Ac in regions of high relative H4 K16Ac in strain (A). Bioinformatic analysis was performed by H.-R. Chung.

### 3.1.2 Acetylation of H4 K16 at telomeric regions was dependent on Sas2, but only partially dependent on the chromatin assembly factors CAF-I and Asf1

#### 3.1.2.1 H4 K16Ac was depleted at subtelomeric regions in *sas2Δ*

Sas2 was previously shown to influence telomeric silencing and to prevent the spreading of heterochromatin by acetylating H4 K16 at subtelomeric regions (Kimura et al. 2002; Suka et al. 2002; Shia et al. 2006). Accordingly, we expected to find reduced levels of H4 K16Ac at telomeric regions in *sas2Δ* cells. For the analysis, the H4 K16Ac levels were normalized across the genome. Black upright bars in the graph represent higher than average acetylation, and grey downward bars indicate lower than average acetylation. According to expectation, H4 K16Ac could be detected at subtelomeric regions in wild-type cells (Fig. 6, 7, upper row). In agreement with earlier work (Kimura et al. 2002; Suka et al. 2002; Shia et al. 2006), relative H4 K16Ac levels were reduced in *sas2Δ* in subtelomeric regions up to approximately 20 kb distance from the telomere, for instance at the right arm of chromosome VI (Fig. 6 second row, grey bars). Here, the difference in H4 K16 acetylation between *sas2Δ* and wild-type is indicated and is also shown for each mutant strain *cac1Δ*, *asf1Δ* and *cac1Δ asf1Δ*. Thus, in *sas2Δ* decreased H4 K16 acetylation levels at the telomeres were below the average acetylation and are indicated by the grey bars that point downwards.

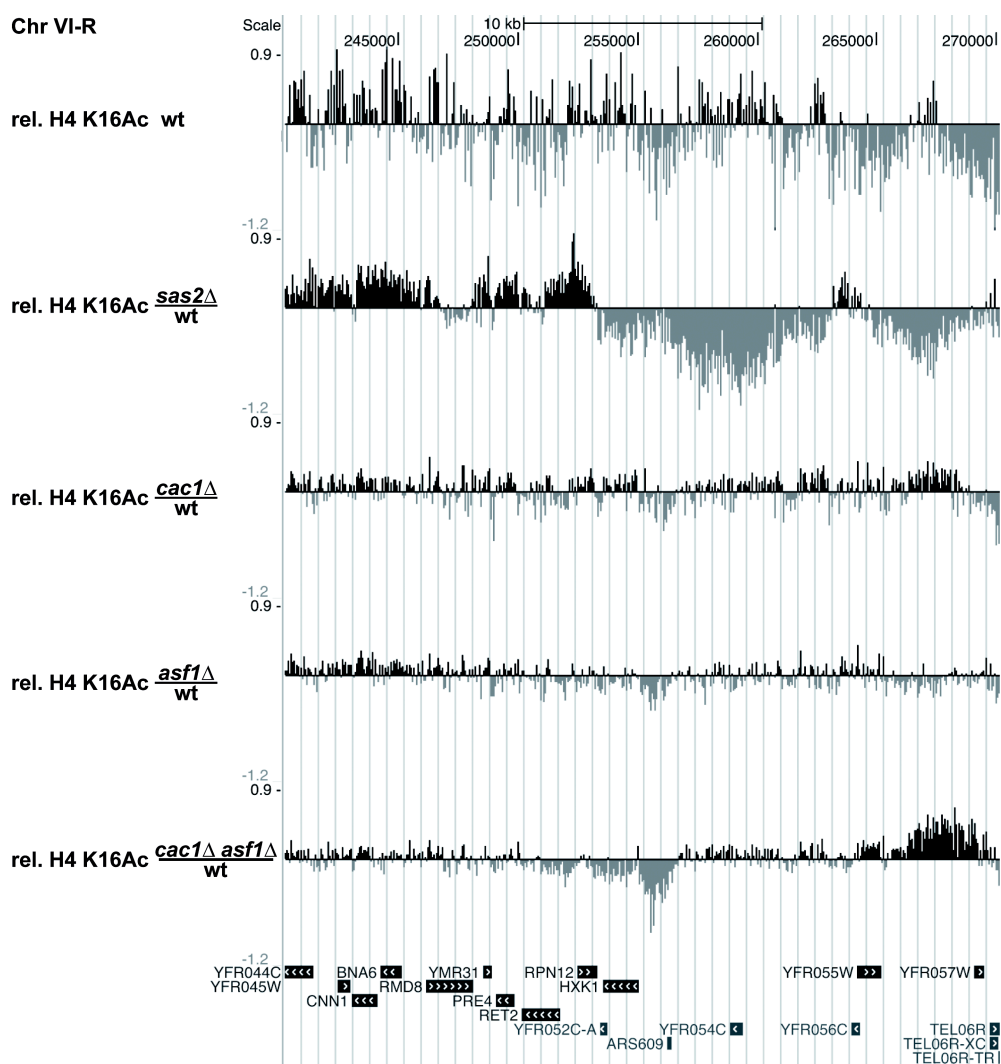


**Figure 6. H4 K16Ac at subtelomeric regions showed dependence on Sas2, and a partial influence of the chromatin assembly factors CAF-I and Asf1.**

H4 K16Ac (relative to H4) was averaged over the whole yeast genome for each strain. Acetylation signals for wt are shown on top. Positive signals are indicated as black bars representing above-average H4 K16Ac, negative signals are indicated as grey bars representing below-average acetylation. The relative H4 K16Ac of all mutant strains (*sas2* $\Delta$ , *cac1* $\Delta$ , *asf1* $\Delta$ , *cac1* $\Delta$  *asf1* $\Delta$ ) is shown as the difference of relative H4 K16Ac in the mutant strain to wild-type relative H4 K16Ac. 25 kb of sequence from Chr VI-R is shown. Underlying annotations at the bottom of the graph indicate positions of protein-coding genes and other features according to the *Saccharomyces* Genome Database (SGD). (Abbreviations at the telomeres: XC - core X, YP - Y' element, XR - subtelomeric repeats.) Bioinformatic analysis was performed by H.-R. Chung. Data was visualized using the UCSC Browser (<http://genome.ucsc.edu/>).

Chromosome ends are mosaic structures that consist of several subtelomeric repeats. The composition of the repeat elements varies between telomeres. The core X element can be found at every end, whereas the Y' element is included at many but not all telomeres. We observed reduced H4 K16Ac in *sas2* $\Delta$  at all subtelomeric regions regardless of whether Y' elements were present at telomeres or not, as shown for a further example at the left arm of chromosome X (X-L) and the right arm of chromosome III (III-R) (Fig. 7 left side, second row and Fig. 8 right side, second row). At the telomeres IX-L, XII-L, XVI-R the core X element displayed nearly unchanged levels of H4 K16Ac in *sas2* $\Delta$  (data not shown). The

acetylation of Y' elements was clearly reduced in *sas2* $\Delta$  cells, although the extent of H4 K16Ac in wild-type could not be defined unambiguously, since these elements consist of highly repetitive sequences which can not be distinguished during signal intensity calculations. Furthermore, our ChIP-chip data allowed a refined view of local H4 K16Ac levels standing in contrast to earlier work. Significantly, we did not observe the continuous increase of H4 K16Ac levels towards centromere-proximal sequences reported earlier (Kimura et al. 2002; Suka et al. 2002) (Fig. 6, first row), i.e. there was no “mound” of H4 K16Ac having been proposed to inhibit SIR spreading. Also, the decrease of H4 K16Ac in *sas2* $\Delta$  was discontinuous (Fig. 6, second row). Thus, our data demonstrated that acetylation by SAS-I was not specifically targeted to subtelomeric regions, for instance by an underlying DNA sequence, and indicated that its distribution in the genome was governed by other, so far unknown principles.

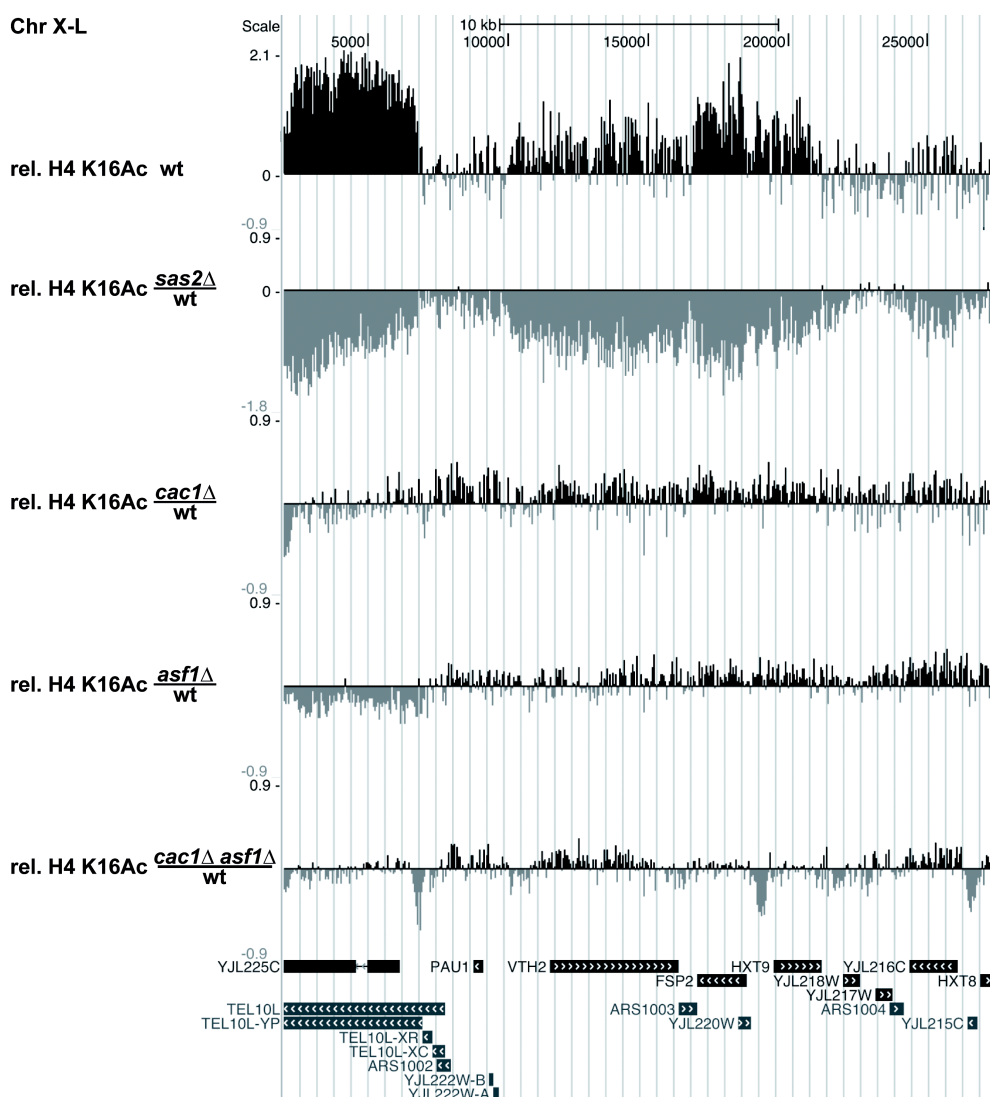


**Figure 7. H4 K16Ac at subtelomeric regions depended on Sas2, and displayed a partial influence of the chromatin assembly factors CAF-I and Asf1.**

30 kb of sequence from Chr X-L is shown. Tiling array data is presented as described in Fig. 6. Bioinformatic analysis was performed by H.-R. Chung.

Interestingly, at chromosome III-R, the zone of H4 K16Ac decrease in *sas2* $\Delta$  cells extended up to and beyond *HMR* (Fig. 8). This observation might explain the suppression of the silencing defect of the mutated *HMR*-E silencer allele *HMRa-e\*\** upon deletion of *SAS2*. This mutation leads to the derepression of *HMRa*. Since H4 K16Ac in *sas2* $\Delta$  cells is decreased and the *HMR* locus is located at the right arm of chromosome III in vicinity of the telomeres, Sir proteins would be enabled to spread up to *HMR* and propagate heterochromatin formation. Therefore, the silencing defect would be repressed due to Sir spreading in the absence of Sas2.

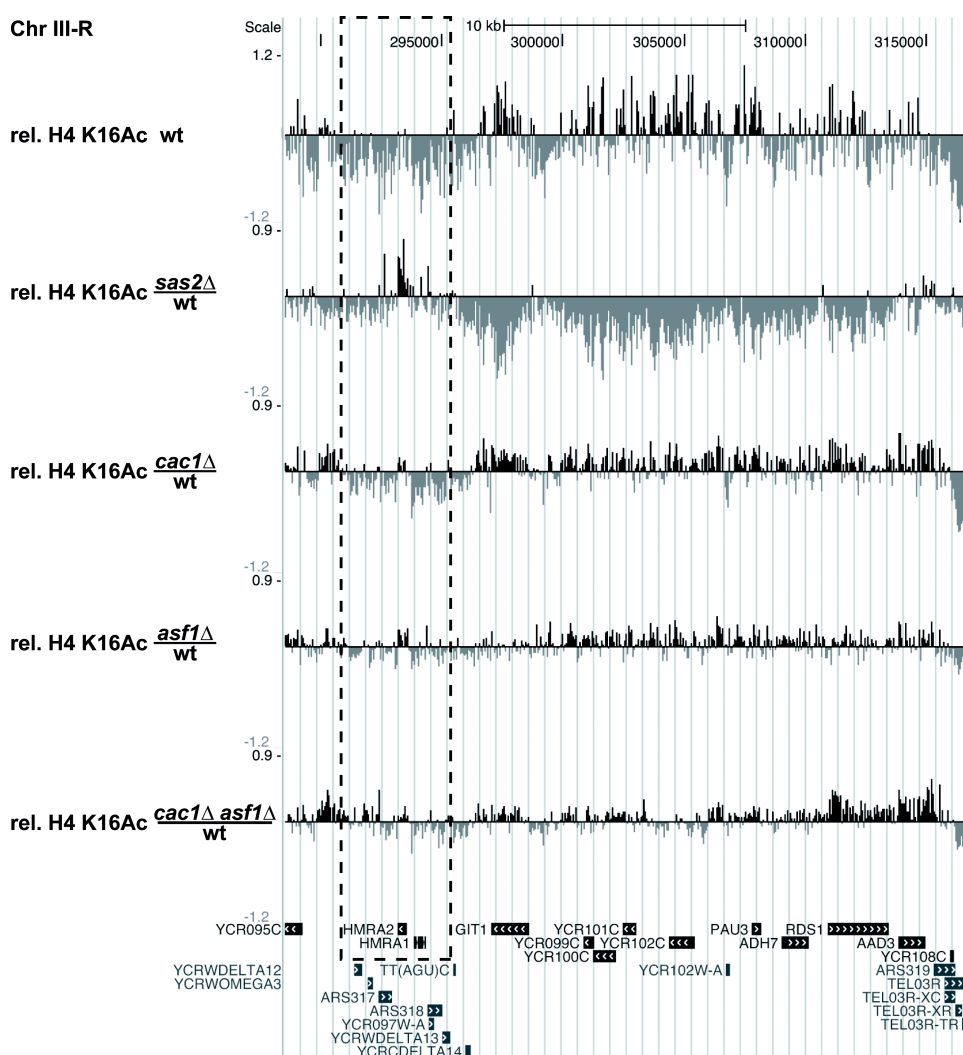


**Figure 8. Relative H4 K16Ac was decreased around *HMR* in *sas2* $\Delta$  cells.**

25 kb of sequence from Chr III-R is shown. The *HMR* locus is marked by the dashed line. Tiling array data is presented as described in Fig. 6. Bioinformatic analysis was performed by H.-R. Chung.

### 3.1.2.2 H4 K16Ac at telomeric regions was partially influenced by the chromatin assembly factors CAF-I and Asf1

Based on the fact that the chromatin assembly factors CAF-I and Asf1 were previously shown to interact with Sas2 (Meijsing and Ehrenhofer-Murray 2001), one could speculate that their deletion would also cause a reduction of H4 K16 acetylation in regions where H4 K16Ac depended on Sas2. As shown above, H4 K16Ac at the subtelomeric regions was dependent on Sas2. We therefore examined these regions (chromosome VI, X and III) in *cac1Δ*, *asf1Δ* and *cac1Δ asf1Δ* strains (Fig. 6, Fig. 7 and Fig. 8 third to last row) to determine the effect of the chromatin assembly factors on H4 K16Ac. Interestingly, there was no major reduction of the H4 K16 acetylation signal as observed in *sas2Δ* cells. The detected patterns in *cac1Δ*, *asf1Δ* and *cac1Δ asf1Δ* revealed only small changes of H4 K16Ac at subtelomeric regions compared to wild-type (compare Fig. 6, Fig. 7 and Fig. 8 first and second with third to last rows). The changes in acetylation level in the *cac1Δ*, *asf1Δ* and *cac1Δ asf1Δ* strains were discontinuous with some signals above and some below the average acetylation level and H4 K16 acetylation did not show an even distribution. Some reduction of H4 K16Ac at telomeric Y' elements was observed in *cac1Δ*, *asf1Δ* and *cac1Δ asf1Δ* but not beyond, as shown e.g. at chromosome X-L (Fig. 7). As an independent measurement for local H4 K16Ac levels, we used conventional ChIP analysis, in which ChIP precipitates were analyzed by quantitative PCR (Fig. 9).

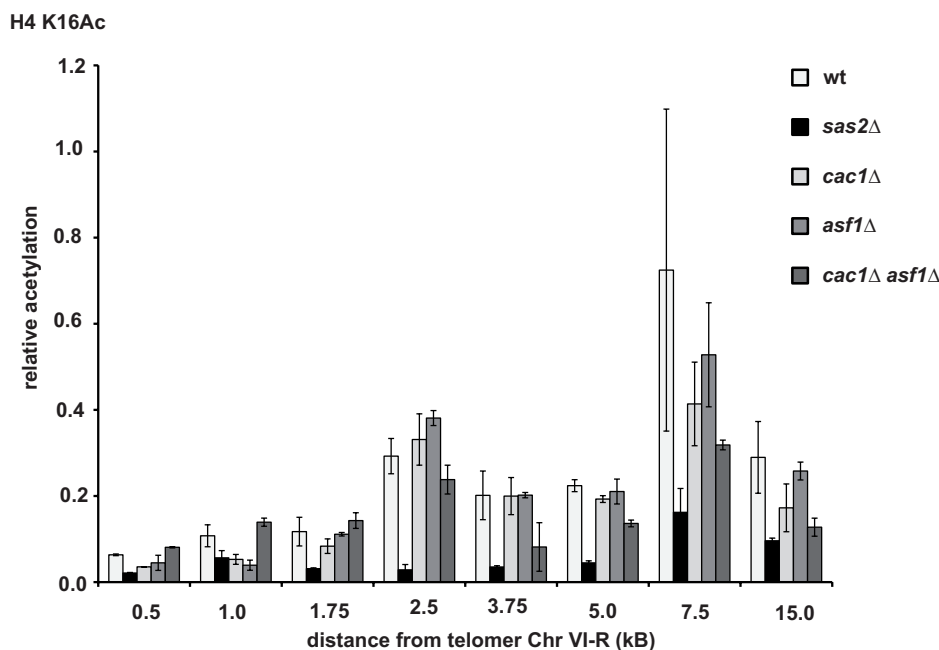


**Figure 9. H4 K16Ac was partially dependent on the chromatin assembly factors CAF-I and Asf1.** ChIP analysis of H4 K16Ac at the right arm of chromosome VI, in wild-type, *sas2Δ*, *cac1Δ*, *asf1Δ* and *cac1Δ asf1Δ* is shown. The relative acetylation, calculated as percent of input, was determined at a distance of 0.5 – 15 kb from the telomere. Error bars represent technical replicates.

Consistent with the tiling array results, we observed at most a mild reduction of H4 K16Ac pattern at the subtelomeric region of chromosome VI-R in *cac1Δ asf1Δ* strains, but not in *cac1Δ* and *asf1Δ* (Fig. 9). In the chromatin assembly factor mutant strains *cac1Δ* and *asf1Δ*, H4 K16Ac was comparable to wild-type acetylation level (Fig. 9). Conversely, upon deletion of *SAS2*, H4 K16Ac was strongly reduced compared to wild-type, which was in agreement with the expectations and the tiling array data, as discussed above. Taken together, the H4 K16 acetylation pattern in the chromatin assembly factor mutant strains *cac1Δ*, *asf1Δ* and *cac1Δ asf1Δ* was distinct from those observed in wild-type and *sas2Δ* cells, which indicated at most a partial influence of the chromatin assembly factors on Sas2-mediated H4 K16 acetylation. One can speculate that the influence of chromatin assembly factors would be detectable only at certain time points, for instance when histone modifications are established or reestablished on chromatin after dis- and reassembly, such as would be the case after DNA replication, transcription or repair.

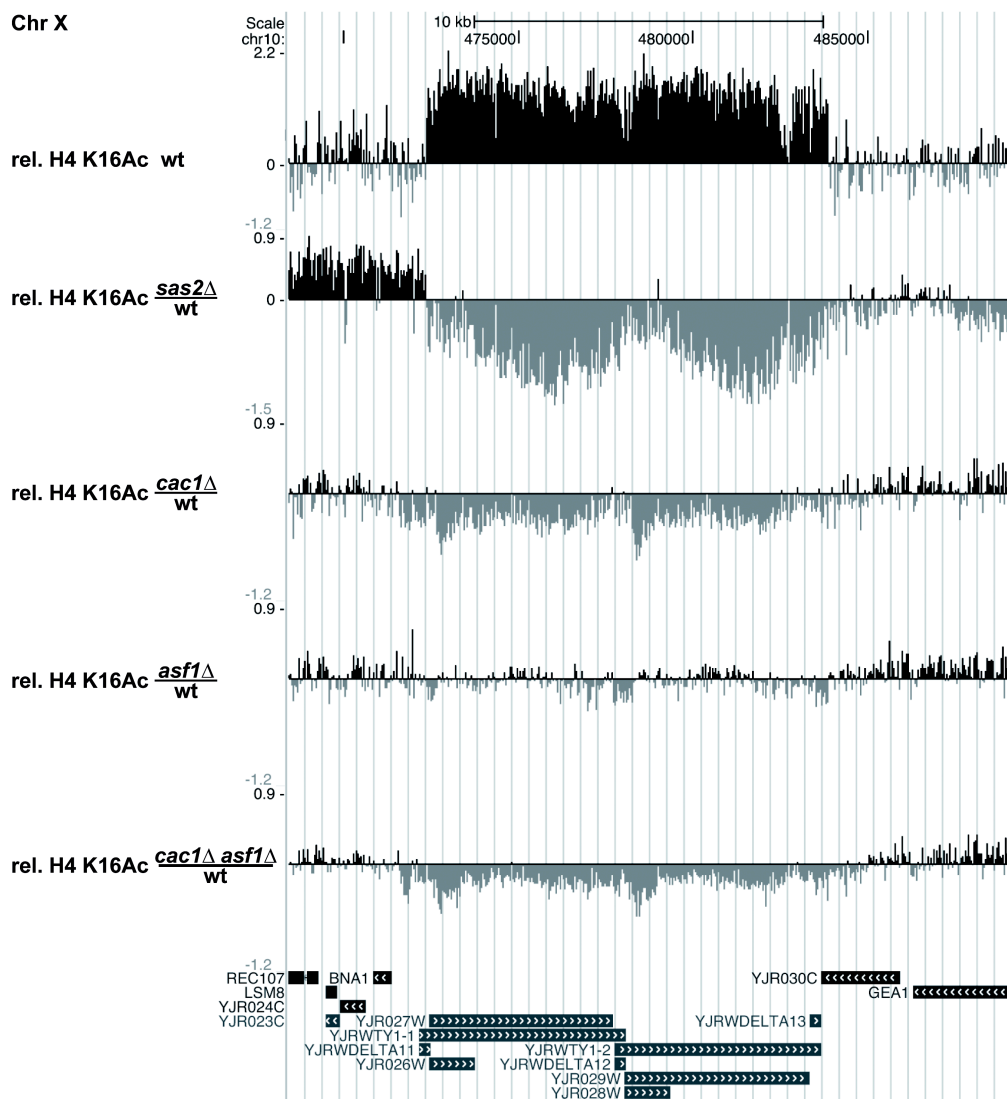
### 3.1.3 Retrotransposons showed H4 K16 acetylation that depended on Sas2

Our analysis above confirmed the expectation that H4 K16Ac was strongly decreased at telomeres in *sas2Δ* cells. We next sought to identify other regions of the genome where lysine 16 acetylation depended on Sas2. Interestingly, we observed a prominent loss of H4 K16Ac at Ty retrotransposons. Retrotransposons are ubiquitous components of eukaryotic genomes. LTR retrotransposons in *S. cerevisiae* are referred to as Ty elements and consist of five distinct groups, designated Ty1, Ty2, Ty3, Ty4 and Ty5 (Kim et al. 1998). Here, *TY1-1* and *TY1-2* on chromosome X as well as *TY2-1* on chromosome XII are shown as examples (Fig. 10A, 11A). A cursory look at H4 K16Ac levels in wild-type (Fig. 10A, 11A, top row) suggest that they are particularly high at Ty elements. However, this interpretation is misleading for the following reason: The yeast genome contains up to 30 Ty elements that are almost indistinguishable in sequence. Thus, in the process of annotation, all H4 K16Ac signals of Ty elements are added up to each single Ty location, thus erroneously giving the impression of a high H4 K16Ac signal. The full length Ty5-1 element on *TEL III-L*, as sole exception, did not show acetylation of H4 K16 (data not shown), maybe due to its location next to the telomeric region. Nevertheless, as also confirmed by conventional ChIP (see below), H4 K16Ac was depleted upon deletion of *SAS2* along the whole body of full-length Ty elements (Fig. 10A, 11A second row). This indicated that the observed H4 K16 acetylation at Ty elements was mediated by Sas2. The dependence of the acetylation on Sas2 was confirmed by ChIP analysis in that H4 K16

acetylation was high in wild-type and diminished in *sas2Δ* cells at both *TY1* and the *TY2* element at chromosomes X and XII, respectively (Fig. 10B, 11B). In the tiling array, H4 K16 acetylation was diminished to some extent at *TY1* upon deletion of *CAC1* and the simultaneous deletion of *CAC1* and *ASF1*, but not as strongly as in *sas2Δ* (Fig. 10A third and last row). At *TY2-1* at chromosome XII, the deletion of the chromatin assembly factors *CAC1* and/ or *ASF1* did not result in a pronounced loss of H4 K16 acetylation (Fig. 11A, third – last row). Measuring the H4 K16Ac level by conventional ChIP analysis at *TY2-1* confirmed that H4 K16Ac was maintained upon deletion of the chromatin assembly factors *CAC1* and *ASF1* (Fig. 11B). Taken together, the results indicated that Sas2 affected acetylation at Ty elements, whereas the influence of chromatin assembly factors was less prominent. However, as will be evident from the results below, low transcription and thus low exchange of histones H3/ H4 correlated with higher levels of H4 K16Ac. We therefore speculate that upon deletion of the chromatin assembly factors *CAC1* and *ASF1* histone exchange would have been slowed down and subsequently led to an accumulation of Sas2-dependent H4 K16Ac.

To investigate a possible function for Sas2 in the expression of Ty elements, a growth assay using a *TY1(ML2)::URA3* construct (Morillon et al. 2002) was performed. The expression of *TY1(ML2)::URA3* was measured by determining the resistance to 5-fluoroorotic acid (5-FOA) in wild-type, *sas2Δ* and as a control, in *xrn1Δ* cells (Fig. 12A). 5-FOA is used as a counter-selective compound due to the fact that it is converted into a toxic metabolite by the Ura3 protein (Boeke et al. 1987). The cytoplasmic 5'-3' exonuclease Xrn1 functions in mRNA decay and was previously shown to be important for the expression of *TY1(ML2)::URA3*, because this construct was less expressed in cells with a deletion of *XRN1* (Berretta et al. 2008). As expected, *xrn1Δ* cells were more resistant to 5-FOA than wild-type cells (Fig. 12A, right panel, bottom rows), indicating that Ty1 was repressed in the absence of Xrn1. The deletion of *SAS2* caused the cells to be less resistant to 5-FOA compared to *xrn1Δ*, but only a mild difference (if at all) was observed between wild-type and *sas2Δ* cells. An 5-FOA resistance comparable to *xrn1Δ* cells was detected in *sas2Δ xrn1Δ* cells (data not shown), indicating that Ty1 repression in *xrn1Δ* cells was not further enhanced by *sas2Δ*. From this result, we concluded that Ty1 expression was not stabilized by Sas2, even though there was strong Sas2-dependent H4 K16Ac at these elements.

A



B

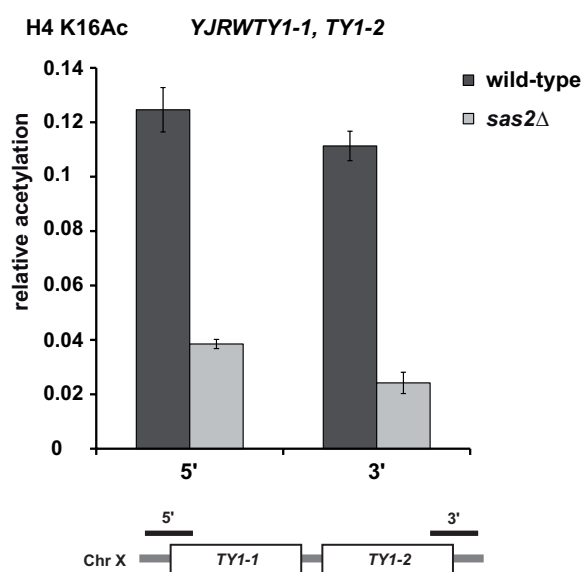


**Figure 10. H4 K16Ac at Ty elements depended on Sas2.**

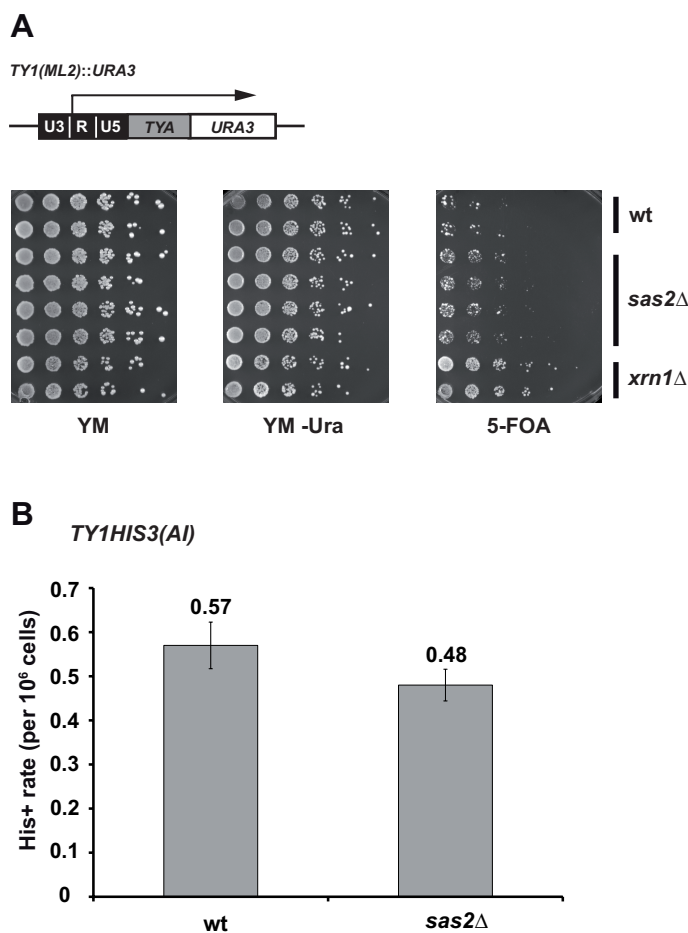
(A) 20 kb of the sequence around Ty1-1 and Ty1-2 at Chr X are shown. Tiling array data is presented as described in Fig. 6. Bioinformatic analysis was performed by H.-R. Chung. (B) ChIP analysis of H4 K16Ac at Ty1-1 and Ty1-2 at Chr X. The relative acetylation level was determined as percent of input. Error bars represent technical replicates. Positions of the products amplified for ChIP analysis are indicated as black bars in the diagram underneath the graph.



**Figure 11. H4 K16Ac was unaffected deletion of the chromatin assembly factors *CAC1* and *ASF1*.**

(A) 10 kb of the sequence around the Ty2-1 element at chromosome XII. Tiling array data is presented as described in Fig. 6. Bioinformatic analysis was performed by H.-R. Chung. (B) ChIP analysis of H4 K16Ac at Ty2-1 on Chr XII. The relative acetylation level was determined as percent of input. Error bars represent technical replicates. Positions of the qPCR products for ChIP analysis are indicated as black bars in the diagram beneath the graph.

To gain further insight into the role of Sas2 at Ty elements, we examined the influence of Sas2 on Ty1 mobility. For this purpose, strains bearing a *HIS3(AI)* insertion at a Ty1 retrotransposon locus (Curcio and Garfinkel 1991) were used. The transposition rate was determined by the number of cells that were able to grow on medium lacking histidine (Fig. 12B). In *sas2Δ* cells, the transposition rate was only slightly reduced compared to wild-type cells. This difference did not appear to be statistically significant and was not comparable to the strongly reduced transposition rate previously detected in *xrn1Δ* (Berretta et al. 2008). Therefore, the role of Sas2 must be of different nature than that of Xrn1. These results indicated that Sas2 did not influence expression or mobility of Ty elements. Thus, we showed that the H4 K16 acetylation at Ty elements strongly depended on Sas2, but the functional relevance of Sas2-mediated H4 K16 acetylation at yeast retrotransposons remains to be determined.

**Figure 12. The influence of Sas2 at Ty1 differed from that of the 5' -3' exonuclease Xrn1.**

(A) Sas2 did not repress expression of Ty1. Growth assay of wt, *sas2Δ*, *xrn1Δ* strains bearing a *TY1(ML2)::URA3* construct. Cells were grown on minimal medium (YM), medium lacking Ura (YM -Ura) and on medium containing 5-FOA (5-fluoro-orotic acid) to test for repression of *TY1(ML2)::URA3*.

(B) The transposition rate of *TY1HIS3(AI)* was not altered by the deletion of *SAS2*. The transposition rate of *TY1HIS3(AI)* in wt and *sas2Δ* was measured as the number of His<sup>+</sup> cells (indicated by the numbers on top of the bars). Cultures were grown at 20 °C to induce transposition. Aliquots were plated on full medium and medium lacking histidine. (For detailed information see material and methods section). Data from three independent experiments is shown with standard deviations.

### 3.1.4 H4 K16 acetylation was decreased at the 3' ends of long ORFs in *sas2Δ* cells

After the investigation of the effect of *sas2Δ*, *cac1Δ*, *asf1Δ*, and *cac1Δ asf1Δ* on global H4 K16 acetylation at telomeric regions and retrotransposons, we examined in more detail other regions. In general, H4 K16 acetylation in wild-type cells was present throughout these regions (Fig. 13 and 14A, first rows). Strikingly, in *sas2Δ* cells, we observed a pronounced depletion of H4 K16Ac specifically within open reading frames (ORFs), but not in intergenic regions (Fig. 13 and 14A, second row).

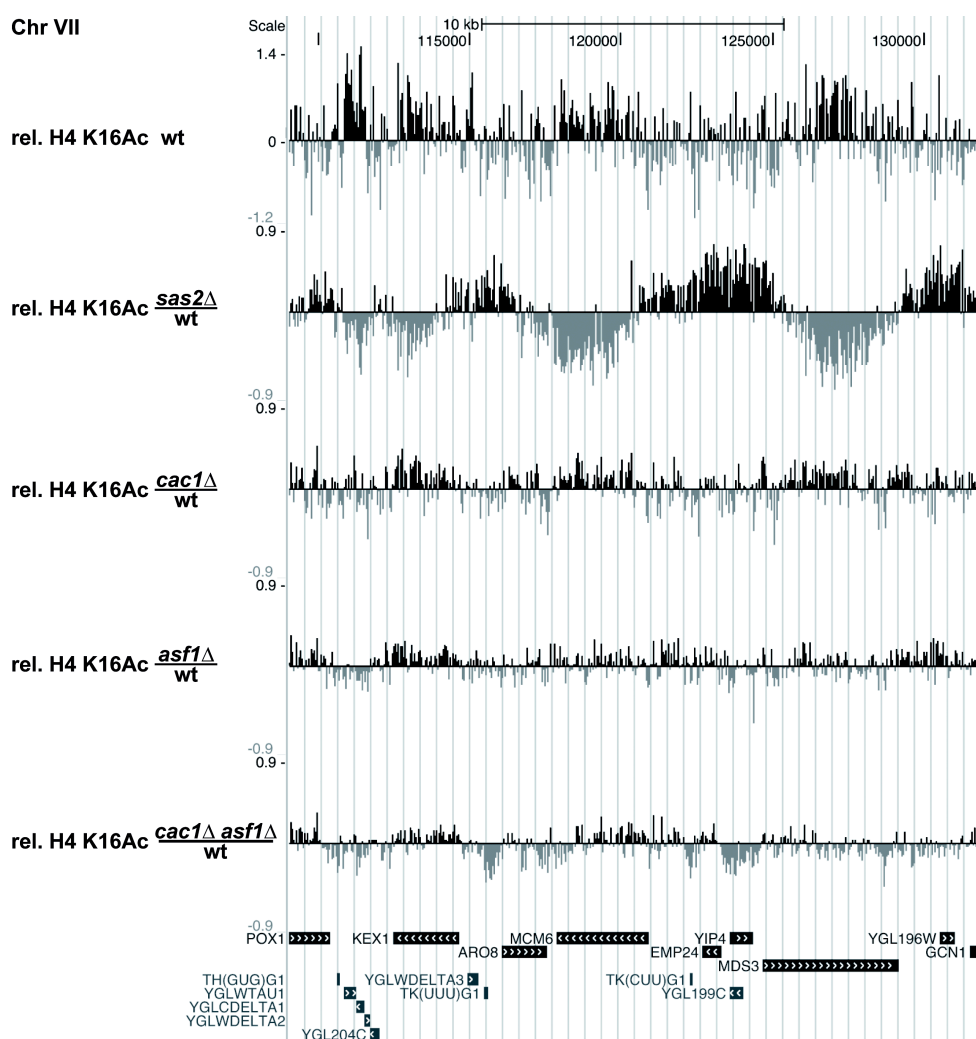


**Figure 13. H4 K16Ac was depleted along ORFs in *sas2Δ* cells.**

Representative region of H4 K16Ac depletion in a region of 20 kb at Chr VII. Tiling array data is presented as described in Fig. 6. Bioinformatic analysis was performed by H.-R. Chung.

This pattern was observed throughout the genome and has gone unnoticed in previous studies. Partially because global H4 K16Ac protein levels were analyzed (Kimura et al. 2002) and region specific experiments were performed, at the subtelomeric region of chromosome VI-R (Kimura et al. 2002; Suka et al. 2002) and also due to technical limitations that is a microarray consisting of spots gained from PCR products (Shia et al. 2006) in contrast to the high resolution tiling arrays used in this study. In other words,



**Figure 14. Depletion of H4 K16Ac at the *CSF1* gene, in *sas2Δ*.**

(A) H4 K16Ac profiling in a region of 35 kb at Chr XII around *CSF1*. Tiling array data is presented as described in Fig. 6. Bioinformatic analysis was performed by H.-R. Chung. (B) ChIP analysis verification of H4 K16Ac at the *CSF1* gene in wt and *sas2Δ*. The relative acetylation, calculated as percent of input, was determined at the 5' end, the center and the 3' region of the gene. Error bars represent technical replicates.

In order to quantitate the observed acetylation pattern, the tiling array data was mapped to RNA expression data of wild-type cells and *sas2Δ* cells (Fig. 15A). This analysis was performed by Ho-Ryun Chung. Transcripts were binned according to transcription frequency, and genes were normalized to 100 % length. In wild-type cells, acetylation was lower in genes that were transcribed more frequently, whereas genes that were less transcribed, showed a higher level of H4 K16Ac (Fig. 15A, left panel) (Kurdistani et al. 2004; Liu et al. 2005) suggesting that H4 K16 acetylation was removed from ORFs during transcription.

Interestingly, there was a marked loss of H4 K16Ac towards the 3' end of genes in *sas2Δ* cells, in particular at those genes with low expression rates, whereas H4 K16Ac remained higher at the 5' region (Fig. 15A, middle panel). Thus, H4 K16 acetylation by SAS-I was most pronounced in the region of the gene where PolIII is in the elongation phase of transcription. Of note, because the ChIP-chip data was normalized for each strain individually, the relative H4 K16Ac level in *sas2Δ* can not be directly compared to the level in wt cells. The average acetylation level in *sas2Δ* cells is likely lower than the average acetylation level in wt, since the deletion of *SAS2* caused a decrease of bulk H4 K16Ac. Nonetheless, investigation of the average change in relative H4 K16Ac in *sas2Δ* as compared to wt (Fig. 15A, right panel) showed that there was less change in the 5' region of ORFs, and that the H4 K16Ac depletion was stronger towards the 3' end of the genes.

This effect was more pronounced in genes with lower expression rates than in the most strongly expressed genes (81 – 100%). Furthermore, the 3' region of genes is characterized by lower H3 exchange rates than the promoter regions (Rufiange et al. 2007), suggesting an inverse correlation between SAS-I dependent acetylation and histone exchange (see below).

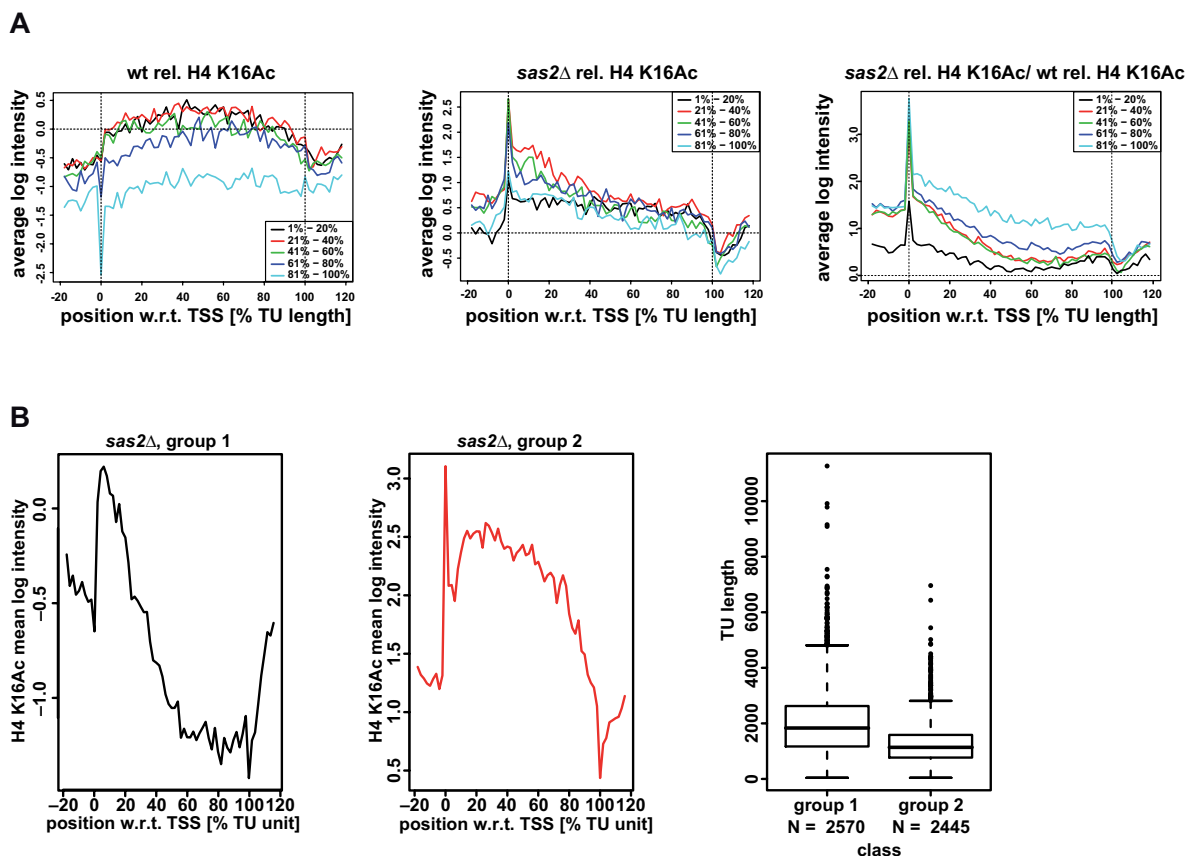


**Figure 15.** *sas2Δ* caused a decrease of H4 K16 acetylation in the 3' region of ORFs.

(A) Quantitative analysis of H4 K16Ac in wt and *sas2Δ*. Yeast genes were binned according to transcription frequency (%) using RNA expression data for wt (left) or *sas2Δ* (middle and right), and transcripts were normalized to 100 % length. The graph shows the average relative H4 K16Ac of binned genes in wt (left) and *sas2Δ* (middle). The graph on the right shows the change in relative H4 K16Ac between *sas2Δ* and wt. (B) Analysis of the H4 K16Ac profile (relative to H4) of *sas2Δ* relative to gene length. Genes were classified by *k*-means clustering. Average H4 K16Ac profile of group 1 and 2, respectively (left and middle panel). Right, box plot of length of transcription units of each group. Note that genes belonging to group 1 were significantly longer than those of group 2 ( $p$ -value <  $2.2e-16$ ). Whiskers extend the box 1.5 times the box height, dots denote outliers. Bioinformatics was performed by H.-R. Chung.

Our visual inspection of the data suggested that the H4 K16Ac pattern in *sas2Δ* cells was more pronounced at long than at short ORFs. To follow this idea, genes were clustered in two groups according to their H4 K16 acetylation profile in *sas2Δ* cells (Fig. 15B, left and middle). The genes of group 1 showed a drop of H4 K16Ac predominantly in the second half of the gene, and these genes were significantly longer than the genes of group 2 (Fig. 15B, right panel). The H4 K16Ac profile of group 2 genes showed an overall higher level of acetylation and a less pronounced decrease in the 3' region as compared to group 1, and these genes were on average shorter than those of group 1. Thus, in summary, this analysis revealed that acetylation of H4 K16 by SAS-I was most pronounced in the 3' region of long genes that have a low transcription rate.

### 3.1.5 *sas2Δ* cells showed resistance to 6-azauracil

Given that the deletion of *SAS2* resulted in a strong genome-wide effect on H4 K16 acetylation within ORFs, the region of genes where RNA Polymerase II (PolII) is in the elongation phase of transcription, we asked whether this was reflected in an effect of *sas2Δ* on transcription elongation by determining the sensitivity of *sas2Δ* cells to 6-azauracil (6-AU). 6-AU causes a reduction of the intracellular nucleotide pools and renders PolII unable to elongate efficiently in the absence of positive transcription elongation factors (Mason and Struhl 2005). Conversely, some chromatin remodeling and modification factors, for instance Isw1 (Morillon et al. 2003a), or the H3 K36 methyltransferase Set2 (Keogh et al. 2005), cause resistance to 6-AU (Fig. 16A and C). Interestingly, *sas2Δ* cells showed a higher resistance to 6-AU than wild-type, suggesting that transcription elongation was facilitated in the absence of Sas2 (Fig. 16A).

While the resistance of *sas2Δ* to 6-AU at high concentrations was less strong than that of *set2Δ* (Fig. 16C), an additional deletion of *SAS2* in a *set2Δ* background caused a slight reduction in 6-AU resistance, thus indicating a possible cooperation of both histone modifying enzymes in transcription elongation (see below). Resistance to 6-AU is contingent upon the ability of cells to induce the *IMD2* gene (Hyle et al. 2003) (see below), a process that is disturbed in the absence of positive-acting elongation factors, but 6-AU sensitivity can also be obtained by means unrelated to elongation (Riles et al. 2004), for instance by influencing the expression of drug transporters (Garcia-Lopez et al. 2010). However, the 6-AU resistance of *sas2Δ* depended upon the elongation factor Dst1 (Fig. 16B), demonstrating that it was not due to unspecific effects of Sas2 on drug transport. Since *IMD2* is located close to the right arm of TEL VIII, it is possible that the effect of *sas2Δ* on telomeric silencing affected *IMD2* expression and thus 6-AU resistance.

However, the *sas2Δ* 6-AU resistance was independent of *SIR2*, *SIR3* (Fig. 16D) and *SIR4* (data not shown), further supporting the notion that the 6-AU resistance was reflecting an effect on transcription elongation. Furthermore, mutation of H4 K16 to arginine, which mimics the deacetylated state, displayed a 6-AU resistance phenotype similar to that of *sas2Δ* (Fig. 16E), indicating that Sas2 exerted a repressive effect on transcription elongation through acetylation of H4 K16.

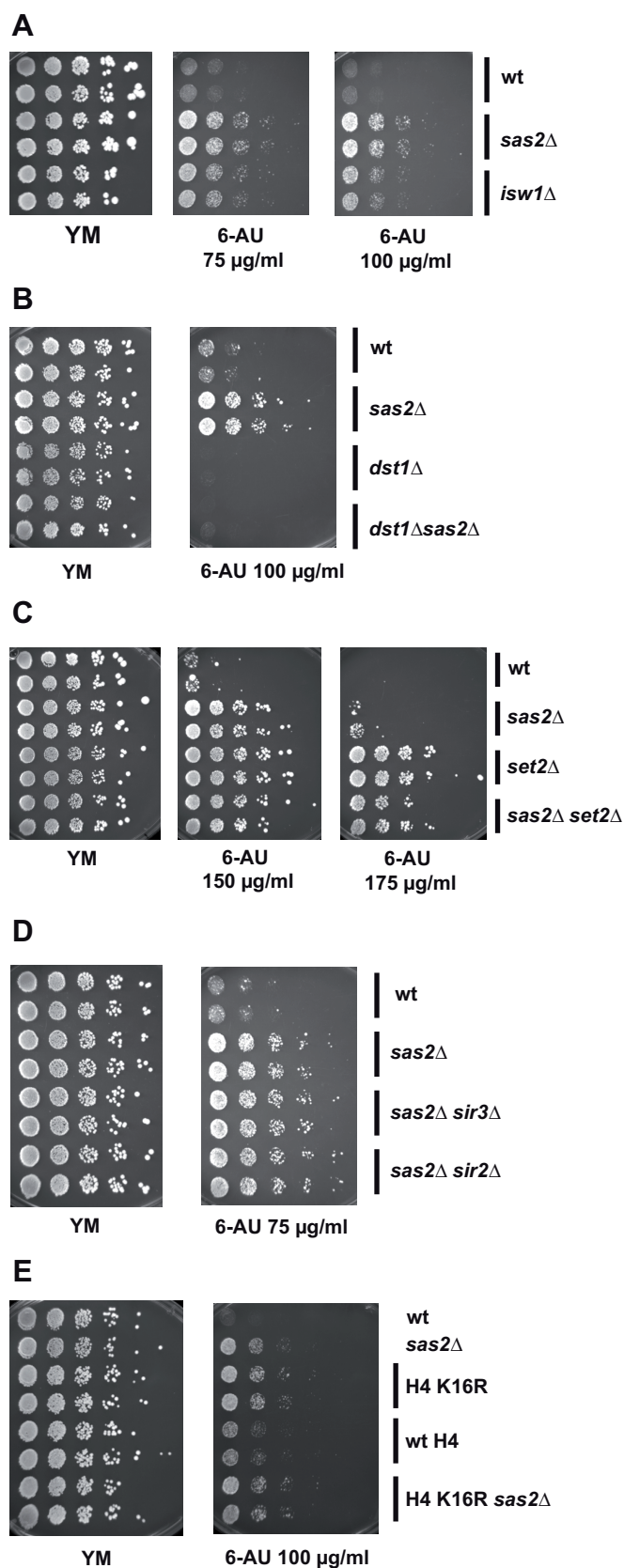


**Figure 16. Deletion of SAS2 caused resistance to 6-azauracil (6-AU).**

(A) *sas2Δ* cells were more 6-AU resistant than *isw1Δ*. (B) *sas2Δ* was epistatic to *dst1Δ*. (C) *sas2Δ* showed a lower 6-AU resistance than *set2Δ*. (D) The 6-AU resistance of *sas2Δ* was independent of telomeric silencing, as indicated by the observation that *sir2Δ* or *sir3Δ* did not alter the 6-AU resistance of *sas2Δ*. (E) Mutation of H4 K16 to arginine (H4 K16R) caused 6-AU resistance. (A-E) Serial dilutions of the indicated strains carrying an *URA3*-marked plasmid were plated on 6-AU containing medium and incubated for three days at 30 °C. Images are courtesy of Prof. A. E. Ehrenhofer-Murray.

### 3.1.5.1 Comparable *IMD2* expression level in wt and *sas2Δ* cells

*IMD2* was previously shown to be induced in the presence of 6-AU (Hyle et al. 2003), and therefore one reason for the resistance of *sas2Δ* cells to 6-AU could be an increased expression of the *IMD2* gene. To investigate this hypothesis, we examined the expression levels of *IMD2* in wild-type and *sas2Δ* cells upon induction with 6-AU for 0, 30 and 120 min (Fig. 17). *IMD2* levels were elevated in both wild-type and *sas2Δ* after 30 and 120 min of 6-AU induction compared to cells without treatment. However, levels in *sas2Δ* did not exceed wild-type *IMD2* expression levels. Deletion of *SAS2* therefore did not affect *IMD2* expression, indicating that 6-AU resistance in *sas2Δ* must occur for reasons other than induction of *IMD2* gene.

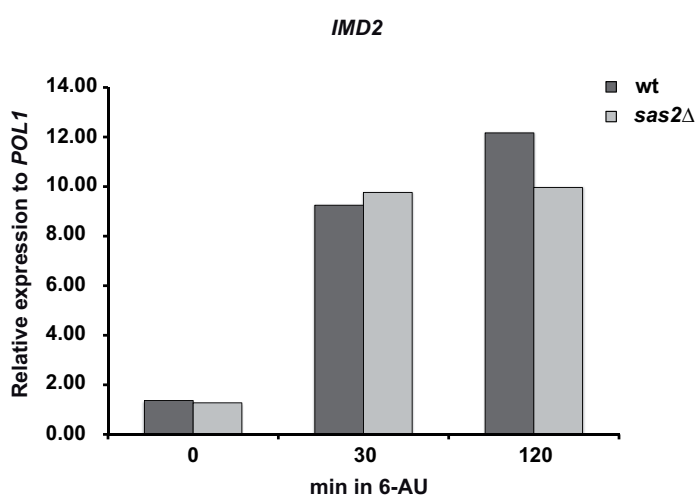


**Figure 17. *IMD2* induction upon 6-AU treatment did not increase in *sas2Δ*.**

RNA expression analysis of the *IMD2* gene upon induction with 6-azauracil (6-AU) for 0, 30 or 120 min in wild-type and *sas2Δ*. Expression levels of *IMD2* were determined by quantitative RT-PCR analysis and normalized to expression levels of the *POL1* gene.

### 3.1.5.2 Increased processivity of transcription in *sas2Δ* cells

There are several possibilities for how transcription elongation can be enhanced *in vivo*, namely by affecting the ability of PolIII to travel along the entire length of the gene (processivity), the elongation rate *per se*, or the coupling of transcription to subsequent RNA processing events (Mason and Struhl 2005).

Since the depletion of H4 K16 acetylation at ORFs and increased resistance to 6-AU in *sas2Δ* suggested a role for Sas2 in transcription elongation, we sought to determine how it affected the distribution and migration of PolIII along a gene. For this purpose, we measured the level of PolIII distribution at three positions within the long (8 kb) *FMP27* gene whose expression is driven by the glucose-repressible *GALI* promoter (*GALIpr*) (Mason and Struhl 2005). PolIII levels in wild-type were normalized to 1.0 at each position. Interestingly, *sas2Δ* cells displayed elevated levels of PolIII at the 3' end of the gene in galactose suggestive of an increased accessibility of this region to PolIII (Fig. 18A). This

trend towards an increased level of PolII at the 3' end was also detected at a second gene, the frequently transcribed *PMAI* (Fig. 18B).

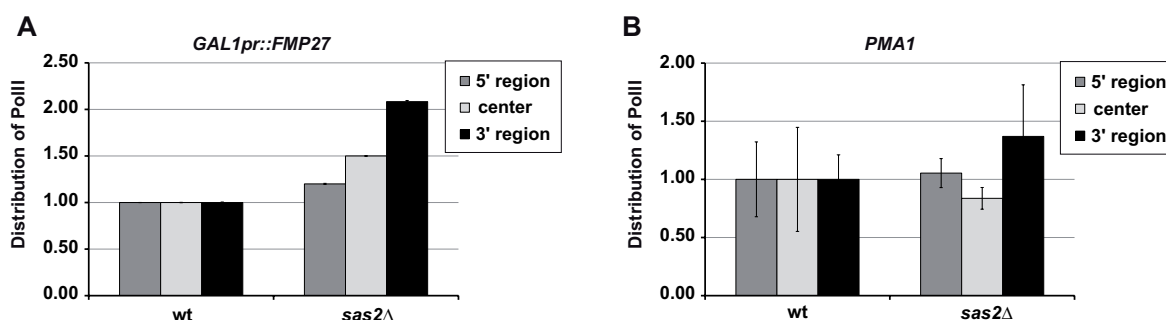


**Figure 18. PolII was present at elevated levels at 3' region of ORFs in *sas2Δ*.**

Distribution of PolII at three indicated positions along *GAL1pr::FMP27* (A) and *PMAI* (B). Cells were grown in galactose (A) or glucose (B), values in wild-type were normalized to 1.0 at each position, error bars represent technical (A) and three independent replicates (B).

Therefore, we furthermore examined the kinetics of PolII dissociation from *GAL1pr::FMP27* upon shift of the cells from galactose to glucose medium in wt and *sas2Δ* cells (Fig. 19A, B) by chromatin immunoprecipitation. The occupancy of PolII was elevated at the 3' end of *FMP27* *sas2Δ* cells. The level of PolII in wt cells, was slightly reduced at 5' region after two minutes and apart from that evenly distributed. This result gave no hint for an affection of the PolII elongation rate upon deletion of Sas2.

Since transcription elongation is associated with different phosphorylation states of the C-terminal domain (CTD) of PolII, we further sought to investigate the influence of *sas2Δ* on two phosphorylation states. Whereas phosphorylation at serine 5 (S5) occurs at the promoter proximal region and is linked to transcription initiation, serine 2 (S2) is phosphorylated during elongation (Hirose and Ohkuma 2007).

To examine the levels of PolII CTD phosphorylation in *sas2Δ* cells, ChIP analysis was performed applying specific antibodies for either S5 or S2 phosphorylation at three different genes (Fig. 20A-F). It has been reported previously that the frequently transcribed gene *PMAI* displayed high levels of S5 phosphorylation at promoter proximal regions and high levels of S2 phosphorylation at regions next to the 3' end (Morillon et al. 2003b). However, using the identical reagents, we were not able to detect this tendency either at *PMAI* (Fig. 20A, B), or at the other tested genes *CSF1* (Fig. 20C, D) and *MPS3* (Fig. 20E, F) in wild-type cells. Furthermore, the detected levels of S5 and S2 phosphorylation in *sas2Δ* cells were indistinguishable from wt in our experiment, but different from the previously reported phosphorylation state of the PolII CTD domain along a gene. In conclusion, these experiments suggested that the processivity, but not the elongation rate of PolII increased in the absence of Sas2.

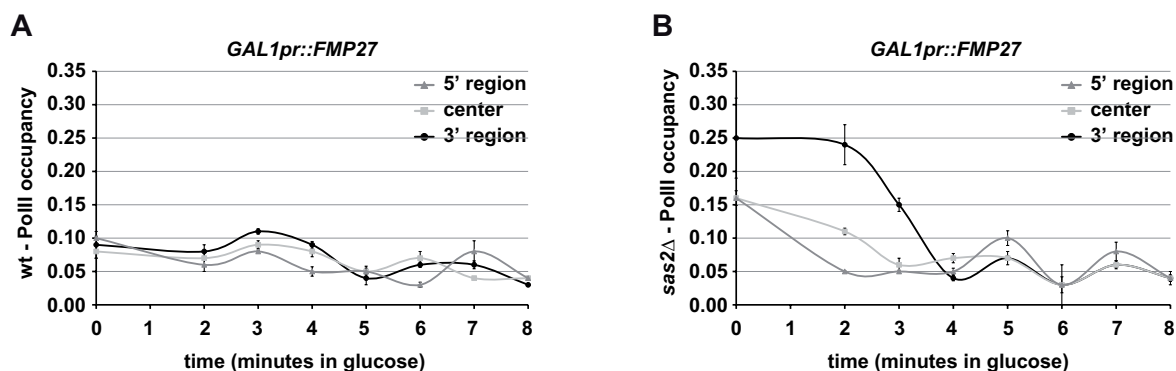


**Figure 19. PolII dissociation was slowed down at the 3' end of *GAL1pr::FMP27* in *sas2Δ*.**

ChIP analysis of the last wave of PolII occupancy at indicated regions of *GAL1pr::FMP27* in wild-type (A) and *sas2Δ* (B). Cells were grown in galactose and samples were taken after shift to glucose at indicated times. The experiment was performed with technical assistance from C. Reiter. Samples were normalized to Input. Error bars present technical replicates.

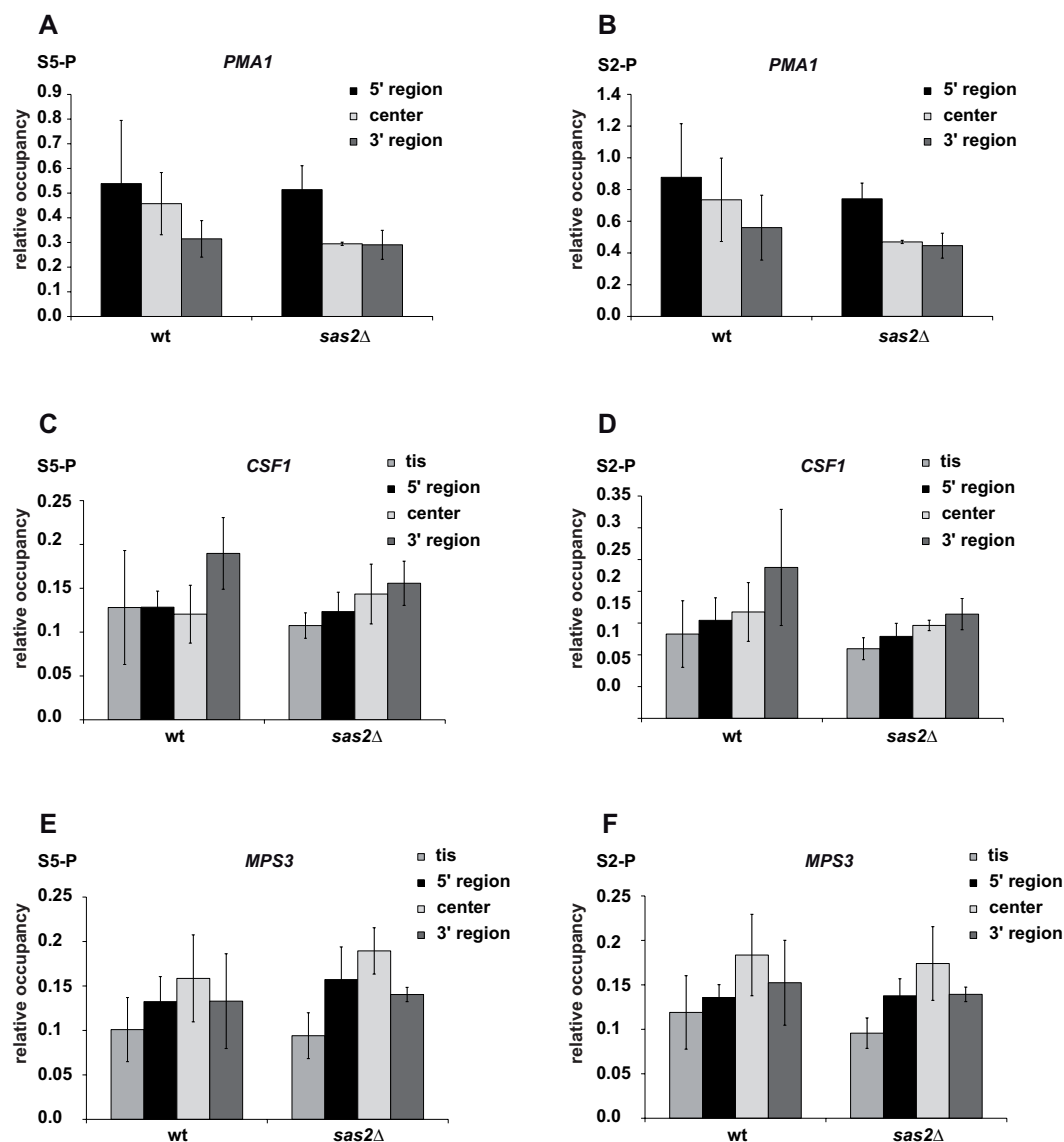


**Figure 20. Levels of PolIII CTD phosphorylation at S5 and S2 of were not altered by *sas2Δ*.**

Occupancy of PolIII phosphorylated at CTD-S5 or S2 was determined at three or four indicated positions (tis: transcription initiation site) at *PMA1* (A, B), *CSF1* (C, D) and *MPS3* (E, F). The relative level of occupancy was determined as percent of input. Error bars represent technical replicates.

### 3.1.6 Accumulation of transcripts at the 3' end of genes in *sas2Δ* cells

One prediction from the data above is that in the absence of Sas2, the chromatin might become more loose, which may then lead to increased accessibility to PolIII transcription from sequences within the ORF. Previous studies found that chromatin that was loosened e.g. by deletion of the chromatin remodeler Isw2 (Whitehouse et al. 2007) or transcription elongation factors (Kaplan et al. 2003) subsequently resulted in inappropriate transcription events. To investigate the possible affection of transcription by Sas2, a genome-wide RNA expression analysis of *sas2Δ* and wild-type cells was performed in cooperation with the group of Lars Steinmetz from the European Molecular Laboratory, Heidelberg. Therefore, total RNA was prepared and hybridized to a custom designed tiling array (David et al. 2006) comprised of both strands of the complete genomic sequence and therefore enables to examine transcription events arising from one strand or the other (bioinformatic processing and analysis performed by Zhenyu Xu and Ho-Ryun Chung). For the analysis genes in the yeast genome were divided into four different groups: genes that were 1) strongly activated, 2) slightly activated, 3) strongly repressed or 4) slightly repressed in *sas2Δ* cells (Fig. 21A and data not shown). Genes that were strongly repressed in *sas2Δ* are those that are located in subtelomeric regions and are therefore repressed by inappropriate SIR spreading (Reifsnyder et al. 1996). They showed visible differences in expression between wild-type and *sas2Δ*, e.g. at TEL-IV (Fig. 21B, compare upper and lower row in each panel). Interestingly, the two main gene clusters, representing the majority of genes of the genome, the slightly activated ( $n = 2586$ ) and slightly repressed genes ( $n = 1526$ ) showed a mild increase in transcript levels at the 3' end of genes, indicating that Sas2 affected transcription mildly, but globally. This was not seen in the other two groups of genes. Both clusters of slightly activated and slightly repressed genes also showed a peak at the 5' end, which might be explained by abortive transcription.

It was shown in previous studies that the deletion of some factors, e.g. the methyltransferase Set2, transcription elongation factors or the chromatin remodeler Isw2 (Kaplan et al. 2003; Carrozza et al. 2005; Whitehouse et al. 2007; Cheung et al. 2008) caused aberrant transcription, so called cryptic transcription. This phenomenon only occurred at a subset of genes and was shown to generate short transcripts of defined length from a defined cryptic transcription initiation start site. However, the accumulation of transcripts at the 3' end of genes we observed upon deletion of *SAS2* seemed to be more diffuse and occurred more frequently than so far found by cryptic transcription initiation. In the case of *sas2Δ*, such defined transcripts, which in cryptic transcription mutants are typically found e.g. at the genes *STE11* and *FLO8* (Carrozza et al. 2005; Cheung et al.

2008), were not detectable by northern blot analysis (data not shown) or in the expression arrays (Fig. 21C). Based on these differences between the previously described cryptic transcription and the accumulation of transcripts we observed in *sas2Δ* cells, we concluded that the effect caused by the deletion of *SAS2* was distinct from cryptic transcription.

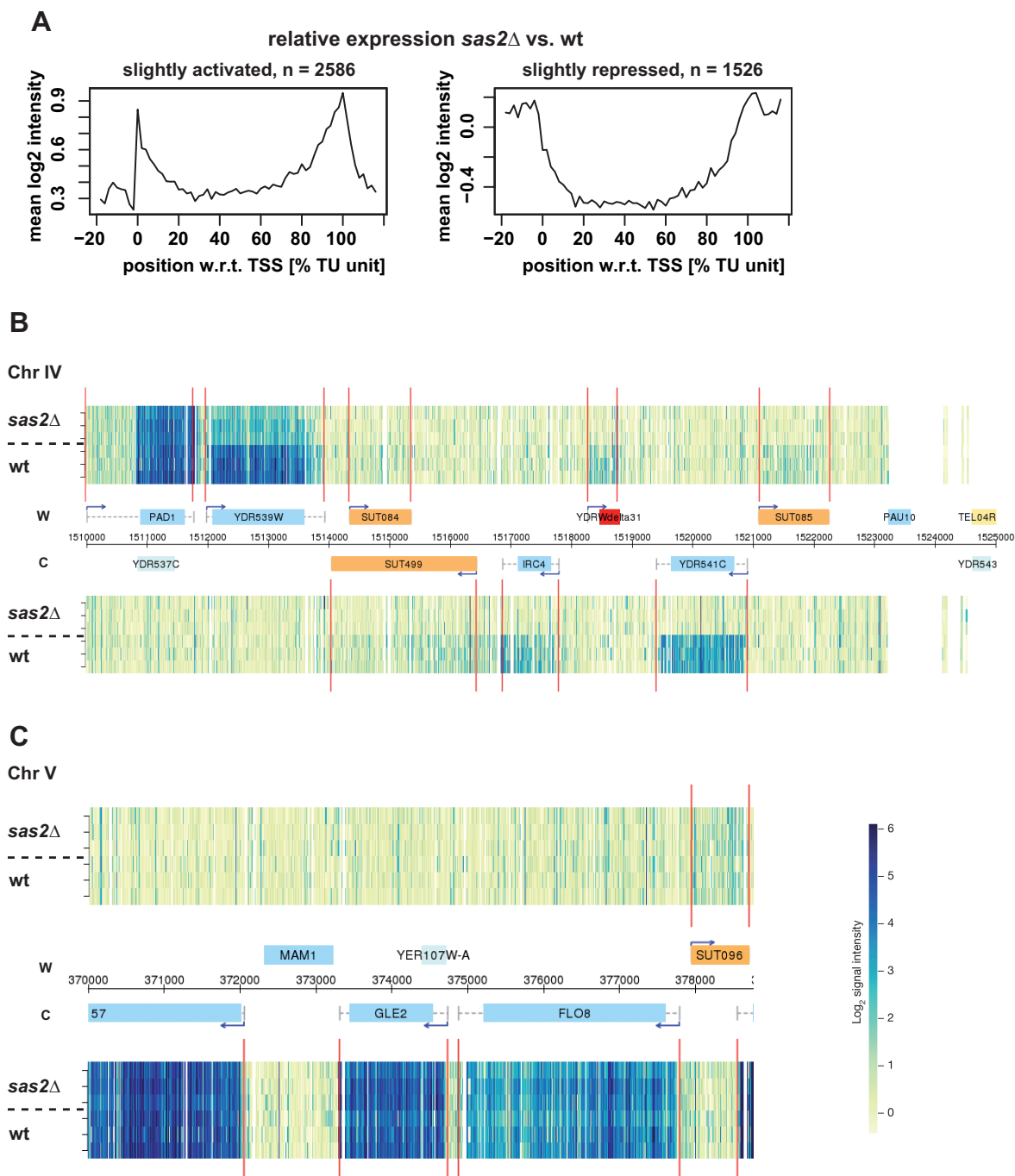


**Figure 21. *sas2Δ* caused an accumulation of transcripts at 3' ends within coding regions.**

(A) RNA expression analysis showed an accumulation of transcripts at the 3' ends of genes that were slightly activated (left) or slightly repressed (right) in *sas2Δ* as classified by k-means clustering (see material and methods). Same-strand transcription in expression clusters from *sas2Δ* versus wt is shown. This also showed increased transcript levels at the 5' end of genes, which may indicate transcription abortion in *sas2Δ*. Bioinformatic analysis performed by H.-R. Chung and Z. Xu. (B) Subtelomeric genes were repressed in *sas2Δ*. Transcript map of expression data along 15 kb of chromosome IV (horizontal axis) for the Watson (W, top) and the Crick (C, bottom) strand. Normalized signal intensities ( $\text{Log}_2$ ), as indicated by color in C, are shown for *sas2Δ* and wild-type (vertical axis), in that blue indicates high expression levels and yellow low expression levels. The three rows for *sas2Δ* and wt indicate the three biological replicates. The vertical

red lines show the inferred transcript boundaries. Genome annotations according to *Saccharomyces* Genome Database (SGD) are shown on the horizontal axis in the center: annotated ORFs (blue boxes) and corresponding UTRs (dashed grey lines), SUTs (stable unannotated transcripts, (Xu et al. 2009) (orange boxes), LTR (red box). Transcription start sites are marked by blue arrows. Numbers indicate coordinates in base pairs. (C) Similar expression levels of *FLO8* in wt and *sas2Δ*. Data is represented as described in B. Experiments were performed with technical help from S. Clauder-Münster. Transcript maps were generated by Z. Xu.

Furthermore, a *GAL1pr*-driven *FLO8-HIS3* reporter construct (Cheung et al. 2008) was used to examine a possible role of Sas2 in cryptic transcription initiation. In this reporter construct, *HIS3* is placed downstream of a cryptic start site within the *FLO8* 3' region, such that cryptic initiation leads to histidine auxotrophy. Full-length *FLO8-HIS3* transcription can be regulated by growth on different carbon sources, since the *FLO8* promoter is replaced by the *GAL1* promoter.

Several mutations that impair transcription elongation have been shown to activate *HIS3* in this construct, including mutations in the genes *SPT6* and *SPT16* that encode transcription elongation factors (Cheung et al. 2008). In agreement with the above data, *sas2Δ* alone was not able to induce cryptic transcription at the reporter construct (data not shown), whereas induction was observed upon mutation of *SPT6* or *SPT16* (Fig. 22A, middle and right panel) (Cheung et al. 2008). However, *FLO8-HIS3* expression was enhanced upon the deletion of *SAS2* in both the *spt6-1004* and the *spt16-197* background (Fig. 22A). *spt6-1004* caused stronger *FLO8-HIS3* expression than *spt16-197* in that cells were mildly His<sup>+</sup> on glucose-containing medium and fully His<sup>+</sup> on galactose medium (Fig. 22A) (Cheung et al. 2008). Accordingly, enhanced cryptic initiation by *sas2Δ* in this background was apparent on glucose-containing medium. Conversely, *FLO8-HIS3* expression in *spt16-197* was only seen under inducing conditions on galactose medium, and *sas2Δ* enhanced this expression. Taken together, *sas2Δ* exerted a mild global effect on the transcript level from within a gene, and it enhanced the initiation of cryptic transcripts caused by defects in elongation factors.

To validate the detected genome-wide effect of *sas2Δ* on 3' transcript levels, we tested if transcript levels at the 3' ends of ORFs were elevated compared to the 5' ends and by determining the 3': 5' ratio at selected genes using quantitative RT-PCR. The ratio of 3' to 5' transcript levels was slightly, but significantly increased upon deletion of *SAS2* (Fig. 22B), indicating that the transcript level was higher at 3' ends than at 5' ends, which confirmed the genome-wide effect of *sas2Δ* on transcription at the level of individual genes. Taken together, these results indicated that transcript levels were mildly influenced by Sas2 on a global scale.

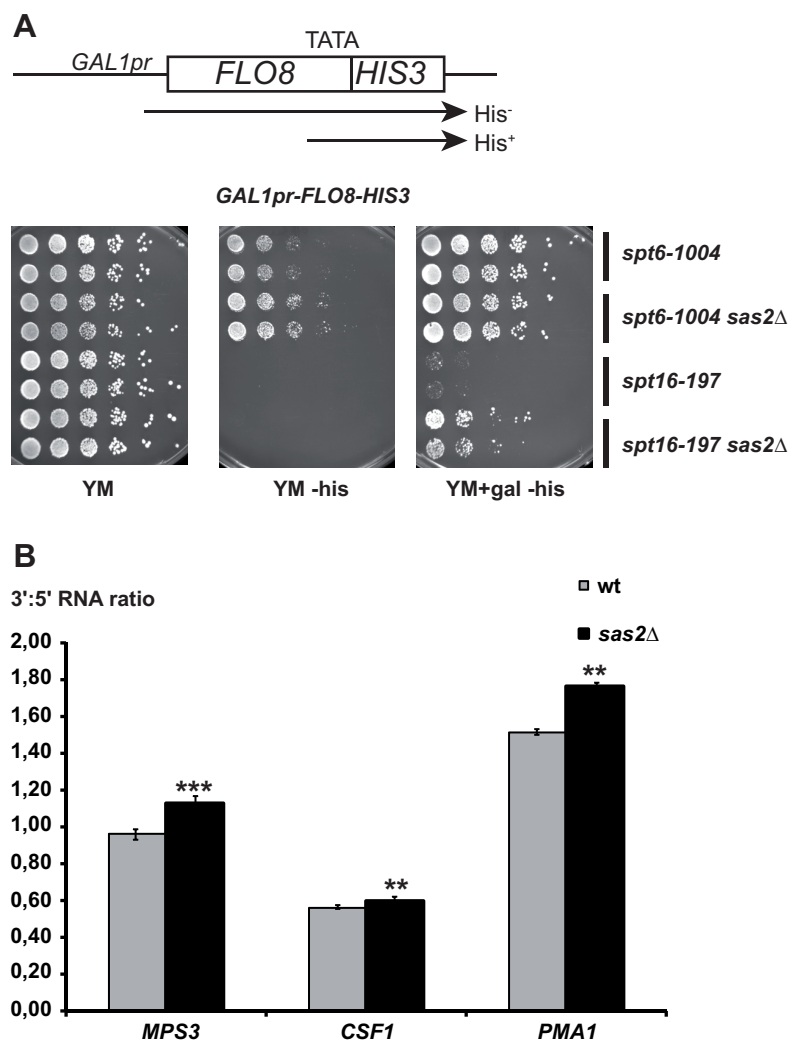


**Figure 22. Accumulation of transcripts at 3' ends in *sas2*Δ.**

(A) *sas2*Δ enhanced accumulation of transcripts from a cryptic promoter from the *pGAL1-FLO8-HIS3* reporter in *spt6-1004* and *spt16-197*. Cells were spotted on the indicated medium. Growth medium containing galactose (+gal) can induce cryptic transcription initiated at *HIS3*, depending on the strainbackground. *sas2*Δ enhanced cryptic initiation in *spt6-1004* and *spt16-197*. (B) 3':5' RNA ratio in *sas2*Δ cells showed a slight, but significant increase at the indicated genes. 3' and 5' RNA expression levels were measured, and the ratio was calculated at the indicated genes in wt and *sas2*Δ cells. Error bars indicate the mean value of three independent RNA preparations. P-values from students t-test are indicated by \*\* ( $p < 0.005$ ), \*\*\* ( $p < 0.001$ ).

### 3.1.7 Partial interdependence of Sas2 and Set2

The H3 K36 methyltransferase Set2 has previously been shown to prevent intragenic transcription (Carrozza et al. 2005; Li et al. 2007b). Since the above data (Fig. 16C) suggested a connection between *sas2*Δ and *set2*Δ and because *sas2*Δ caused a mild increase in cryptic transcription, we therefore asked whether H3 K36 methylation was influenced by Sas2-dependent H4 K16 acetylation and vice versa. Significantly, H3 K36Me<sub>3</sub> was reduced across the whole gene body of *CSF1* in *sas2*Δ as compared to wild-type. However, the reduction was not as pronounced as in *set2*Δ cells (Fig. 23A). This finding indicated that the Sas2-mediated H4 K16 acetylation was required for full

trimethylation of H3 K36 by Set2 at the *CSF1* gene. Conversely, H4 K16 acetylation was only slightly reduced by *set2Δ* in the 3' region ( $p < 0.06$ ), but not throughout the gene body of *CSF1* (Fig. 23B). However, this dependence of H3 K36Me3 on Sas2 did not hold for another gene, the frequently transcribed *PMA1*. Here, we neither found a significant reduction of H3 K36Me3 in *sas2Δ* nor significantly changed levels of H4 K16 acetylation in *set2Δ* cells (Fig. 23C, D). These findings suggested that a cooperation between Sas2 and Set2 took at least place at some genes. There, Sas2 and Set2 are likely to cooperate in establishing chromatin states within ORFs in that Sas2 partially influenced the subsequent histone methylation by Set2. That Sas2 and Set2 might act in cooperation was also supported by the finding that the additional deletion of *SAS2* in the *set2Δ* background caused a slight reduction in 6-AU resistance (see above, Fig. 16C).

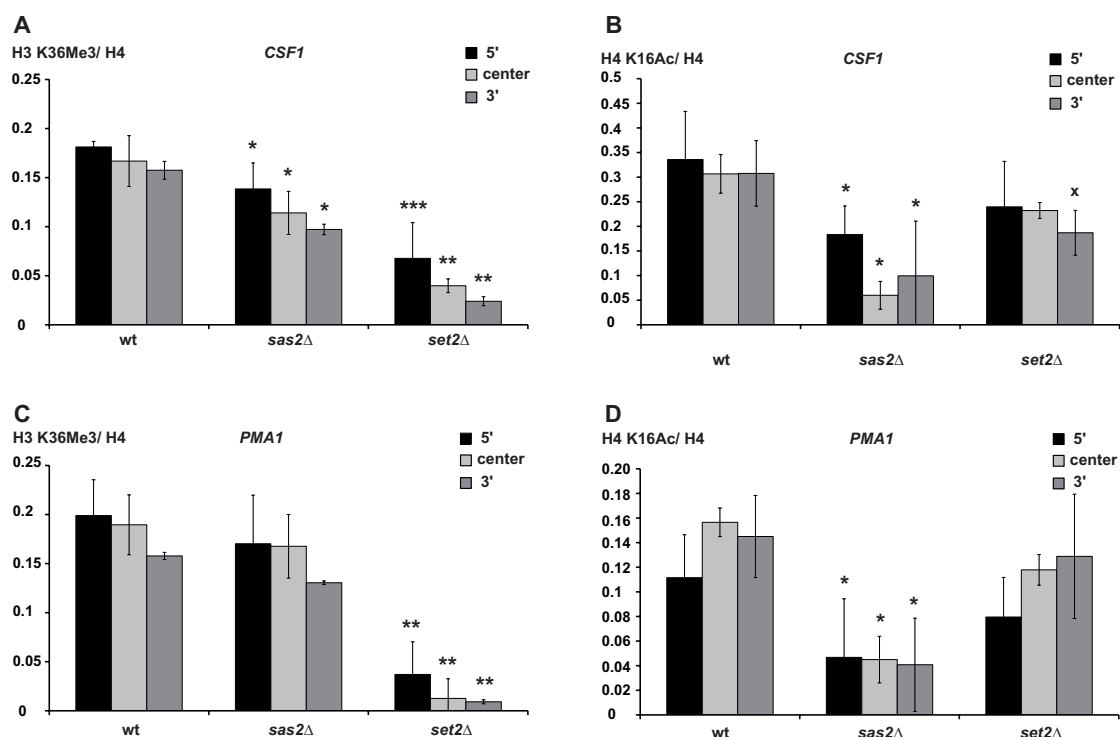


**Figure 23. Influence of Sas2 on Set2-mediated H3 K36 methylation.**

(A-D) Influence of Sas2 and Set2 on H3 K36Me3 and H4 K16Ac, respectively, was examined by ChIP analysis. Fragments amplified by qPCR at the *CSF1* (A, B) and *PMA1* gene (C, D) were located at the 5' region, center of the gene and 3' region. H3 K36Me3 and H4 K16Ac was normalized relative to nucleosome density (unmodified H4). Error bars indicate the standard deviation of three independent experiments. P-values indicated by \* ( $p < 0.05$ ), \*\* ( $p < 0.005$ ), \*\*\* ( $p < 0.001$ ) and <sup>x</sup> ( $p < 0.06$ ) show the statistical significance of changes in histone modifications. Experiment was performed with technical help from J. Weber.

### **3.1.8 Sas2-dependent H4 K16 acetylation was predominantly found in regions of low histone exchange and low H3 K56 acetylation**

Our analysis above showed that Sas2-mediated acetylation was predominantly deposited on long ORFs with a low transcription rate, raising the question as to how this pattern of H4 K16Ac deposition is generated. Of note, low transcription rates are associated with low levels of histone H3 exchange as well as with low levels of H3 K56 acetylation along a gene (Rufiange et al. 2007), thus suggesting a correlation between low histone exchange and high levels of Sas2-dependent H4 K16Ac.

Importantly, a correlation analysis of our genome-wide H4 K16Ac data from wild-type cells with H3 K56Ac data (Rufiange et al. 2007) revealed that these modifications were mutually exclusive in that regions with high H3 K56Ac showed low H4 K16Ac and vice versa (Fig. 24A) (bioinformatic analysis performed by Ho-Ryun Chung). Since H3 K56Ac marks sequences with high histone exchange (Rufiange et al. 2007), this showed that the histones incorporated during histone exchange were hypoacetylated on H4 K16. On the other hand, the observation that low H3 K56Ac, and thus low exchange, correlated with higher H4 K16Ac indicated that K16 acetylation occurred at a time point other than histone exchange.

One prediction from this analysis would be that H4 K16 acetylation mediated by Sas2 would be reduced upon deletion of *SAS2* at regions that displayed low histone exchange and low levels of H3 K56Ac and that this loss would be less pronounced in regions with high exchange. Significantly, we found a strong correlation of the pattern of reduced H4 K16Ac in *sas2Δ* and low histone exchange and low H3 K56Ac (Fig. 24B). Histone exchange was previously shown to be high at promoter regions (Rufiange et al. 2007) and these regions were less affected by the deletion of *SAS2*. The drop of H4 K16 acetylation in *sas2Δ* was observed along the gene body and thus correlated with regions of reduced exchange along the ORF (Rufiange et al. 2007). Also, intergenic regions with high H3 exchange were less susceptible to loss of H4 K16Ac in *sas2Δ*. In conclusion, this showed that Sas2-dependent H4 K16 acetylation was deposited in the genome outside of transcription- and histone exchange-dependent histone turnover. Since SAS-I interacts with CAF-I that performs DNA replication-coupled chromatin assembly on possibility would be that Sas2-mediated acetylation might be deposited during this process. To this end, the question at which time point Sas2-mediated H4 K16 acetylation is introduced on chromatin was addressed in the next set of experiments (see below).

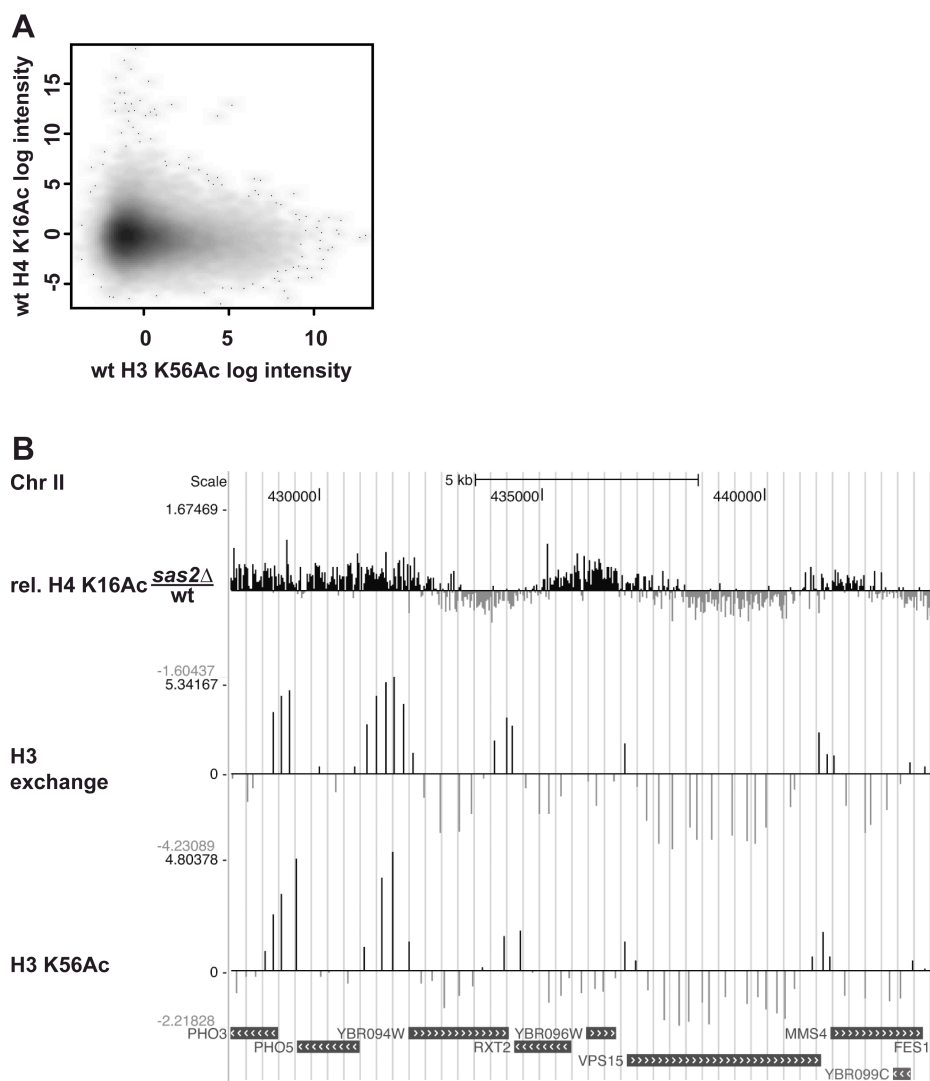


**Figure 24. H4 K16Ac was present in regions with low H3 K56 Ac and low histone H3 exchange.**

(A) Correlation analysis of relative H4 K16Ac and H3 K56Ac (Rufiange et al. 2007). (B) Comparison of the change of relative H4 K16Ac in *sas2Δ* compared to wt with H3 exchange and H3 K56Ac levels (Rufiange et al. 2007). The data is represented as in Fig. 6. Bioinformatic analysis by H.-R. Chung.

### 3.1.9 H4 K16Ac in *CAC1* and/ or *ASF1* deletion strains was less changed in regions with low histone exchange

We showed above that the chromatin assembly factors CAF-I and Asf1 display a partial influence on Sas2-mediated H4 K16 acetylation. Asf1 is not exclusively associated to replication-coupled assembly but was also shown to be involved in replication-independent histone exchange (Robinson and Schultz 2003; Green et al. 2005).

Since both factors are involved in nucleosome dis- and reassembly, we furthermore sought to investigate the correlation of the changes in H4 K16Ac in *cac1Δ*, *asf1Δ* and *cac1Δ asf1Δ* strains with the H3 exchange data (Rufiange et al. 2007). We observed a moderate but consistent reduction of H4 K16Ac in *cac1Δ*, *asf1Δ* and *cac1Δ asf1Δ* cells in regions with high histone exchange and high levels of H3 K56Ac (Fig. 25 third to last row). This pattern appeared in anticorrelation to the observed decrease of H4 K16Ac in *sas2Δ* cells along the gene body, at regions with low exchange (see above) and matched the result that H4 K16Ac was low in regions that are strongly transcribed. Additionally, the reduction in *cac1Δ*, *asf1Δ* and *cac1Δ asf1Δ* correlated with regions low in H4 K16Ac in wild-type (Fig. 25, compare third to fifth row with the first row) indicating that there was a low level of H4 K16Ac incorporated into chromatin in regions of high levels of exchange that was dependent on CAF-I and Asf1.

Conversely, at regions of low histone exchange, H4 K16Ac was less changed in *cac1Δ*, *asf1Δ* and *cac1Δ asf1Δ* cells, indicating that in these particular regions the removal of H4 K16Ac was dependent on CAF-I and Asf1 (Fig. 25 third to last row). One explanation for this mild change might therefore be that H4 K16Ac accumulated due to reduced exchange in the absence of *CAC1* and *ASF1*. Taken together, H4 K16Ac was absent at high levels of transcription-coupled histone exchange and H3 K56Ac and then again accumulated at regions with low exchange in the absence of *CAC1* and *ASF1*. Still, the question remained when H4 K16 acetylation is deposited into chromatin and if this incorporation would be dependent on CAF-I and Asf1.



## **3.2 Cell-cycle dependent deposition of H4 K16 acetylation by Sas2**

### **3.2.1 Generation of a repressible *SAS2* allele was achieved by construction of a heat-inducible N-degron**

The experiments described above led us to hypothesize that Sas2 deposits H4 K16 acetylation in chromatin during DNA replication-coupled chromatin assembly. In order to test this hypothesis experimentally, we designed the following experiment. In a first step, Sas2 would be shut off to remove all Sas2-dependent H4 K16Ac, and cells would then be arrested in the G1 phase of the cell cycle. Cells would then be split, and one half would be kept in the G1 cell-cycle arrest, whereas the other half would be released to progress through the subsequent S-phase. At the same time, Sas2 would be switched on in both samples. Due to the depletion of H4 K16Ac at the beginning of the experiment, differences in newly acetylated H4 K16Ac level upon Sas2 induction should be detectable between arrested and released cells. This should allow us to determine whether the deposition of H4 K16 acetylation appeared to be coupled to the S-phase of the cell cycle.

In order to perform this experiment, we required a repressible *SAS2* allele that could quickly be switched on again. The first approach was made using a construct where a myc-tagged Sas2 was under the control of the *MET3* promoter, which is repressed in the presence of methionine. To test for effective repression, Western blot analysis was performed. Sas2 was detected in cells carrying a myc-Sas2 plasmid where *SAS2* was under the control of its natural promoter (Fig. 26A, lanes 3-5). Sas2 levels were higher in cells bearing the *MET3pr-SAS2* construct that were grown in medium without methionine (Fig. 26A, lanes 5-7). The addition of 400  $\mu$ M methionine minimally reduced the expression, but even a high concentration of 800  $\mu$ M methionine did not cause a complete reduction, and Sas2 was still detectable (Fig. 26A, far right lanes). Even though this construct did not fully repress Sas2, its functionality was tested using a genetic mating assay. This assay takes advantage of the reduced mating ability of *sir1 $\Delta$  sas2 $\Delta$  MATa* cells with a *MAT $\alpha$*  tester strain due to the derepression of *HML $\alpha$* . The mating ability could be restored by complementation with a functional *SAS2* (Fig. 26B) (Reifsnyder et al. 1996; Ehrenhofer-Murray et al. 1997). *MET3pr-SAS2* was able to restore the mating ability to the same extent as wild-type *SAS2* on medium lacking methionine (Fig. 26B, middle panel). Under repressive conditions (+Met), *MET3pr-SAS2* still complemented the mating defect of the *sir1 $\Delta$  sas2 $\Delta$*  strain (Fig. 26B, right panel), indicating that the repression of *MET3pr-SAS2* by methionine was not sufficient for a full loss of Sas2 function.

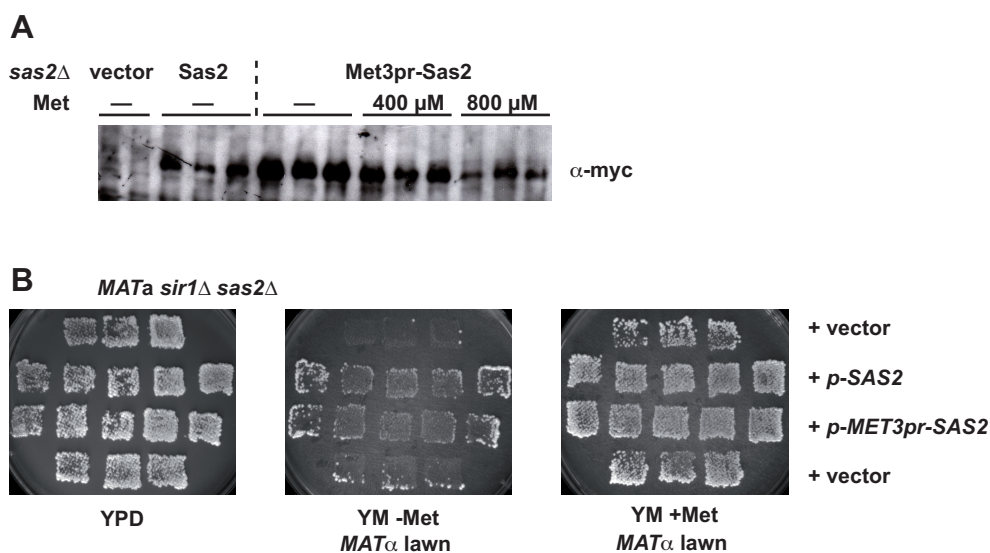


**Figure 26. Myc-tagged Sas2 under the control of the methionine repressible promoter *MET3*.**

(A) Incomplete repression of Met3pr-6xmyc-Sas2 in the presence of methionine. Western blot analysis using  $\alpha$ -myc antibody of whole cell extracts from cells with *sas2Δ* background bearing plasmids: lanes 1-2 empty vector, lanes 3-5 6xmyc-Sas2, lanes 6-14 Met3pr-6xmyc-Sas2. Strains with Met3pr-6xmyc-Sas2 were grown in medium containing 400  $\mu$ M, 800 $\mu$ M methionine to repress Sas2 or without methionine. (B) *p-MET3pr-SAS2* was able to complement the *HML $\alpha$*  silencing defect of *MATa sir1Δ sas2Δ* cells. Cells were tested for their mating ability with a *MAT $\alpha$*  mating tester strain. *p-MET3pr-SAS2* cells were grown on plates with 400  $\mu$ M methionine prior to the mating test.

A next attempt was made by applying the N-terminal tagging technique (Janke et al. 2004) in which the *SAS2* promoter was replaced with a galactose-inducible promoter, *GALLpr*, and Sas2 concomitantly was tagged with three HA-tags. Western blot analysis showed that 3x HA-Sas2 was not detectable under repressive conditions in medium with glucose compared to non-repressive conditions with galactose as the only carbon source (Fig. 27A, upper panel). Furthermore, as expected, H4 K16 acetylation was also strongly, but not completely reduced in the absence of Sas2 in glucose containing medium (Fig. 27A, middle panel). This is likely due to the fact that there are other HATs that also carry out H4 K16 acetylation, e.g. Esa1 (Suka et al. 2002). Sas2 functionality was tested performing a mating assay with strains containing the silencing defective *HMRa-e\*\** allele. *MAT $\alpha$*  cells bearing the *HMRa-e\*\** allele are mating-defective due to derepression of their *HMRa* locus by mutations in the *HMR-E* silencer. The defective mating phenotype was suppressed by the deletion of *SAS2*, as was previously shown (Ehrenhofer-Murray et al. 1997) (Fig. 27B, first row), because cells containing *SAS2* showed less efficient mating compared to *sas2Δ*. The mating ability of the *GALLpr-SAS2* strain, which was grown under repressive conditions (glucose) before mating, was higher than in *SAS2* cells, but still lower than in the *sas2Δ* strain. Since this effect was not very explicit, the construct was integrated into a *TEL VII L* background and further tested for functionality in a *URA3* silencing assay. Once again, under repressive conditions the *GALLpr-SAS2* construct was

able to complement the silencing defect (data not shown). This result indicated that the *GALLpr-SAS2* construct still produced low levels of Sas2 under repressing condition, even though Sas2 protein was not detectable by Western analysis (Fig. 27A), and it thus was not of use for the planned experiment. Furthermore, a similar *SAS2* construct consisting of the weaker *GALS* promoter (Janke et al. 2004) was also tested for functionality, but also did not show sufficient repression in glucose containing medium (data not shown). The reason why both constructs failed to repress Sas2 efficiently remained unclear.

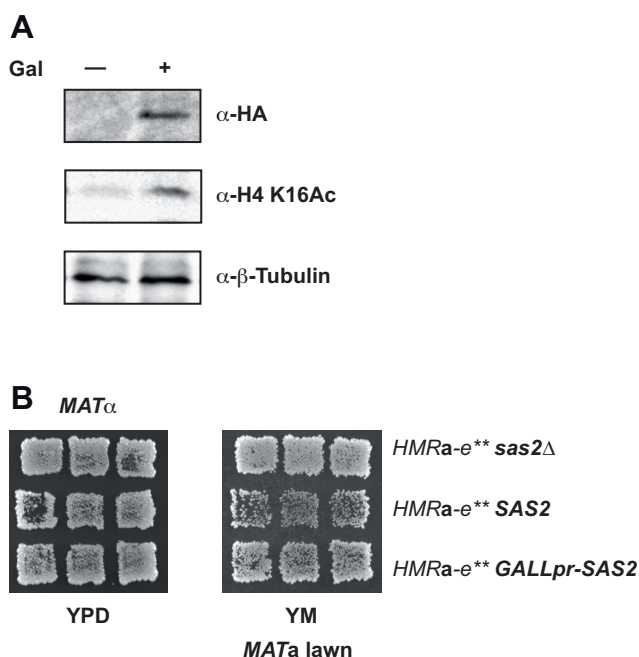


**Figure 27. Repression of *GALLpr-SAS2* was still able to complement the *HMRa-e\*\** silencing defect.**

(A) Western blot analysis of whole-cell extracts of the galactose-inducible and glucose-repressible GalLpr-3x HA-Sas2 construct and its influence on H4 K16Ac. HA-Sas2 was not detected under repressive conditions, but in the presence of galactose with an antibody against the HA epitope tag (first row). H4 K16Ac was strongly reduced in the absence of Sas2 (second row).  $\beta$ -Tubulin immunoblot served as a loading control (third row). (B) *GALLpr-SAS2* complemented *HMRa-e\*\**. *MAT $\alpha$*  *HMRa-e\*\** cells with *sas2 $\Delta$* , *SAS2* and *GALLpr-SAS2* grown under repressive conditions with glucose were tested for their ability to mate with a *MATa* mating tester strain.

We speculated that maybe a resetting of some epigenetic modifications during meiosis would be necessary to obtain a complete repression. To test this hypothesis, we crossed a *sas2 $\Delta$  TEL VII-L::URA3* strain with a strain bearing the *GALLpr-SAS2* construct. The *GALLpr-SAS2 TEL VII-L::URA3* strain derived from the cross was tested for functionality in a telomeric *URA3* silencing assay. The loss of *SAS2* led to a derepression of telomeric *URA3*, as was previously shown (Xu et al. 1999) (Fig. 28, right panel), as shown by the inability of *sas2 $\Delta$*  cells to grow on 5-FOA containing medium. An intact *SAS2* allele restored the silencing of *URA3*. This was also observed for the *GALLpr-SAS2* strain, although *URA3* silencing was slightly weaker than that of Sas2 (Fig. 28, right panel). At

any rate, the detected resistance to 5-FOA showed that the repression of *SAS2* in *GALLpr-SAS2* was insufficient.

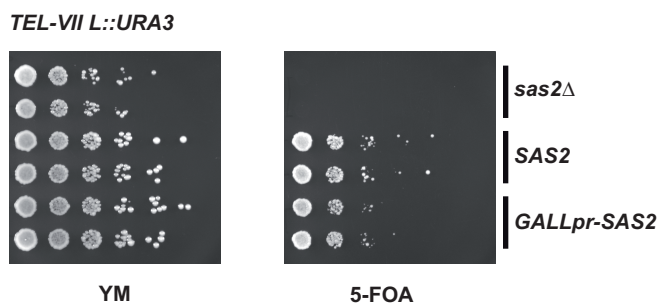


**Figure 28. *GALLpr-SAS2* segregants derived from a genetic cross, did not derepress *TEL-VII L::URA3* under repressive conditions.**

A *sas2Δ TEL-VII L::URA3* strain was crossed with a *GALLpr-SAS2* strain. After tetrad dissection, the appropriate segregants were tested under repressive conditions (glucose) for telomeric silencing on medium containing 5-FOA. *sas2Δ* and *SAS2* served as controls.

Furthermore, we tested if a *GALLpr-SAS2* construct integrated on a plasmid yielded a repressible *Sas2*, because plasmid-borne *SAS2* has previously been observed to complement the *URA3* silencing of *sas2Δ* less efficiently than genomic *SAS2* (Fig. 29, compare row 1 and 4). No difference was detected between *p-SAS2* and *p-GALLpr-SAS2* and both plasmids showed the same level of complementation. This result indicated that the repression of *Sas2* did not improve by integrating *GALLpr-SAS2* on a plasmid.

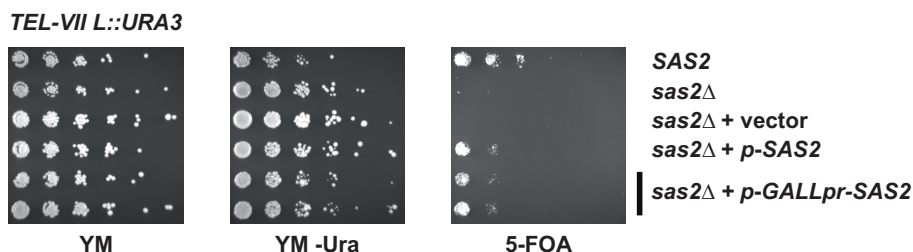


**Figure 29. *GALLpr-SAS2* on a plasmid showed less complementation of *sas2Δ TEL-VII L::URA3* than a genomic integration, but still insufficient repression of *Sas2* under repressive conditions.**

*GALLpr-SAS2* was integrated on *p-SAS2* in a *sas2Δ TEL-VII L::URA3* strain and tested for *URA3* silencing under repressive conditions (glucose) on medium containing 5-FOA, together with genomic *SAS2* (first row), genomic *sas2Δ* (second row), *sas2Δ* and empty plasmid (third row), *sas2Δ* and plasmid with *SAS2* (fourth row).

In a final approach, we chose a heat-inducible degron to achieve the rapid degradation of *Sas2*. For this purpose, *SAS2* was fused to a temperature-sensitive, but stable N-terminal fragment of mouse dihydrofolate reductase (DHFR) (Dohmen et al. 1994), which contains a cryptic N-degron that is only activated at the restrictive temperature of 37 °C and leads to the degradation of the protein. This process is accelerated by simultaneous overproduction of the E3 ubiquitin ligase Ubr1, which is additionally regulated by a galactose-inducible

promoter (Labib et al. 2000; Makise et al. 2008). The Sas2 heat-inducible fusion protein was termed Sas2-td and also contained one HA-tag. Unfortunately, it was not detectable by Western blot, and the degradation of Sas2-td therefore could not be controlled by following Sas2 protein levels (data not shown). However, we could show that H4 K16 acetylation was strongly reduced under restrictive conditions at 37 °C and galactose induction (Fig. 30A), suggesting that the degradation of Sas2-td was successful. In order to verify the functionality of *SAS2-td*, the construct was introduced into a *MATa sir1Δ* strain and tested for mating with a *MATα* tester strain after growth under permissive and non-permissive conditions. In the presence of Sas2 after incubation in glucose-containing medium at 30 °C (permissive), cells were able to mate, indicating repression of *HMLα* (Fig. 30B, first and second panel). After incubation at restrictive conditions with galactose at 37 °C, a non-mating phenotype was observed in *sir1Δ SAS2-td* cells (Fig. 30B, third and fourth panel). This effect was caused by the derepression of *HMLα* that occurred in the absence of both *SIR1* and *SAS2*, indicating that Sas2 was efficiently degraded. The construct was not subjected to further tests of functionality. Taken together, a reliable repression of Sas2 was achieved by the fusion to a heat-inducible degenon. Therefore, the Sas2-td construct was applied in further experiments described in the following section.

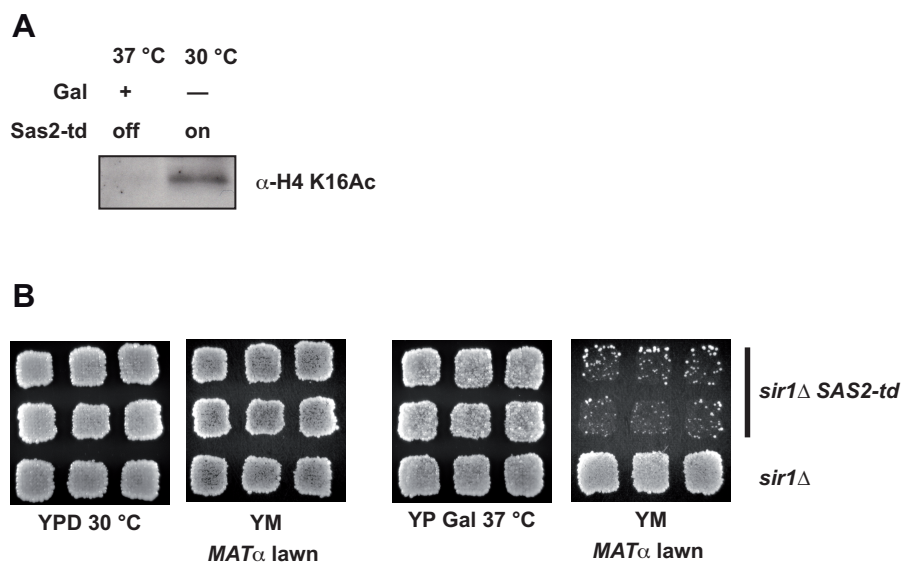


**Figure 30. Under restrictive conditions the heat-inducible degenon mutant Sas2-td decreased H4 K16Ac and caused derepression of *HMLα* silencing.**

(A, B) *CUP1pr-Ub-Arg-DHFR<sup>ts</sup>-HA-sas2 (SAS2-td)* was integrated in a *UBR1* overexpression strain to efficiently degrade Sas2 in the presence of galactose at 37 °C. (A) Western blot analysis for H4 K16Ac with Sas2-td shut off (galactose, 37 °C) and switched on (glucose, 30 °C) showed reduction of H4 K16Ac under restrictive conditions. (B) The *SAS2-td* construct in a *sir1Δ* background was tested for the repression of the *HMLα* silencing defect with a *MATα* mating tester. *SAS2-td* under permissive conditions (glucose, 30 °C, left panels) did not cause an *HMLα* silencing defect in *sir1Δ*, whereas *SAS2-td* grown under restrictive conditions (galactose, 37 °C, right panels) caused *HMLα* derepression indicating loss of Sas2 function.

### 3.2.2 Dynamics of H4 K16 acetylation by Sas2 were cell-cycle dependent

Chromatin is a dynamic structure that regulates access to the DNA for cellular processes such as DNA replication, transcription and DNA repair. This is, among others, achieved by the disassembly and reassembly of nucleosomes, which is carried out by chromatin assembly factors. The HAT Sas2 was previously shown to interact with the chromatin assembly factors CAF-I and Asf1 (Meijsing and Ehrenhofer-Murray 2001), and these also interacted with PCNA. This fact, as well as the experiments described above, led to the hypothesis that Sas2-mediated H4 K16 acetylation might be introduced in a replication-coupled fashion.

In order to address this issue, we performed cell-cycle experiments with cells bearing the repressible Sas2-td construct as outlined above (3.2.1). Figure 31A shows a schematic representation of the experiment. Cells were first synchronized with nocodazole in G2/ M phase to facilitate the following G1 arrest with  $\alpha$ -factor<sup>1</sup>. At this time, cells were grown under conditions where Sas2 was shut off and H4 K16 acetylation should be diminished. Subsequently, half of the cells were released to the following S-phase and cell cycle by washing out  $\alpha$ -factor, whereas the other half was maintained in the G1 arrest. In both cases, the cells were shifted to glucose-containing medium and 30 °C in order to induce SAS2 expression and H4 K16 acetylation.

As expected, we found that H4 K16 acetylation was strongly reduced in arrested cells in the absence of Sas2 (Fig. 31B, time point 0, sample A). Interestingly, upon SAS2 induction, cells that remained in G1 arrest for one hour still exhibited a reduced H4 K16 acetylation level (Fig. 31B, sample B) comparable to that in the absence of Sas2 (Fig. 31B, time point 0, sample A). This showed that, despite the induction of Sas2, the H4 K16Ac remained low, indicating that there was only little H4 K16 acetylation by Sas2 in G1. However, it is also possible that Sas2 was not induced efficiently in G1, or that the Sas2 promoter was less stable in this phase. In contrast, cells that were released to the subsequent S-Phase, showed increased levels of global H4 K16 acetylation (Fig. 31B, lane C), suggesting that Sas2 performed acetylation activity associated with replication-coupled chromatin assembly during S-Phase. After two hours, the level of H4 K16 acetylation was not further elevated in released cells, indicating that the H4 K16Ac level was restored already after the first round of DNA replication subsequent to the G1 arrest.

---

<sup>1</sup>  $\alpha$ -factor is a yeast mating pheromone, which is used to cause arrest of *MATa* cells in the G1 phase of the cell cycle

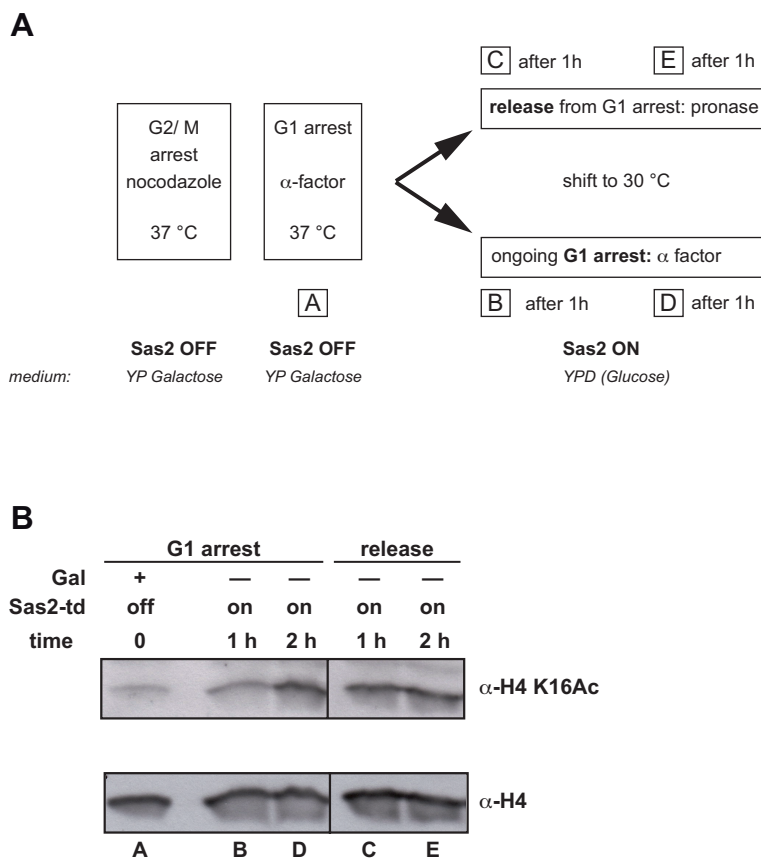


**Figure 31. Sas2-mediated H4 K16 acetylation was dependent on progression through S-phase.**

(A) An asynchronous culture of *ubr1* $\Delta$ ::*GAL-MYC-UBR1*::*HIS3 SAS2-td* was grown over night and then subjected to each step of the experimental protocol presented here. Sas2-td was shut off in the presence of galactose and growth at 37 °C, and switched on after a shift to glucose and growth at 30 °C. Samples marked by framed capitals were taken at the indicated time points. (B) G1-arrested cells showed reduced H4 K16 acetylation compared to cells released into S-phase. The H4 K16Ac status was determined in whole-cell extracts by Western blot analysis. Similar levels of H4 were detected (lower panel). DNA content and thus cell cycle phase was monitored by FACS analysis (data not shown).

Cells that were maintained in G1 arrest displayed elevated H4 K16Ac after two hours. This increase of H4 K16Ac might be caused by a low level of histone synthesis that also occurs during G1 these histones would be subsequently incorporated and acetylated by Sas2. Alternatively, there may be a slower rate of H4 K16Ac incorporation, such that full acetylation in the genome is only reached after 2 hours. These results suggested that the acetylation of H4 K16 by Sas2 was carried out coupled to DNA replication. Since this experiment did not give information about the incorporation of the acetylated histones, we furthermore planned to examine the cell-cycle dependent *in vivo* chromatin acetylation by ChIP-chip analysis.

## 4. Discussion

Sas2, a member of the MYST family of acetyltransferases, has so far been shown to prevent the spreading of heterochromatin at telomeres and to be involved in silencing of the *HM* and rDNA loci. Here, we investigated which regions in the genome of *S. cerevisiae* showed H4 K16 acetylation that depended on Sas2. We found that H4 K16Ac was affected genome-wide, but not uniformly, in the absence of Sas2. Besides the subtelomeres, a pronounced effect of *SAS2* deletion was found at coding regions, and we found evidence that Sas2 influenced transcription elongation, because *sas2Δ* cells were more resistant to 6-AU and showed slightly higher occupancy of PolII at 3' regions of ORFs. A deletion of *SAS2* furthermore resulted in the accumulation of transcripts at 3' ends but was distinct from cryptic transcription initiation. Since the H4 K16Ac was high in regions with low exchange, we argued that K16 is deposited on chromatin independently of transcription. This was furthermore supported by the observation that Sas2-dependent H4 K16Ac deposition depended on S-phase of the cell cycle, which might provide a hint as to a function of Sas2 besides its role in blocking the spreading of heterochromatin.

### **4.1 Sas2 influenced H4 K16Ac on a global scale**

In this study, we examined the Sas2-dependent H4 K16Ac on a genome-wide scale by applying a H4 K16Ac-specific antibody and high resolution tiling arrays representing the complete yeast genome. We found that H4 K16Ac was globally decreased in *sas2Δ* cells compared to wild-type, which was in agreement with Kimura et al. (Kimura et al. 2002) who showed a reduction of the global H4 K16Ac protein level in the absence of *SAS2* and another study that also reported the genome-wide reduction of H4 K16Ac in *sas2Δ* (Shia et al. 2006). Although *sas2Δ* caused a global reduction of H4 K16Ac, the loss was not evenly distributed, some regions were more affected and some were less affected by the loss of *SAS2* apart from the telomeres. Our analysis revealed a major loss of H4 K16Ac along ORFs that was not found in intergenic regions. This difference was not observed in the previous study (Shia et al. 2006) and was probably due to some differences in the experimental procedure. Firstly, we used tiling arrays with 25-mer probes and 5 bp probe spacing tiled through the complete yeast genome, providing in total 3.2 million perfect match/ mismatch probes and thereby a high resolution that allowed a detailed analysis. The microarrays used by Shia et al. contained 14.000 spots of PCR products including ORFs

and intergenic regions. Secondly, we performed additional ChIP-chip applying an antibody for unmodified H4, which allowed us to normalize our H4 K16Ac data to nucleosome distribution, whereas the previous study normalized the data to input. Taken together, our data indicate that the acetylation status of ORFs was strongly influenced by Sas2. This leads to the assumption that Sas2 can be found associated to ORFs. Although Sas2 has been previously found associated to the rDNA locus (Meijsing and Ehrenhofer-Murray 2001), we were not able to detect significant levels of Sas2 at ORFs nor telomeres or Ty elements (data not shown). This fact might be due to a possible indirect association of Sas2 or the investigation of a time point when Sas2 is not present at the chromatin, since we found that Sas2 acted in an S-phase dependent manner (see below). Furthermore, other groups reported that they were also not able to detect association of Sas2 with specific sequences (Dang et al. 2009; Jacobson and Pillus 2009). However, this could also be due to technical limitations of the ChIP method.

As expected, we furthermore found that H4 K16Ac was strongly reduced at subtelomeric regions upon deletion of *SAS2*, which confirmed the findings of previous studies (Kimura et al. 2002; Suka et al. 2002; Shia et al. 2006). In fact, our data provide a refined view of H4 K16 acetylation at the subtelomere, since we did not observe a continuous gradient of acetylation towards centromere-proximal regions in wild-type in contrast to previous studies (Kimura et al. 2002; Suka et al. 2002).

Interestingly, another region depleted of H4 K16Ac that we identified in *sas2Δ* was the region around the *HMR* locus at chromosome III. Since a deletion of *SAS2* suppresses the silencing defect of the mutated *HMR*-E silencer allele *HMRa-e\*\** (Ehrenhofer-Murray et al. 1997), we thus hypothesize that the silencing is reestablished by the spreading of heterochromatin mediated by the Sir proteins. The SIR complex is hence allowed to spread further to more centromere-proximal regions upon deletion of *SAS2* and spreads up to and beyond the *HMR* locus that is located adjacent to the subtelomeric region. This spreading across the *HMR* locus even occurs if the Sir complex is unable to bind to the mutated Rap1 and Abf1 binding sites which is the case at *HMRa-e\*\**. Through the Sir spreading, *HMRa* is subsequently repressed, and the  $\alpha$ -mating ability of *MAT $\alpha$*  strains is restored. To confirm this hypothesis, ChIP analysis of the Sir complex in a *sas2Δ* background around the *HMR* locus will be necessary.

The global data analysis of this study revealed that despite the global reduction, H4 K16 acetylation was not lost completely in *sas2Δ* cells, which was also shown previously on the protein level (Kimura et al. 2002). The question remains, which other HAT (or HATs) targets the residual H4 K16Ac, for instance at intergenic regions and 5' ends of the coding

regions. Another HAT that is known to target H4 K16 besides other H4 lysine residues is the NuA4-associated enzyme Esa1 (Smith et al. 1998; Clarke et al. 1999). However, ChIP analysis of a previous study showed that H4 K16Ac in a conditional *esa1* mutation in a *sas2Δ* background did not lead to a complete loss of the H4 K16 acetylation signal (Suka et al. 2002). The level at telomere proximal regions in that study was no further reduced in the double mutation than by *sas2Δ* alone. On the other hand, at the *INO1* coding region, especially at promoter-distal regions, H4 K16Ac was cumulatively reduced in *esa1ts sas2Δ* (Suka et al. 2002). This fact could argue for a participation of both Sas2 and Esa1 at coding regions, which has already been shown in the case of Esa1 (Robert et al. 2004) and will be discussed below for Sas2. At present, no further acetyltransferase is known to be specific for H4 K16, but it was shown that K16 is acetylated in 80 % of all H4 molecules, and also most of the monoacetylated H4 is acetylated at this residue (Smith et al. 2003). It would be interesting to know to which percentage this acetylation is reduced upon deletion of *SAS2*. Future investigations have to reveal if there is another, so far unknown HAT with redundant activity for H4 K16. In summary, we showed in this study that Sas2 displayed a global influence on H4 K16 acetylation in *S. cerevisiae*.

## **4.2 The possible function of Sas2 at Ty elements**

In our genome-wide analysis of Sas2-mediated H4 K16 acetylation, we found that H4 K16Ac was strongly reduced in *sas2Δ* cells at nearly all retrotransposons of *S. cerevisiae*, the Ty elements. The real extent of H4 K16 acetylation at Ty elements remained uncertain because the approximately 30 Ty elements contain many repetitive elements, which make the sequences indistinguishable in data analysis. Nonetheless, reduction of H4 K16Ac in the absence of Sas2, which was also confirmed by ChIP analysis, strongly suggested a dependence of chromatin modification of Ty elements on Sas2. However, the functional analysis showed that Sas2 was not involved in the stabilization of the expression or transposition of Ty1, which was in contrast to the 5'-3' exoribonuclease Xrn1 as shown in a previous study (Berretta et al. 2008). The question what function Sas2 exhibits at Ty elements therefore remains open. That Ty elements can be regulated by chromatin modifications and modifiers was previously shown (Berretta et al. 2008). In that study, a barrier established by Set1 and H3 K4me was suggested to restrict the silencing of Ty1 to this region. It was furthermore shown that deacetylation also mediated silencing of Ty1 (Berretta et al. 2008), but it was not shown which residues were involved. Since Sas2 participates in the boundary function at telomeres and is involved in

silencing at the *HM* loci, it is conceivable that it helps to maintain silencing of Ty elements restricted to their regions. It was also shown for another boundary participator, Sir4 that it determines the integration site of the Ty5 element (Xie et al. 2001). However, because deletion of *SAS2* did not influence expression or transposition of Ty1, we speculate that Sas2 might influence another part of the Ty1 silencing pathway. Furthermore, it is possible that diverse mechanisms function in Ty silencing which could also be redundant in function. This might explain why the deletion of *SAS2* did not display an influence on expression and transposition of Ty1. In the end, further experiments are necessary to elucidate the role of Sas2-mediated H4 K16Ac at Ty elements. Since Sas2-mediated H4 K16Ac is high in regions that are less transcribed and show little histone exchange (discussed below), which applies to the Ty elements one could speculate that these regions therefore strongly depend on Sas2.

### **4.3 The deletion of *SAS2* influenced transcription elongation**

A surprising result in our genome-wide H4 K16Ac analysis was the finding that H4 K16Ac was depleted along the majority of ORFs. The resulting question was if a deletion of *sas2Δ* affected transcription elongation, since ORFs are the region where PolII acts in its elongation phase. To test this, we took advantage of the drug 6-azauracil (6-AU), which can be used to measure the affection of elongation, because it depletes the nucleotide pools of a cell, and PolII is then unable to proceed through transcription elongation unless positive transcription elongation factors are available.

Unexpectedly, we discovered that *sas2Δ* showed the unusual phenotype of resistance to 6-AU. This was surprising, because many factors that are required for transcription elongation, for instance Dst1 are known to cause 6-AU sensitivity (Hubert et al. 1983). The resistance to 6-AU indicated the opposite, namely that transcription elongation was facilitated (Mason and Struhl 2005) in *sas2Δ* cells. Because 6-AU affects the induction of the IMP dehydrogenase encoded by the *IMD2* gene (Hyle et al. 2003), we tested if an increased expression of *IMD2* upon 6-AU treatment was caused in *sas2Δ*. The expression levels of *IMD2* in *sas2Δ* did not exceed that from wt, and therefore the resistance of *sas2Δ* to 6-AU must be caused by other means. Furthermore, sensitivity to 6-AU can be caused by mutations that affect other processes than transcription or induction of *IMD2* (Riles et al. 2004), and resistance to 6-AU can be caused by the overexpression of drug transporter *SNG1* (Garcia-Lopez et al. 2010), also an effect independent of elongation. We can exclude an unspecific effect of *sas2Δ*, because simultaneous deletion of *SAS2* and *DST1*, a

positive transcription elongation factor, showed sensitivity to 6-AU like a *dst1Δ* alone. Therefore, the effect of *sas2Δ* was dependent on the Dst1 elongation factor.

To gain further insight into the biochemical aspects of transcription elongation in the absence of *SAS2*, we investigated the occupancy and distribution of PolIII. We found the processivity of PolIII to be affected in *sas2Δ* cells, but not the elongation rate, because the level of PolIII occupancy was elevated at 3' ends of *PMAI* and the Gal-inducible *FMP27* gene. At other genes we examined an elevated PolIII occupancy was not detectable. However, this finding was unexpected, because it suggests that chromatin with reduced H4 K16Ac is more accessible for cellular processes like transcription, which on the other hand, implies that H4 K16Ac and the presence of Sas2 is inhibitory. Whether the effect of Sas2 on PolIII or elongation was direct or indirect remains to be determined, since we and others were not able to detect Sas2 association at specific regions (Dang et al. 2009; Jacobson and Pillus 2009). So far, H4 K16Ac was reported to be associated with open chromatin, since it inhibits higher-order formation (Shogren-Knaak et al. 2006). Furthermore, PolIII elongation was linked to histone deacetylation, which is important to restore repressive chromatin after transcription (Joshi and Struhl 2005). It was also shown in mammalian cells, that H4 K16Ac provides a combinatorial code for the recruiting of a transcription elongation factor by BRD4 and thereby influences transcription elongation (Zippo et al. 2009). H4 K16Ac is not inhibitory per se, but it could act through protein-histone interactions and recruit factors at a certain time point. It was shown that the transcription factor Bdf1, which is associated with acetylated chromatin, only binds to hypoacetylated H4 K16 (Kurdistani et al. 2004). In conclusion, our results indicate that *sas2Δ* caused increased processivity of PolIII at least in a subset of genes.

#### **4.4 *sas2Δ* influenced the level of transcription on a global scale**

Our results so far indicated an influence of Sas2 on transcription elongation. Because elongation is one aspect of transcription, we furthermore investigated the influence of *sas2Δ* on transcription. If chromatin in the absence of *SAS2* becomes more loose, would this lead to increased transcription activity in the cell? We investigated this issue by performing a genome-wide expression analysis in wt and *sas2Δ* cells. Interestingly, next to the expected repression of subtelomeric genes we found a genome-wide accumulation of transcripts at the 3' end at the majority of genes relative to wild-type (Fig. 32). The observed effect at the 3' ends occurred in two groups of genes, the slightly repressed and the slightly activated genes. A second, smaller peak at the 5' prime end that was also

detected in these two groups may be caused by abortive transcription initiation. The two remaining groups, the strongly activated and strongly repressed genes, showed the highest change in expression but did not show an accumulation of transcripts at 3' ends. In agreement with previous studies, we found that the genes near the telomeres depended on Sas2 for their expression (Kimura et al. 2002; Shia et al. 2006). But the accumulation of transcripts at the 3' regions of ORFs has gone unnoticed in those previous studies, again due to the technology used in those studies (Kimura et al. 2002; Shia et al. 2006).

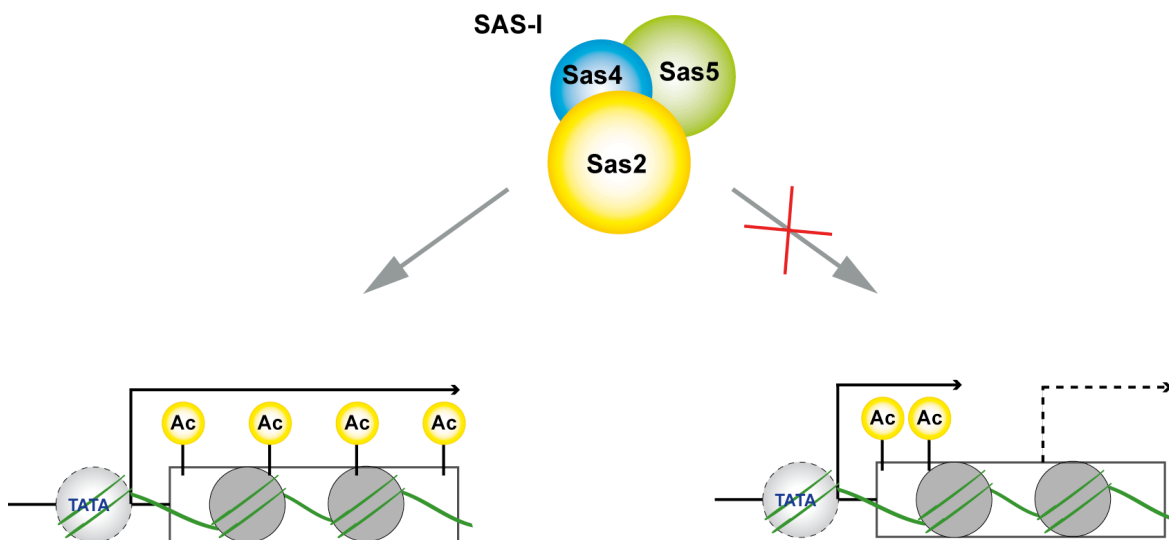


**Figure 32. Model for the influence of Sas2 on transcription.**

Normal transcription in the presence of Sas2 (left side). The deletion of *SAS2* leads to an accumulation of transcripts at the 3' end of ORFs (dashed arrow) (right side).

In contrast to our analysis, which identified an accumulation of transcripts in the two slightly affected groups of genes, one of the previous studies examined only genes that were affected by more than twofold change in expression (Kimura et al. 2002). Another study observed effects on transcription caused by a H4 K16R mutation. These effects were grouped into specific and unspecific effects, and the specific effects were proposed to be mediated by Bdf1 and Sir 3 binding (Dion et al. 2007). To confirm our genome-wide findings, we performed a local analysis of the 3': 5' ratio at three individual genes. These genes showed a slight but significant increase of transcripts at their 3' end. An increased 3': 5' ratio at some genes was also reported to occur upon the deletion of *ASF1* and this effect was linked to the loss of histone deposition activities of Asf1 to prevent transcription from within coding regions (Schwabish and Struhl 2006). In connection with our above results, we assume that the generation of transcripts at the 3' ends is caused by the increased occupancy of PolII at 3' ends in *sas2Δ*, although increased PolII occupancy was

not found at all genes. This may be comparable with an effect that was found in *Drosophila*, where a stalled PolIII maintains an open chromatin structure and is able to enhance gene expression (Gilchrist et al. 2008). In conclusion, we found that, in addition to the influence on transcription elongation, Sas2 furthermore slightly influenced transcription and caused an accumulation of transcripts at their 3' ends of ORFs. This mild genome-wide affection in the absence of *SAS2* might not be surprising since the deletion of *SAS2* does not cause lethality.

Is the accumulation of transcripts from within the ORFs at the 3' ends due to cryptic transcription initiation caused by deletion of *SAS2*? A deletion of *SAS2* alone did not cause cryptic transcription initiation at a *FLO8::HIS3* reporter construct (Cheung et al. 2008). Furthermore, no additional transcripts were detectable at the *FLO8* or *STE11* genes (data not shown), which were previously shown to contain cryptic initiation sites (Kaplan et al. 2003; Carrozza et al. 2005; Cheung et al. 2008). Interestingly, the additional deletion of *SAS2* in the combination with mutations in the genes encoding transcription elongation factors, *spt16-197* and *spt6-1004*, exacerbated the cryptic transcription measured using the *FLO8::HIS3* reporter construct. For several reasons we propose that the detected accumulation of transcripts in *sas2Δ* cells is distinct from the type of cryptic transcription that was reported for several mutants and derives from within coding regions. Cryptic initiation starts at defined, alternative transcription start sites, cryptic TATA boxes that become available if repressive chromatin is not properly restored after PolIII elongation, e.g. at the *FLO8* gene (Kaplan et al. 2003). By starting at defined sites, the cryptic transcripts have a defined length. Although cryptic transcription is a widespread phenomenon, it occurs at a subset of genes (~1000 genes) (Cheung et al. 2008). In contrast, the accumulation of transcripts in *sas2Δ* cells was found at the majority (4112 genes) of about 6300 yeast genes, making it a genome-wide phenomenon. Recently, it was reported that pervasive transcription occurs bidirectionally and is widespread in the yeast genome (David et al. 2006; Neil et al. 2009; Xu et al. 2009). Although the expression arrays applied in this study were capable of detecting sense and antisense transcription (David et al. 2006), in the absence of *SAS2*, antisense transcription was not detectable (H.- R. Chung, data not shown). Although plenty of studies have related several types of pervasive transcription and antisense transcription to biological functions (Martens et al. 2004; Cheung et al. 2008), so far we cannot state a function of the accumulated transcripts for *sas2Δ*.

#### **4.5 Cooperation of Sas2 and Set2 in the repression of transcription elongation**

The absence of the H3 K36 methyltransferase Set2 was linked to the occurrence of intragenic transcription initiation (Carrozza et al. 2005; Li et al. 2007b). Set2 was shown to travel with PolIII (Krogan et al. 2003; Kizer et al. 2005) and to recruit Rpd3S via H3 K36Me, which subsequently deacetylates ORFs and restores repressive chromatin (Carrozza et al. 2005; Li et al. 2007b). In this study, we made the observation that an additional deletion of *SAS2* in a *set2Δ* background caused reduction of the resistance to 6-AU compared to *set2Δ* alone. This result suggested an interdependence of both factors and brought us to further examine a possible cooperation between Sas2 and Set2. The prediction would be that if the two modifications depended on each other, H3 K36Me3 would be reduced in a *sas2Δ* and H4 K16Ac reduced in a *set2Δ* background, although this prediction stands in contrast to several studies that described increased the bulk acetylation in *set2Δ* cells (Carrozza et al. 2005; Keogh et al. 2005; Li et al. 2007b). In our analysis, the full level of H3 K36Me3 at the *CSF1* gene depended on Sas2, whereas H4 K16Ac at the 3' end was slightly influenced by Set2. At a second individual gene that was examined, the highly transcribed *PMAI* gene, this mutual influence was not observed. Interestingly, our findings are contrary to the previously identified increase of bulk acetylation in the absence of Set2 (Carrozza et al. 2005; Keogh et al. 2005; Li et al. 2007b). That H3 K36 methylation can regulate chromatin acetylation was observed in another study (Bell et al. 2007). Increased H4 K16Ac levels were found upon deletion of dHypb, which has sequence similarity with Set2 and is one of the two *Drosophila* H3 K36 methyltransferases. A knock-down of the second methyltransferase dMes-4, which performs di- and trimethylation of H3 K36 in *Drosophila*, on the contrary resulted in a decrease in H4 K16Ac (Bell et al. 2007), an effect that is comparable to our observation at the *CSF1* gene. Taken together, we discovered a cooperation of Set2 and Sas2 in the repression of transcription elongation and a slight, but significant decrease of H4 K16Ac at *CSF1* upon deletion of Set2. Therefore, a partial co-regulation of Set2 and Sas2 in *S. cerevisiae* seemed to occur here.

#### **4.6 Sas2-dependent H4 K16 acetylation was associated with regions of low H3 exchange**

In the investigations of this study, a pronounced influence of Sas2 on H4 K16Ac within ORFs, rather than intergenic regions, was observed. For a detailed examination of this effect, we correlated the relative H4 K16Ac data of wt and *sas2* $\Delta$  to the gene expression data of wt and *sas2* $\Delta$ , respectively. As reported previously, in wild-type high H4 K16Ac correlated with low rates of gene expression and H4 K16Ac was low at frequently transcribed ORFs (Kurdistani et al. 2004; Liu et al. 2005), suggesting the removal of H4 K16Ac from ORFs during transcription. Upon deletion of *SAS2*, H4 K16Ac at 5' ends was less changed, but was strongly depleted towards 3' ends. During gene expression, histones are exchanged and H3 K56Ac was shown to be correlated with this replication-independent histone exchange (Xu et al. 2005; Ruffiange et al. 2007). The correlation analysis of our study revealed that H4 K16Ac was high in regions with low H3 K56 and vice versa: a finding that was in line with another study showing that H3 K56Ac did not influence H4 K16Ac (Xu et al. 2007). Furthermore, a high turnover rate of histones was previously related to low levels of H4 K16Ac, and low turnover was related to higher H4 K16Ac (Dion et al. 2007). If the H4 K16Ac at regions with low histone turnover depended on Sas2, one can expect that H4 K16Ac in these regions would be strongly reduced in the absence of Sas2. We show evidence that Sas2 is responsible for the acetylation of H4 K16Ac at regions with low replication-independent exchange. Thus, Sas2-mediated H4 K16Ac must be incorporated into chromatin at a time point other than transcription, because this modification is lost during high transcription-dependent and independent histone turnover. According to this notion, our data indicate that the H4 K16Ac is incorporated using a mechanism coupled to DNA replication as will be discussed below. In conclusion, H4 K16Ac mediated by Sas2 is high in regions with low H3 K56Ac and low histone exchange.

#### **4.7 The influence of CAF-I and Asf1 on H4 K16Ac**

The HAT Sas2 interacts with the chromatin assembly factors CAF-I and Asf1 (Meijsing and Ehrenhofer-Murray 2001). Therefore, we sought to investigate if and at which regions CAF-I and Asf1 influence the Sas2-mediated H4 K16Ac. Globally, the overall levels of H4 K16Ac in *cac1* $\Delta$  and *asf1* $\Delta$  did not change much, but the deletion of both chromatin assembly factors (*cac1* $\Delta$  *asf1* $\Delta$ ) showed a slight decrease. The patterns of H4 K16Ac in *cac1* $\Delta$ , *asf1* $\Delta$  and *cac1* $\Delta$  *asf1* $\Delta$  cells appeared to be very similar, which was in line with

our global data analysis. This observation suggests a redundant influence of both enzymes on H4 K16Ac, which would be in line with At the subtelomeric region, the region described best for the influence of Sas2 on H4 K16Ac, small changes in H4 K16Ac were detected upon the deletion of *CAC1* and *ASF1* on H4 K16Ac was observed. Although telomeric silencing is reduced in *cac1Δ* cells (Enomoto et al. 1997), this effect did not seem to be related to the reduction in subtelomeric H4 K16Ac. Furthermore, this also did not seem to be the case in the *CAC1 ASF1* double deletion, which exhibits telomeric silencing defects (Singer et al. 1998; Krawitz et al. 2002).

For *cac1Δ*, it was previously shown that Sir2 levels were reduced at silent loci, which is likely to cause the defects in silencing (Tamburini et al. 2006). This observation may explain why H4 K16Ac levels in the CHIP analysis in *cac1Δ* cells was less reduced compared to the absence of Sas2, and partially exceeds wild-type level. In the comparison of our H4 K16Ac data with H3 K56Ac and H3 exchange data from Rufiange et al. (Rufiange et al. 2007), we noticed a specific pattern in *cac1Δ*, *asf1Δ* and *cac1Δ asf1Δ* cells that was in anticorrelation with the H3 exchange data. H4 K16Ac in these strains was reduced in regions with high exchange. Only a mild change in H4 K16Ac was observed in regions with low exchange, those regions that were depleted in H4 K16Ac upon the loss of Sas2. It was shown previously, that H3 levels are reduced at silent loci in *cac1Δ* cells (Tamburini et al. 2006). Compared to that, the H4 K16Ac in *cac1Δ* cells shows only minor changes. For the deletion of *ASF1*, a slightly lower (Prado et al. 2004) as well as a slightly higher nucleosome density (Adkins and Tyler 2004) was reported. However, the reported changes in nucleosome density were not dramatic. No extensive changes in nucleosome density of the endogenous  $2\mu$  plasmid were furthermore reported for the deletion of both chromatin assembly factors *CAC1* and *ASF1* (Adkins and Tyler 2004), although *cac1Δ asf1Δ* cells exhibit severe growth defects (Tyler et al. 1999). Since H4 K16Ac was less changed in the absence of CAF-I and/ or Asf1 in regions of low exchange, where H4 K16Ac depends on Sas2, we hypothesize that H4 K16Ac was accumulated. We assume that H4 K16Ac accumulated due to less histone exchange in these cells. We furthermore observed an accumulation of H4 K16Ac at Ty elements in *cac1Δ*, *asf1Δ*, *cac1Δ asf1Δ*. In conclusion, the exchange of H4 K16-acetylated nucleosomes at these regions may depend on CAF-I and Asf1.

Taken together, our findings show a partial influence of the chromatin assembly factors CAF-I and Asf1 on H4 K16Ac and suggest that exchange of H4 K16Ac in regions of low histone exchange depends on CAF-I and Asf1. Since both chromatin assembly factors are

linked to replication-coupled chromatin assembly (Tyler et al. 1999; Ransom et al. 2010), the influence of CAF-I and Asf1 might be supposedly best observed during replication.

#### **4.8 Replication-coupled deposition of H4 K16Ac by Sas2**

Because our results described above suggested an incorporation of Sas2-mediated H4 K16Ac independently of transcription, we sought to examine if H4 K16Ac is deposited coupled to DNA replication. Our experimental approach (see Chapter 3.2) required a construct of Sas2 that could be shut off and switched on reliably. In our attempt to produce a repressible Sas2, several approaches were tested. The *MET3* promoter did not reduce Sas2 levels completely, and this *SAS2* allele was still functional under repressive conditions. The use of a galactose inducible promoter decreased the Sas2 level completely under repressive conditions as measurable by Sas2 protein level. However, this Sas2 construct was still able to complement the *HMRa-e\*\** silencing defect under repressive conditions.

Finally, the construction of a heat inducible degron-Sas2 (Sas2-td) with the parallel induction of the ubiquitin ligase Ubr1 in order to increase the degradation of Sas2, resulted in a repressible Sas2-td that showed no residual Sas2 function under repressive conditions. In order to investigate the time-point of deposition of H4 K16Ac during the cell cycle, we conducted the experiment using the Sas2-td construct. We found that upon induction of Sas2, H4 K16Ac was fully regained upon release of the cells into the subsequent S-phase. After two hours, the H4 K16Ac level in released cells was not further increased, indicating that full acetylation levels of H4 K16Ac were reached after completing one S-phase. Cells that were maintained in G1, showed a reduced H4 K16Ac level upon Sas2 induction that was comparable to that observed in cells upon Sas2 shut-off. Since the bulk of histone synthesis is coupled to DNA replication (Jackson and Chalkley 1985), it is possible that Sas2 only acetylates freshly synthesized histones, because we observed that H4 K16Ac is high after release to S-phase and reduced in cells maintained in G1. In cells that were maintained in G1 arrest the H4 K16Ac level was increased after two hours. One explanation for this may be that histone synthesis, to a minor extent, also occurs in G1 phase (Jackson and Chalkley 1985). Another explanation is that histone exchange occurring in G1 arrest that is independent of replication (Linger and Tyler 2006), leads to the incorporation of histones which are acetylated by Sas2.

Histones typically carry certain posttranslational modifications prior to their incorporation into chromatin after DNA replication (Sobel et al. 1995; Loyola et al. 2006). H4 carries a

modification pattern of acetylation at K5 and K12 that marks it as freshly synthesized (Sobel et al. 1995). These freshly synthesized histones are deposited onto the replicated DNA by CAF-I and Asf1 (Tyler et al. 1999). Since Sas2 interacts with CAF-I (and also Asf1), two ways of reestablishment of the H4 K16 acetylation mark are thinkable, either before or after incorporation of the histone into chromatin (Meijsing and Ehrenhofer-Murray 2001). Whether Sas2 acetylates histones prior to deposition to chromatin or afterwards, cannot be concluded from our experiment, which does not distinguish between acetylation of free or chromatin-bound histones and thus remains unclear. Furthermore, the dependence of the incorporation of H4 K16Ac on CAF-I and/ or Asf1 remains to be determined.

However, our experiment suggests that the bulk acetylation of Sas2 at H4 K16 occurs coupled to DNA replication, implying a role for Sas2-mediated H4 K16Ac in the inheritance and reestablishment of chromatin states after replication.

#### **4.9 A genome-wide function of Sas2-mediated H4K16Ac**

Sas2 belongs to the family of MYST HAT acetyltransferases and influences transcriptional silencing at telomeres, *HM* loci and the rDNA locus. Sas2 acetylates H4 K16 and thereby prevents spreading of SIR-mediated heterochromatin at telomeres (Kimura et al. 2002; Suka et al. 2002; Shia et al. 2006). With this study, we have expanded the view on the functions of Sas2 besides its well-known boundary function. Sas2 influences H4 K16 acetylation on a global scale, and H4 K16Ac is lost at ORFs in the absence of Sas2. The results suggest that Sas2 exhibits a mild global effect on transcription, since we firstly found that a *sas2Δ* caused resistance to 6-AU, which indicates an effect on transcription elongation and secondly, that *sas2Δ* caused a mild increase in processivity of PolII and an accumulation of transcripts at the 3' ORF region. Although the effect on transcription is distinct from intragenic transcription, the results suggest that Sas2 participates in maintaining genome integrity by preventing pervasive transcription events. The H4 K16Ac signal is removed during transcription, since we, in agreement with others (Liu et al. 2005; Dion et al. 2007) observed that high exchange correlates with low H4 K16Ac levels. This fact raises the question at which time H4 K16Ac is then integrated.

We show that the acetylation of H4 K16 by Sas2 occurs coupled to DNA replication, which is in line with the previously identified interaction of Sas2 with CAF-I, a replication-coupled chromatin assembly factor. H4 K16Ac might therefore serve as a genome-wide mark for replicated chromatin and might be important for the inheritance of

---

epigenetic states in that it reestablishes epigenetic states that restrict SIR and heterochromatin expansion. The established pattern is then subject to changes due to cellular processes, e.g. during transcription and histone exchange. Thereby, H4 K16Ac at different locations might underlie different modes of changes. At ORFs H4 K16Ac will be removed at every transcription cycle and reestablished at every chromatin replication. The removal will be less at intergenic regions. At the telomeric boundary H4 K16Ac remains present in equilibrium with SIR to prevent the propagation of heterochromatin into euchromatic regions. Taken together, this study reveals a global function of Sas2-mediated H4 K16Ac and relates it to histone exchange, transcription elongation and DNA replication.

In mammalian cells, H4 K16Ac is targeted by the human MOF (hMOF), which also belongs to the MYST HAT family. MOF is generally associated with open chromatin and further acts as supporting factor for DNA repair (Gupta et al. 2005). H4 K16Ac is involved in many interplays with other modifications and was also linked to transcription elongation, as was recently shown for instance in a combination with H3 S10Ph and H3 K9Ac that serves as a platform to recruit BRD4 and subsequently stimulates transcription elongation (Zippo et al. 2009). In *Drosophila*, H4 K16 acetylated by MOF regulates dosage compensation by targeting the promoter and 3' ends of genes at the male X chromosome. Additionally, it regulates gene expression at autosomes and in the female genome by binding primarily to promoters (Kind et al. 2008). In summary, although the enzymes Sas2, hMOF and MOF are structurally related and share substrate specificity, the different species have established specific functions and mechanisms to affect the structure of chromatin.

## 5. References

- Adkins, M.W., Howar, S.R., and Tyler, J.K. 2004. Chromatin disassembly mediated by the histone chaperone Asf1 is essential for transcriptional activation of the yeast PHO5 and PHO8 genes. *Mol Cell* **14**(5): 657-666.
- Adkins, M.W. and Tyler, J.K. 2004. The histone chaperone Asf1p mediates global chromatin disassembly in vivo. *J Biol Chem* **279**(50): 52069-52074.
- Adkins, M.W., Williams, S.K., Linger, J., and Tyler, J.K. 2007. Chromatin disassembly from the PHO5 promoter is essential for the recruitment of the general transcription machinery and coactivators. *Mol Cell Biol* **27**(18): 6372-6382.
- Annunziato, A.T. and Seale, R.L. 1983. Histone deacetylation is required for the maturation of newly replicated chromatin. *J Biol Chem* **258**(20): 12675-12684.
- Barbaric, S., Reinke, H., and Horz, W. 2003. Multiple mechanistically distinct functions of SAGA at the PHO5 promoter. *Mol Cell Biol* **23**(10): 3468-3476.
- Beiter, T., Reich, E., Williams, R.W., and Simon, P. 2009. Antisense transcription: a critical look in both directions. *Cell Mol Life Sci* **66**(1): 94-112.
- Bell, O., Wirbelauer, C., Hild, M., Scharf, A.N., Schwaiger, M., MacAlpine, D.M., Zilbermann, F., van Leeuwen, F., Bell, S.P., Imhof, A. et al. 2007. Localized H3K36 methylation states define histone H4K16 acetylation during transcriptional elongation in *Drosophila*. *EMBO J* **26**(24): 4974-4984.
- Belotserkovskaya, R., Oh, S., Bondarenko, V.A., Orphanides, G., Studitsky, V.M., and Reinberg, D. 2003. FACT facilitates transcription-dependent nucleosome alteration. *Science* **301**(5636): 1090-1093.
- Benjamini, Y. and Hochberg, Y. 1995. Controlling the false discovery rate: a practical and powerful approach to multiple testing. *Journal of the Royal Statistical Society Series B: Statistical Methodology* **57**: 289-300.
- Benson, L.J., Gu, Y., Yakovleva, T., Tong, K., Barrows, C., Strack, C.L., Cook, R.G., Mizzen, C.A., and Annunziato, A.T. 2006. Modifications of H3 and H4 during chromatin replication, nucleosome assembly, and histone exchange. *J Biol Chem* **281**(14): 9287-9296.
- Berretta, J. and Morillon, A. 2009. Pervasive transcription constitutes a new level of eukaryotic genome regulation. *EMBO Rep* **10**(9): 973-982.
- Berretta, J., Pinskaya, M., and Morillon, A. 2008. A cryptic unstable transcript mediates transcriptional trans-silencing of the Ty1 retrotransposon in *S. cerevisiae*. *Genes Dev* **22**(5): 615-626.

- Boeke, J.D. and Devine, S.E. 1998. Yeast retrotransposons: finding a nice quiet neighborhood. *Cell* **93**(7): 1087-1089.
- Boeke, J.D., Trueheart, J., Natsoulis, G., and Fink, G.R. 1987. 5-Fluoroorotic acid as a selective agent in yeast molecular genetics. *Methods Enzymol* **154**: 164-175.
- Carmen, A.A., Milne, L., and Grunstein, M. 2002. Acetylation of the yeast histone H4 N terminus regulates its binding to heterochromatin protein SIR3. *J Biol Chem* **277**(7): 4778-4781.
- Carrozza, M.J., Utley, R.T., Workman, J.L., and Cote, J. 2003. The diverse functions of histone acetyltransferase complexes. *Trends Genet* **19**(6): 321-329.
- Carrozza, M.J., Li, B., Florens, L., Suganuma, T., Swanson, S.K., Lee, K.K., Shia, W.J., Anderson, S., Yates, J., Washburn, M.P. et al. 2005. Histone H3 methylation by Set2 directs deacetylation of coding regions by Rpd3S to suppress spurious intragenic transcription. *Cell* **123**(4): 581-592.
- Chen, C.C., Carson, J.J., Feser, J., Tamburini, B., Zabaronick, S., Linger, J., and Tyler, J.K. 2008. Acetylated lysine 56 on histone H3 drives chromatin assembly after repair and signals for the completion of repair. *Cell* **134**(2): 231-243.
- Cheung, P., Tanner, K.G., Cheung, W.L., Sassone-Corsi, P., Denu, J.M., and Allis, C.D. 2000. Synergistic coupling of histone H3 phosphorylation and acetylation in response to epidermal growth factor stimulation. *Mol Cell* **5**(6): 905-915.
- Cheung, V., Chua, G., Batada, N.N., Landry, C.R., Michnick, S.W., Hughes, T.R., and Winston, F. 2008. Chromatin- and transcription-related factors repress transcription from within coding regions throughout the *Saccharomyces cerevisiae* genome. *PLoS Biol* **6**(11): e277.
- Chung, H.R. and Vingron, M. 2009. Comparison of sequence-dependent tiling array normalization approaches. *BMC Bioinformatics* **10**: 204.
- Clapier, C.R. and Cairns, B.R. 2009. The biology of chromatin remodeling complexes. *Annu Rev Biochem* **78**: 273-304.
- Clarke, A.S., Lowell, J.E., Jacobson, S.J., and Pillus, L. 1999. Esa1p is an essential histone acetyltransferase required for cell cycle progression. *Mol Cell Biol* **19**(4): 2515-2526.
- Clarke, D.J., O'Neill, L.P., and Turner, B.M. 1993. Selective use of H4 acetylation sites in the yeast *Saccharomyces cerevisiae*. *Biochem J* **294** ( Pt 2): 557-561.
- Curcio, M.J. and Garfinkel, D.J. 1991. Single-step selection for Ty1 element retrotransposition. *Proc Natl Acad Sci U S A* **88**(3): 936-940.

- Dang, W., Steffen, K.K., Perry, R., Dorsey, J.A., Johnson, F.B., Shilatifard, A., Kaeberlein, M., Kennedy, B.K., and Berger, S.L. 2009. Histone H4 lysine 16 acetylation regulates cellular lifespan. *Nature* **459**(7248): 802-807.
- David, L., Huber, W., Granovskaia, M., Toedling, J., Palm, C.J., Bofkin, L., Jones, T., Davis, R.W., and Steinmetz, L.M. 2006. A high-resolution map of transcription in the yeast genome. *Proc Natl Acad Sci U S A* **103**(14): 5320-5325.
- Dion, M.F., Kaplan, T., Kim, M., Buratowski, S., Friedman, N., and Rando, O.J. 2007. Dynamics of replication-independent histone turnover in budding yeast. *Science* **315**(5817): 1405-1408.
- Dohmen, R.J., Wu, P., and Varshavsky, A. 1994. Heat-inducible degron: a method for constructing temperature-sensitive mutants. *Science* **263**(5151): 1273-1276.
- Downs, J.A., Kosmidou, E., Morgan, A., and Jackson, S.P. 2003. Suppression of homologous recombination by the *Saccharomyces cerevisiae* linker histone. *Mol Cell* **11**(6): 1685-1692.
- Drinnenberg, I.A., Weinberg, D.E., Xie, K.T., Mower, J.P., Wolfe, K.H., Fink, G.R., and Bartel, D.P. 2009. RNAi in budding yeast. *Science* **326**(5952): 544-550.
- Driscoll, R., Hudson, A., and Jackson, S.P. 2007. Yeast Rtt109 promotes genome stability by acetylating histone H3 on lysine 56. *Science* **315**(5812): 649-652.
- Dujon, B. 1996. The yeast genome project: what did we learn? *Trends Genet* **12**(7): 263-270.
- Ehrenhofer-Murray, A.E. 2004. Chromatin dynamics at DNA replication, transcription and repair. *Eur J Biochem* **271**(12): 2335-2349.
- Ehrenhofer-Murray, A.E., Rivier, D.H., and Rine, J. 1997. The role of Sas2, an acetyltransferase homologue of *Saccharomyces cerevisiae*, in silencing and ORC function. *Genetics* **145**(4): 923-934.
- Ehrentraut, S., Weber, J.M., Dybowski, J.N., Hoffmann, D., and Ehrenhofer-Murray, A.E. 2010. Rpd3-dependent boundary formation at telomeres by removal of Sir2 substrate. *Proc Natl Acad Sci U S A* **107**(12): 5522-5527.
- Ekwall, K. 2005. Genome-wide analysis of HDAC function. *Trends Genet* **21**(11): 608-615.
- English, C.M., Adkins, M.W., Carson, J.J., Churchill, M.E., and Tyler, J.K. 2006. Structural basis for the histone chaperone activity of Asf1. *Cell* **127**(3): 495-508.
- Enomoto, S. and Berman, J. 1998. Chromatin assembly factor I contributes to the maintenance, but not the re-establishment, of silencing at the yeast silent mating loci. *Genes Dev* **12**(2): 219-232.

- Enomoto, S., McCune-Zierath, P.D., Gerami-Nejad, M., Sanders, M.A., and Berman, J. 1997. RLF2, a subunit of yeast chromatin assembly factor-I, is required for telomeric chromatin function in vivo. *Genes Dev* **11**(3): 358-370.
- Finch, J.T. and Klug, A. 1976. Solenoidal model for superstructure in chromatin. *Proc Natl Acad Sci U S A* **73**(6): 1897-1901.
- Fraga, M.F., Ballestar, E., Villar-Garea, A., Boix-Chornet, M., Espada, J., Schotta, G., Bonaldi, T., Haydon, C., Ropero, S., Petrie, K. et al. 2005. Loss of acetylation at Lys16 and trimethylation at Lys20 of histone H4 is a common hallmark of human cancer. *Nat Genet* **37**(4): 391-400.
- Fuda, N.J., Ardehali, M.B., and Lis, J.T. 2009. Defining mechanisms that regulate RNA polymerase II transcription in vivo. *Nature* **461**(7261): 186-192.
- Fukuda, H., Sano, N., Muto, S., and Horikoshi, M. 2006. Simple histone acetylation plays a complex role in the regulation of gene expression. *Brief Funct Genomic Proteomic* **5**(3): 190-208.
- Garcia-Lopez, M.C., Miron-Garcia, M.C., Garrido-Godino, A.I., Mingorance, C., and Navarro, F. 2010. Overexpression of SNG1 causes 6-azauracil resistance in *Saccharomyces cerevisiae*. *Curr Genet* **56**(3): 251-263.
- Gilchrist, D.A., Nechaev, S., Lee, C., Ghosh, S.K., Collins, J.B., Li, L., Gilmour, D.S., and Adelman, K. 2008. NELF-mediated stalling of Pol II can enhance gene expression by blocking promoter-proximal nucleosome assembly. *Genes Dev* **22**(14): 1921-1933.
- Goffeau, A., Barrell, B.G., Bussey, H., Davis, R.W., Dujon, B., Feldmann, H., Galibert, F., Hoheisel, J.D., Jacq, C., Johnston, M. et al. 1996. Life with 6000 genes. *Science* **274**(5287): 546, 563-547.
- Gottschling, D.E., Aparicio, O.M., Billington, B.L., and Zakian, V.A. 1990. Position effect at *S. cerevisiae* telomeres: reversible repression of Pol II transcription. *Cell* **63**(4): 751-762.
- Green, E.M., Antczak, A.J., Bailey, A.O., Franco, A.A., Wu, K.J., Yates, J.R., 3rd, and Kaufman, P.D. 2005. Replication-independent histone deposition by the HIR complex and Asf1. *Curr Biol* **15**(22): 2044-2049.
- Grewal, S.I. and Jia, S. 2007. Heterochromatin revisited. *Nat Rev Genet* **8**(1): 35-46.
- Groth, A., Ray-Gallet, D., Quivy, J.P., Lukas, J., Bartek, J., and Almouzni, G. 2005. Human Asf1 regulates the flow of S phase histones during replicational stress. *Mol Cell* **17**(2): 301-311.
- Groth, A., Rocha, W., Verreault, A., and Almouzni, G. 2007. Chromatin challenges during DNA replication and repair. *Cell* **128**(4): 721-733.

- Gupta, A., Sharma, G.G., Young, C.S., Agarwal, M., Smith, E.R., Paull, T.T., Lucchesi, J.C., Khanna, K.K., Ludwig, T., and Pandita, T.K. 2005. Involvement of human MOF in ATM function. *Mol Cell Biol* **25**(12): 5292-5305.
- Hirose, Y. and Ohkuma, Y. 2007. Phosphorylation of the C-terminal domain of RNA polymerase II plays central roles in the integrated events of eucaryotic gene expression. *J Biochem* **141**(5): 601-608.
- Huang, H., Hong, J.Y., Burck, C.L., and Liebman, S.W. 1999. Host genes that affect the target-site distribution of the yeast retrotransposon Ty1. *Genetics* **151**(4): 1393-1407.
- Huber, W., Toedling, J., and Steinmetz, L.M. 2006. Transcript mapping with high-density oligonucleotide tiling arrays. *Bioinformatics* **22**(16): 1963-1970.
- Hubert, J.C., Guyonvarch, A., Kammerer, B., Exinger, F., Liljelund, P., and Lacroute, F. 1983. Complete sequence of a eukaryotic regulatory gene. *EMBO J* **2**(11): 2071-2073.
- Huisinga, K.L. and Pugh, B.F. 2004. A genome-wide housekeeping role for TFIID and a highly regulated stress-related role for SAGA in *Saccharomyces cerevisiae*. *Mol Cell* **13**(4): 573-585.
- Hyle, J.W., Shaw, R.J., and Reines, D. 2003. Functional distinctions between IMP dehydrogenase genes in providing mycophenolate resistance and guanine prototrophy to yeast. *J Biol Chem* **278**(31): 28470-28478.
- Imai, S., Armstrong, C.M., Kaeberlein, M., and Guarente, L. 2000. Transcriptional silencing and longevity protein Sir2 is an NAD-dependent histone deacetylase. *Nature* **403**(6771): 795-800.
- Jackson, V. and Chalkley, R. 1985. Histone synthesis and deposition in the G1 and S phases of hepatoma tissue culture cells. *Biochemistry* **24**(24): 6921-6930.
- Jacobson, S. and Pillus, L. 2009. The SAGA subunit Ada2 functions in transcriptional silencing. *Mol Cell Biol* **29**(22): 6033-6045.
- Jamai, A., Puglisi, A., and Strubin, M. 2009. Histone chaperone spt16 promotes redeposition of the original h3-h4 histones evicted by elongating RNA polymerase. *Mol Cell* **35**(3): 377-383.
- Janke, C., Magiera, M.M., Rathfelder, N., Taxis, C., Reber, S., Maekawa, H., Moreno-Borchart, A., Doenges, G., Schwob, E., Schiebel, E. et al. 2004. A versatile toolbox for PCR-based tagging of yeast genes: new fluorescent proteins, more markers and promoter substitution cassettes. *Yeast* **21**(11): 947-962.
- Jiang, C. and Pugh, B.F. 2009. Nucleosome positioning and gene regulation: advances through genomics. *Nat Rev Genet* **10**(3): 161-172.

- Joshi, A.A. and Struhl, K. 2005. Eaf3 chromodomain interaction with methylated H3-K36 links histone deacetylation to Pol II elongation. *Mol Cell* **20**(6): 971-978.
- Kaplan, C.D., Laprade, L., and Winston, F. 2003. Transcription elongation factors repress transcription initiation from cryptic sites. *Science* **301**(5636): 1096-1099.
- Kaufman, P.D. 1996. Nucleosome assembly: the CAF and the HAT. *Curr Opin Cell Biol* **8**(3): 369-373.
- Keogh, M.C., Kurdistani, S.K., Morris, S.A., Ahn, S.H., Podolny, V., Collins, S.R., Schuldiner, M., Chin, K., Punna, T., Thompson, N.J. et al. 2005. Cotranscriptional set2 methylation of histone H3 lysine 36 recruits a repressive Rpd3 complex. *Cell* **123**(4): 593-605.
- Kim, H.J., Seol, J.H., and Cho, E.J. 2009. Potential role of the histone chaperone, CAF-1, in transcription. *BMB Rep* **42**(4): 227-231.
- Kim, H.J., Seol, J.H., Han, J.W., Youn, H.D., and Cho, E.J. 2007. Histone chaperones regulate histone exchange during transcription. *EMBO J* **26**(21): 4467-4474.
- Kim, J.A. and Haber, J.E. 2009. Chromatin assembly factors Asf1 and CAF-1 have overlapping roles in deactivating the DNA damage checkpoint when DNA repair is complete. *Proc Natl Acad Sci U S A* **106**(4): 1151-1156.
- Kim, J.M., Vanguri, S., Boeke, J.D., Gabriel, A., and Voytas, D.F. 1998. Transposable elements and genome organization: a comprehensive survey of retrotransposons revealed by the complete *Saccharomyces cerevisiae* genome sequence. *Genome Res* **8**(5): 464-478.
- Kimura, A., Umehara, T., and Horikoshi, M. 2002. Chromosomal gradient of histone acetylation established by Sas2p and Sir2p functions as a shield against gene silencing. *Nat Genet* **32**(3): 370-377.
- Kind, J., Vaquerizas, J.M., Gebhardt, P., Gentzel, M., Luscombe, N.M., Bertone, P., and Akhtar, A. 2008. Genome-wide analysis reveals MOF as a key regulator of dosage compensation and gene expression in *Drosophila*. *Cell* **133**(5): 813-828.
- Kizer, K.O., Phatnani, H.P., Shibata, Y., Hall, H., Greenleaf, A.L., and Strahl, B.D. 2005. A novel domain in Set2 mediates RNA polymerase II interaction and couples histone H3 K36 methylation with transcript elongation. *Mol Cell Biol* **25**(8): 3305-3316.
- Korber, P., Barbaric, S., Luckenbach, T., Schmid, A., Schermer, U.J., Blaschke, D., and Horz, W. 2006. The histone chaperone Asf1 increases the rate of histone eviction at the yeast PHO5 and PHO8 promoters. *J Biol Chem* **281**(9): 5539-5545.
- Kouzarides, T. 2007. Chromatin modifications and their function. *Cell* **128**(4): 693-705.

- Kozak, M.L., Chavez, A., Dang, W., Berger, S.L., Ashok, A., Guo, X., and Johnson, F.B. 2010. Inactivation of the Sas2 histone acetyltransferase delays senescence driven by telomere dysfunction. *EMBO J* **29**(1): 158-170.
- Krawitz, D.C., Kama, T., and Kaufman, P.D. 2002. Chromatin assembly factor I mutants defective for PCNA binding require Asf1/Hir proteins for silencing. *Mol Cell Biol* **22**(2): 614-625.
- Krogan, N.J., Kim, M., Tong, A., Golshani, A., Cagney, G., Canadien, V., Richards, D.P., Beattie, B.K., Emili, A., Boone, C. et al. 2003. Methylation of histone H3 by Set2 in *Saccharomyces cerevisiae* is linked to transcriptional elongation by RNA polymerase II. *Mol Cell Biol* **23**(12): 4207-4218.
- Kulaeva, O.I., Gaykalova, D.A., and Studitsky, V.M. 2007. Transcription through chromatin by RNA polymerase II: histone displacement and exchange. *Mutat Res* **618**(1-2): 116-129.
- Kurdistani, S.K., Tavazoie, S., and Grunstein, M. 2004. Mapping global histone acetylation patterns to gene expression. *Cell* **117**(6): 721-733.
- Labib, K., Tercero, J.A., and Diffley, J.F. 2000. Uninterrupted MCM2-7 function required for DNA replication fork progression. *Science* **288**(5471): 1643-1647.
- Laemmli, U.K. 1970. Cleavage of structural proteins during the assembly of the head of bacteriophage T4. *Nature* **227**(5259): 680-685.
- Le, S., Davis, C., Konopka, J.B., and Sternglanz, R. 1997. Two new S-phase-specific genes from *Saccharomyces cerevisiae*. *Yeast* **13**(11): 1029-1042.
- Lee, C.K., Shibata, Y., Rao, B., Strahl, B.D., and Lieb, J.D. 2004. Evidence for nucleosome depletion at active regulatory regions genome-wide. *Nat Genet* **36**(8): 900-905.
- Lee, W., Tillo, D., Bray, N., Morse, R.H., Davis, R.W., Hughes, T.R., and Nislow, C. 2007. A high-resolution atlas of nucleosome occupancy in yeast. *Nat Genet* **39**(10): 1235-1244.
- Li, B., Carey, M., and Workman, J.L. 2007a. The role of chromatin during transcription. *Cell* **128**(4): 707-719.
- Li, B., Gogol, M., Carey, M., Pattenden, S.G., Seidel, C., and Workman, J.L. 2007b. Infrequently transcribed long genes depend on the Set2/Rpd3S pathway for accurate transcription. *Genes Dev* **21**(11): 1422-1430.
- Li, B., Howe, L., Anderson, S., Yates, J.R., 3rd, and Workman, J.L. 2003. The Set2 histone methyltransferase functions through the phosphorylated carboxyl-terminal domain of RNA polymerase II. *J Biol Chem* **278**(11): 8897-8903.

- Linger, J. and Tyler, J.K. 2006. Global replication-independent histone H4 exchange in budding yeast. *Eukaryot Cell* **5**(10): 1780-1787.
- Liu, C.L., Kaplan, T., Kim, M., Buratowski, S., Schreiber, S.L., Friedman, N., and Rando, O.J. 2005. Single-nucleosome mapping of histone modifications in *S. cerevisiae*. *PLoS Biol* **3**(10): e328.
- Lo, W.S., Trievel, R.C., Rojas, J.R., Duggan, L., Hsu, J.Y., Allis, C.D., Marmorstein, R., and Berger, S.L. 2000. Phosphorylation of serine 10 in histone H3 is functionally linked in vitro and in vivo to Gcn5-mediated acetylation at lysine 14. *Mol Cell* **5**(6): 917-926.
- Loyola, A., Bonaldi, T., Roche, D., Imhof, A., and Almouzni, G. 2006. PTMs on H3 variants before chromatin assembly potentiate their final epigenetic state. *Mol Cell* **24**(2): 309-316.
- Luger, K., Mader, A.W., Richmond, R.K., Sargent, D.F., and Richmond, T.J. 1997. Crystal structure of the nucleosome core particle at 2.8 Å resolution. *Nature* **389**(6648): 251-260.
- Luger, K. and Richmond, T.J. 1998. The histone tails of the nucleosome. *Curr Opin Genet Dev* **8**(2): 140-146.
- Luke, B., Panza, A., Redon, S., Iglesias, N., Li, Z., and Lingner, J. 2008. The Rat1p 5' to 3' exonuclease degrades telomeric repeat-containing RNA and promotes telomere elongation in *Saccharomyces cerevisiae*. *Mol Cell* **32**(4): 465-477.
- Maeshima, K., Hihara, S., and Eltsov, M. Chromatin structure: does the 30-nm fibre exist in vivo? *Curr Opin Cell Biol* **22**(3): 291-297.
- Makise, M., Matsui, N., Yamairi, F., Takahashi, N., Takehara, M., Asano, T., and Mizushima, T. 2008. Analysis of origin recognition complex in *saccharomyces cerevisiae* by use of Degron mutants. *J Biochem* **143**(4): 455-465.
- Malone, C.D. and Hannon, G.J. 2009. Small RNAs as guardians of the genome. *Cell* **136**(4): 656-668.
- Martens, J.A., Laprade, L., and Winston, F. 2004. Intergenic transcription is required to repress the *Saccharomyces cerevisiae* SER3 gene. *Nature* **429**(6991): 571-574.
- Mason, P.B. and Struhl, K. 2005. Distinction and relationship between elongation rate and processivity of RNA polymerase II in vivo. *Mol Cell* **17**(6): 831-840.
- Masumoto, H., Hawke, D., Kobayashi, R., and Verreault, A. 2005. A role for cell-cycle-regulated histone H3 lysine 56 acetylation in the DNA damage response. *Nature* **436**(7048): 294-298.

- Matsuda, E. and Garfinkel, D.J. 2009. Posttranslational interference of Ty1 retrotransposition by antisense RNAs. *Proc Natl Acad Sci U S A* **106**(37): 15657-15662.
- Meijsing, S.H. and Ehrenhofer-Murray, A.E. 2001. The silencing complex SAS-I links histone acetylation to the assembly of repressed chromatin by CAF-I and Asf1 in *Saccharomyces cerevisiae*. *Genes Dev* **15**(23): 3169-3182.
- Meneghini, M.D., Wu, M., and Madhani, H.D. 2003. Conserved histone variant H2A.Z protects euchromatin from the ectopic spread of silent heterochromatin. *Cell* **112**(5): 725-736.
- Millar, C.B. and Grunstein, M. 2006. Genome-wide patterns of histone modifications in yeast. *Nat Rev Mol Cell Biol* **7**(9): 657-666.
- Moazed, D. 2001. Common themes in mechanisms of gene silencing. *Mol Cell* **8**(3): 489-498.
- Morillon, A., Benard, L., Springer, M., and Lesage, P. 2002. Differential effects of chromatin and Gcn4 on the 50-fold range of expression among individual yeast Ty1 retrotransposons. *Mol Cell Biol* **22**(7): 2078-2088.
- Morillon, A., Karabetsou, N., O'Sullivan, J., Kent, N., Proudfoot, N., and Mellor, J. 2003a. Isw1 chromatin remodeling ATPase coordinates transcription elongation and termination by RNA polymerase II. *Cell* **115**(4): 425-435.
- Morillon, A., O'Sullivan, J., Azad, A., Proudfoot, N., and Mellor, J. 2003b. Regulation of elongating RNA polymerase II by forkhead transcription factors in yeast. *Science* **300**(5618): 492-495.
- Muller, H.J. 1930. Types of visible variations induced by X-rays in *Drosophila*. *Journal of Genetics* **22**: 299-335.
- Neil, H., Malabat, C., d'Aubenton-Carafa, Y., Xu, Z., Steinmetz, L.M., and Jacquier, A. 2009. Widespread bidirectional promoters are the major source of cryptic transcripts in yeast. *Nature* **457**(7232): 1038-1042.
- Ng, H.H., Robert, F., Young, R.A., and Struhl, K. 2003. Targeted recruitment of Set1 histone methylase by elongating Pol II provides a localized mark and memory of recent transcriptional activity. *Mol Cell* **11**(3): 709-719.
- Okamoto, I. and Heard, E. 2009. Lessons from comparative analysis of X-chromosome inactivation in mammals. *Chromosome Res* **17**(5): 659-669.
- Osada, S., Sutton, A., Muster, N., Brown, C.E., Yates, J.R., 3rd, Sternglanz, R., and Workman, J.L. 2001. The yeast SAS (something about silencing) protein complex contains a MYST-type putative acetyltransferase and functions with chromatin assembly factor ASF1. *Genes Dev* **15**(23): 3155-3168.

- Osley, M.A. 1991. The regulation of histone synthesis in the cell cycle. *Annu Rev Biochem* **60**: 827-861.
- Patterton, H.G., Landel, C.C., Landsman, D., Peterson, C.L., and Simpson, R.T. 1998. The biochemical and phenotypic characterization of Hho1p, the putative linker histone H1 of *Saccharomyces cerevisiae*. *J Biol Chem* **273**(13): 7268-7276.
- Perrod, S. and Gasser, S.M. 2003. Long-range silencing and position effects at telomeres and centromeres: parallels and differences. *Cell Mol Life Sci* **60**(11): 2303-2318.
- Pokholok, D.K., Harbison, C.T., Levine, S., Cole, M., Hannett, N.M., Lee, T.I., Bell, G.W., Walker, K., Rolfe, P.A., Herbolsheimer, E. et al. 2005. Genome-wide map of nucleosome acetylation and methylation in yeast. *Cell* **122**(4): 517-527.
- Prado, F., Cortes-Ledesma, F., and Aguilera, A. 2004. The absence of the yeast chromatin assembly factor Asf1 increases genomic instability and sister chromatid exchange. *EMBO Rep* **5**(5): 497-502.
- Rando, O.J. and Chang, H.Y. 2009. Genome-wide views of chromatin structure. *Annu Rev Biochem* **78**: 245-271.
- Ransom, M., Dennehey, B.K., and Tyler, J.K. 2010. Chaperoning histones during DNA replication and repair. *Cell* **140**(2): 183-195.
- Rea, S., Xouri, G., and Akhtar, A. 2007. Males absent on the first (MOF): from flies to humans. *Oncogene* **26**(37): 5385-5394.
- Reifsnnyder, C., Lowell, J., Clarke, A., and Pillus, L. 1996. Yeast SAS silencing genes and human genes associated with AML and HIV-1 Tat interactions are homologous with acetyltransferases. *Nat Genet* **14**(1): 42-49.
- Riles, L., Shaw, R.J., Johnston, M., and Reines, D. 2004. Large-scale screening of yeast mutants for sensitivity to the IMP dehydrogenase inhibitor 6-azauracil. *Yeast* **21**(3): 241-248.
- Robert, F., Pokholok, D.K., Hannett, N.M., Rinaldi, N.J., Chandy, M., Rolfe, A., Workman, J.L., Gifford, D.K., and Young, R.A. 2004. Global position and recruitment of HATs and HDACs in the yeast genome. *Mol Cell* **16**(2): 199-209.
- Robinson, K.M. and Schultz, M.C. 2003. Replication-independent assembly of nucleosome arrays in a novel yeast chromatin reconstitution system involves antisilencing factor Asf1p and chromodomain protein Chd1p. *Mol Cell Biol* **23**(22): 7937-7946.
- Robyr, D., Suka, Y., Xenarios, I., Kurdistani, S.K., Wang, A., Suka, N., and Grunstein, M. 2002. Microarray deacetylation maps determine genome-wide functions for yeast histone deacetylases. *Cell* **109**(4): 437-446.

- Rufiange, A., Jacques, P.E., Bhat, W., Robert, F., and Nourani, A. 2007. Genome-wide replication-independent histone H3 exchange occurs predominantly at promoters and implicates H3 K56 acetylation and Asf1. *Mol Cell* **27**(3): 393-405.
- Rusche, L.N., Kirchmaier, A.L., and Rine, J. 2003. The establishment, inheritance, and function of silenced chromatin in *Saccharomyces cerevisiae*. *Annu Rev Biochem* **72**: 481-516.
- Rusche, L.N. and Lynch, P.J. 2009. Assembling heterochromatin in the appropriate places: A boost is needed. *J Cell Physiol* **219**(3): 525-528.
- Sambrook, J., Fritsch, E.F., and Maniatis, T. 1989. *Molecular Cloning: A Laboratory Manual*. Cold Spring Harbor Laboratory Press
- Santos-Rosa, H., Schneider, R., Bannister, A.J., Sherriff, J., Bernstein, B.E., Emre, N.C., Schreiber, S.L., Mellor, J., and Kouzarides, T. 2002. Active genes are trimethylated at K4 of histone H3. *Nature* **419**(6905): 407-411.
- Schaper, S., Franke, J., Meijnsing, S.H., and Ehrenhofer-Murray, A.E. 2005. Nuclear import of the histone acetyltransferase complex SAS-I in *Saccharomyces cerevisiae*. *J Cell Sci* **118**(Pt 7): 1473-1484.
- Scharf, A.N., Meier, K., Seitz, V., Kremmer, E., Brehm, A., and Imhof, A. 2009. Monomethylation of lysine 20 on histone H4 facilitates chromatin maturation. *Mol Cell Biol* **29**(1): 57-67.
- Schwabish, M.A. and Struhl, K. 2004. Evidence for eviction and rapid deposition of histones upon transcriptional elongation by RNA polymerase II. *Mol Cell Biol* **24**(23): 10111-10117.
- Schwabish, M.A. and Struhl, K. 2006. Asf1 mediates histone eviction and deposition during elongation by RNA polymerase II. *Mol Cell* **22**(3): 415-422.
- Sharp, J.A., Fouts, E.T., Krawitz, D.C., and Kaufman, P.D. 2001. Yeast histone deposition protein Asf1p requires Hir proteins and PCNA for heterochromatic silencing. *Curr Biol* **11**(7): 463-473.
- Sherman, F. 1991. Getting started with yeast. *Methods Enzymol* **194**: 3-21.
- Shia, W.J., Li, B., and Workman, J.L. 2006. SAS-mediated acetylation of histone H4 Lys 16 is required for H2A.Z incorporation at subtelomeric regions in *Saccharomyces cerevisiae*. *Genes Dev* **20**(18): 2507-2512.
- Shibahara, K. and Stillman, B. 1999. Replication-dependent marking of DNA by PCNA facilitates CAF-1-coupled inheritance of chromatin. *Cell* **96**(4): 575-585.

- Shogren-Knaak, M., Ishii, H., Sun, J.M., Pazin, M.J., Davie, J.R., and Peterson, C.L. 2006. Histone H4-K16 acetylation controls chromatin structure and protein interactions. *Science* **311**(5762): 844-847.
- Singer, M.S., Kahana, A., Wolf, A.J., Meisinger, L.L., Peterson, S.E., Goggin, C., Mahowald, M., and Gottschling, D.E. 1998. Identification of high-copy disruptors of telomeric silencing in *Saccharomyces cerevisiae*. *Genetics* **150**(2): 613-632.
- Smith, C.M., Gafken, P.R., Zhang, Z., Gottschling, D.E., Smith, J.B., and Smith, D.L. 2003. Mass spectrometric quantification of acetylation at specific lysines within the amino-terminal tail of histone H4. *Anal Biochem* **316**(1): 23-33.
- Smith, E.R., Eisen, A., Gu, W., Sattah, M., Pannuti, A., Zhou, J., Cook, R.G., Lucchesi, J.C., and Allis, C.D. 1998. ESA1 is a histone acetyltransferase that is essential for growth in yeast. *Proc Natl Acad Sci U S A* **95**(7): 3561-3565.
- Sobel, R.E., Cook, R.G., Perry, C.A., Annunziato, A.T., and Allis, C.D. 1995. Conservation of deposition-related acetylation sites in newly synthesized histones H3 and H4. *Proc Natl Acad Sci U S A* **92**(4): 1237-1241.
- Steinmetz, E.J., Warren, C.L., Kuehner, J.N., Panbehi, B., Ansari, A.Z., and Brow, D.A. 2006. Genome-wide distribution of yeast RNA polymerase II and its control by Sen1 helicase. *Mol Cell* **24**(5): 735-746.
- Sterner, D.E. and Berger, S.L. 2000. Acetylation of histones and transcription-related factors. *Microbiol Mol Biol Rev* **64**(2): 435-459.
- Suganuma, T. and Workman, J.L. 2008. Crosstalk among Histone Modifications. *Cell* **135**(4): 604-607.
- Suk, K., Choi, J., Suzuki, Y., Ozturk, S.B., Mellor, J.C., Wong, K.H., Mackay, J.L., Gregory, R.I., and Roth, F.P. 2011. Reconstitution of human RNA interference in budding yeast. *Nucleic Acids Res.*
- Suka, N., Luo, K., and Grunstein, M. 2002. Sir2p and Sas2p opposingly regulate acetylation of yeast histone H4 lysine16 and spreading of heterochromatin. *Nat Genet* **32**(3): 378-383.
- Sutton, A., Shia, W.J., Band, D., Kaufman, P.D., Osada, S., Workman, J.L., and Sternglanz, R. 2003. Sas4 and Sas5 are required for the histone acetyltransferase activity of Sas2 in the SAS complex. *J Biol Chem* **278**(19): 16887-16892.
- Taipale, M., Rea, S., Richter, K., Vilar, A., Lichter, P., Imhof, A., and Akhtar, A. 2005. hMOF histone acetyltransferase is required for histone H4 lysine 16 acetylation in mammalian cells. *Mol Cell Biol* **25**(15): 6798-6810.
- Tamburini, B.A., Carson, J.J., Linger, J.G., and Tyler, J.K. 2006. Dominant mutants of the *Saccharomyces cerevisiae* ASF1 histone chaperone bypass the need for CAF-1 in

- transcriptional silencing by altering histone and Sir protein recruitment. *Genetics* **173**(2): 599-610.
- Tyler, J.K., Adams, C.R., Chen, S.R., Kobayashi, R., Kamakaka, R.T., and Kadonaga, J.T. 1999. The RCAF complex mediates chromatin assembly during DNA replication and repair. *Nature* **402**(6761): 555-560.
- Verreault, A., Kaufman, P.D., Kobayashi, R., and Stillman, B. 1996. Nucleosome assembly by a complex of CAF-1 and acetylated histones H3/H4. *Cell* **87**(1): 95-104.
- Wach, A., Brachat, A., Pohlmann, R., and Philippsen, P. 1994. New heterologous modules for classical or PCR-based gene disruptions in *Saccharomyces cerevisiae*. *Yeast* **10**(13): 1793-1808.
- Weber, J.M., Irlbacher, H., and Ehrenhofer-Murray, A.E. 2008. Control of replication initiation by the Sum1/Rfm1/Hst1 histone deacetylase. *BMC Mol Biol* **9**: 100.
- Whitehouse, I., Rando, O.J., Delrow, J., and Tsukiyama, T. 2007. Chromatin remodelling at promoters suppresses antisense transcription. *Nature* **450**(7172): 1031-1035.
- Widom, J. and Klug, A. 1985. Structure of the 300A chromatin filament: X-ray diffraction from oriented samples. *Cell* **43**(1): 207-213.
- Williams, S.K. and Tyler, J.K. 2007. Transcriptional regulation by chromatin disassembly and reassembly. *Curr Opin Genet Dev* **17**(2): 88-93.
- Wirbelauer, C., Bell, O., and Schubeler, D. 2005. Variant histone H3.3 is deposited at sites of nucleosomal displacement throughout transcribed genes while active histone modifications show a promoter-proximal bias. *Genes Dev* **19**(15): 1761-1766.
- Workman, J.L. 2006. Nucleosome displacement in transcription. *Genes Dev* **20**(15): 2009-2017.
- Wright, J.H., Gottschling, D.E., and Zakian, V.A. 1992. *Saccharomyces telomeres* assume a non-nucleosomal chromatin structure. *Genes Dev* **6**(2): 197-210.
- Xie, W., Gai, X., Zhu, Y., Zappulla, D.C., Sternglanz, R., and Voytas, D.F. 2001. Targeting of the yeast Ty5 retrotransposon to silent chromatin is mediated by interactions between integrase and Sir4p. *Mol Cell Biol* **21**(19): 6606-6614.
- Xu, E.Y., Kim, S., and Rivier, D.H. 1999. SAS4 and SAS5 are locus-specific regulators of silencing in *Saccharomyces cerevisiae*. *Genetics* **153**(1): 25-33.
- Xu, F., Zhang, K., and Grunstein, M. 2005. Acetylation in histone H3 globular domain regulates gene expression in yeast. *Cell* **121**(3): 375-385.

- Xu, F., Zhang, Q., Zhang, K., Xie, W., and Grunstein, M. 2007. Sir2 deacetylates histone H3 lysine 56 to regulate telomeric heterochromatin structure in yeast. *Mol Cell* **27**(6): 890-900.
- Xu, Z., Wei, W., Gagneur, J., Perocchi, F., Clauder-Munster, S., Camblong, J., Guffanti, E., Stutz, F., Huber, W., and Steinmetz, L.M. 2009. Bidirectional promoters generate pervasive transcription in yeast. *Nature* **457**(7232): 1033-1037.
- Yuan, G.C., Liu, Y.J., Dion, M.F., Slack, M.D., Wu, L.F., Altschuler, S.J., and Rando, O.J. 2005. Genome-scale identification of nucleosome positions in *S. cerevisiae*. *Science* **309**(5734): 626-630.
- Zhu, Y., Dai, J., Fuerst, P.G., and Voytas, D.F. 2003. Controlling integration specificity of a yeast retrotransposon. *Proc Natl Acad Sci U S A* **100**(10): 5891-5895.
- Zippo, A., Serafini, R., Rocchigiani, M., Pennacchini, S., Krepelova, A., and Oliviero, S. 2009. Histone crosstalk between H3S10ph and H4K16ac generates a histone code that mediates transcription elongation. *Cell* **138**(6): 1122-1136.
- Zofall, M., Fischer, T., Zhang, K., Zhou, M., Cui, B., Veenstra, T.D., and Grewal, S.I. 2009. Histone H2A.Z cooperates with RNAi and heterochromatin factors to suppress antisense RNAs. *Nature* **461**(7262): 419-422.

## Danksagung

Ich danke insbesondere Ann Ehrenhofer-Murray für die Bereitstellung dieses spannenden Promotionsthemas, für die Unterstützung in allen Aspekten während der Anfertigung dieser Arbeit, für *scientific advice* und immerwährende Diskussionsbereitschaft.

Mein herzlicher Dank gilt Allen, die an der Durchführung und Analyse von Experimenten, die dieser Arbeit zu Grunde liegen, beteiligt waren. Ho-Ryun Chung für die Analyse der ChIP-chip und Expressionsdaten; Ludger Klein-Hitpass für die Hybridisierungen der ChIP-chip DNA; Lars Steinmetz und Sandra Clauder-Münster sowie Zenyu Xu für die Aufarbeitung und Hybridisierung des RNA Materials und die Analyse der Expressionsdaten; Jan Weber für die Hilfe mit ChIP Analysen und qPCRs; Christian Reiter für die Hilfe bei zeitgenauer Probennahme für ChIP.

Ich bedanke mich bei den wissenschaftlichen Leitern anderer Labore: Antonin Morillon, Amine Nourani, Fred Winston und Tohru Mizushima, die Hefestämme für diese Arbeit zur Verfügung gestellt haben.

Ich bedanke mich bei allen Kollegen und ehemaligen Kollegen der Arbeitsgruppe für die angenehme Arbeitsatmosphäre. Ich danke besonders Rita für ihre Hilfsbereitschaft und Unterstützung, Martina und Jessica für ständigen Nachschub an Platten und Medien, Karolin für exzellente experimentelle Unterstützung, Andja, Christiane und Rolf. Herzlichen Dank an Christian, Juliane und Martin sowie an Corinna und Jacqueline, ich habe die Zeit mit Euch genossen. Ich danke den ZMB Arbeitsgruppen für ihre Hilfsbereitschaft und Beratung, besonders der AG Ehrmann für Hilfe und Rat mit der qPCR Maschine.

Mein herzlicher Dank gilt meiner Familie und Jan-Martin für ihre immerwährende Unterstützung.

---

## Lebenslauf - Franziska Heise

Der Lebenslauf ist in der Online-Version aus Gründen des Datenschutzes nicht enthalten

### **Publikationen**

**Heise F.**, Chung H.-R., Weber J. M., Xu Z., Klein-Hitpass L., Steinmetz L. M., Vingron M., Ehrenhofer-Murray A. E. (submitted) *Genome-wide H4 K16 acetylation by SAS-I is deposited independently of transcription and histone exchange*

Chung H.-R., Dunkel I., **Heise F.**, Linke C., Krobitch S., Ehrenhofer-Murray A. E., Sperling S. R., and Vingron M. *The Effect of Micrococcal Nuclease Digestion on Nucleosome Positioning Data*  
PLoS One. 2010; 5(12): e15754

Schirling C., Heseding C., **Heise F.**, Kesper D., Klebes A., Klein-Hitpass L., Vortkamp A., Hoffmann D., Saumweber H., Ehrenhofer-Murray A.E. *Widespread regulation of gene expression in the Drosophila genome by the histone acetyltransferase dTip60*  
Chromosoma. 2010 Feb;119(1):99-113.

---

## **Konferenzen und Posterpräsentationen**

**Heise F.**, Chung H.-R., Weber J.M., Klein-Hitpass L., Steinmetz L.M., Vingron M., Ehrenhofer-Murray A.E. (2010); Genome-wide control of histone acetylation by the SAS-I complex in *Saccharomyces cerevisiae*. *Posterpräsentation im Rahmen des 9. Forschungstag der Medizinischen Fakultät des Universtätsklinikums Essen*

**Heise F.**, Chung H.-R., Weber J.M., Klein-Hitpass L., Xu Z., Steinmetz L.M., Vingron M., Ehrenhofer-Murray A.E. (2010); Genome-wide regulation of H4 K16Ac by the HAT SAS-I. *Posterpräsentation auf der 9<sup>th</sup> EMBL Conference , Transcription and Chromatin, Heidelberg, Germany*

**Seifert F.**, Chung H.-R., Weber J.M., Klein-Hitpass L., Steinmetz L.M., Vingron M., Ehrenhofer-Murray A.E. (2009); A new role for the HAT Sas2 in the suppression of cryptic initiation in *Saccharomyces cerevisiae*. *Posterpräsentation im Rahmen des 8. Forschungstag der Medizinischen Fakultät des Universtätsklinikums Essen*

**Seifert F.**, Chung H.-R., Klein-Hitpass L., Vingron M., Ehrenhofer-Murray A.E. (2009); Influence of chromatin assembly factors on Sas2-mediated H4 K16 acetylation in *Saccharomyces cerevisiae*. *Posterpräsentation auf der Chromatin, Replication and Chromosomal Stability Conference, University of Copenhagen, Denmark*

**Seifert F.**, Ehrenhofer-Murray A.E. (2007); Interaction of chromatin assembly factors with the histone acetyltransferase complex SAS-I in *Saccharomyces cerevisiae*. *Posterpräsentation auf dem 3<sup>rd</sup> Annual Meeting, EU 6<sup>th</sup> Framework Programme “The Epigenome” Network of Excellence (2004-2009), The Royal Swedish Academy of Sciences Stockholm, Sweden*

Essen, den 16.03.2011

**Erklärung:**

Hiermit erkläre ich, gemäß § 6 Abs. (2) f) der Promotionsordnung der Fakultäten für Biologie, Chemie und Mathematik zur Erlangung der Dr. rer. nat., dass ich das Arbeitsgebiet, dem das Thema "Genome-wide control of H4 K16 acetylation by the SAS-I complex in *Saccharomyces cerevisiae*" zuzuordnen ist, in Forschung und Lehre vertrete und den Antrag von Franziska Heise befürworte und die Betreuung auch im Falle eines Weggangs, wenn nicht wichtige Gründe dem entgegenstehen, weiterführen werde.

Essen, den \_\_\_\_\_

**Erklärung:**

Hiermit erkläre ich, gemäß § 7 Abs. (2) c) + e) der Promotionsordnung der Fakultäten für Biologie, Chemie und Mathematik zur Erlangung des Dr. rer. nat., dass ich die vorliegende Dissertation selbstständig verfasst und mich keiner anderen als der angegebenen Hilfsmittel bedient habe.

Essen, den \_\_\_\_\_

**Erklärung:**

Hiermit erkläre ich, gemäß § 7 Abs. (2) d) + f) der Promotionsordnung der Fakultäten für Biologie, Chemie und Mathematik zur Erlangung des Dr. rer. nat., dass ich keine anderen Promotionen bzw. Promotionsversuche in der Vergangenheit durchgeführt habe und, dass diese Arbeit von keiner anderen Fakultät/ Fachbereich abgelehnt worden ist.

Essen, den \_\_\_\_\_